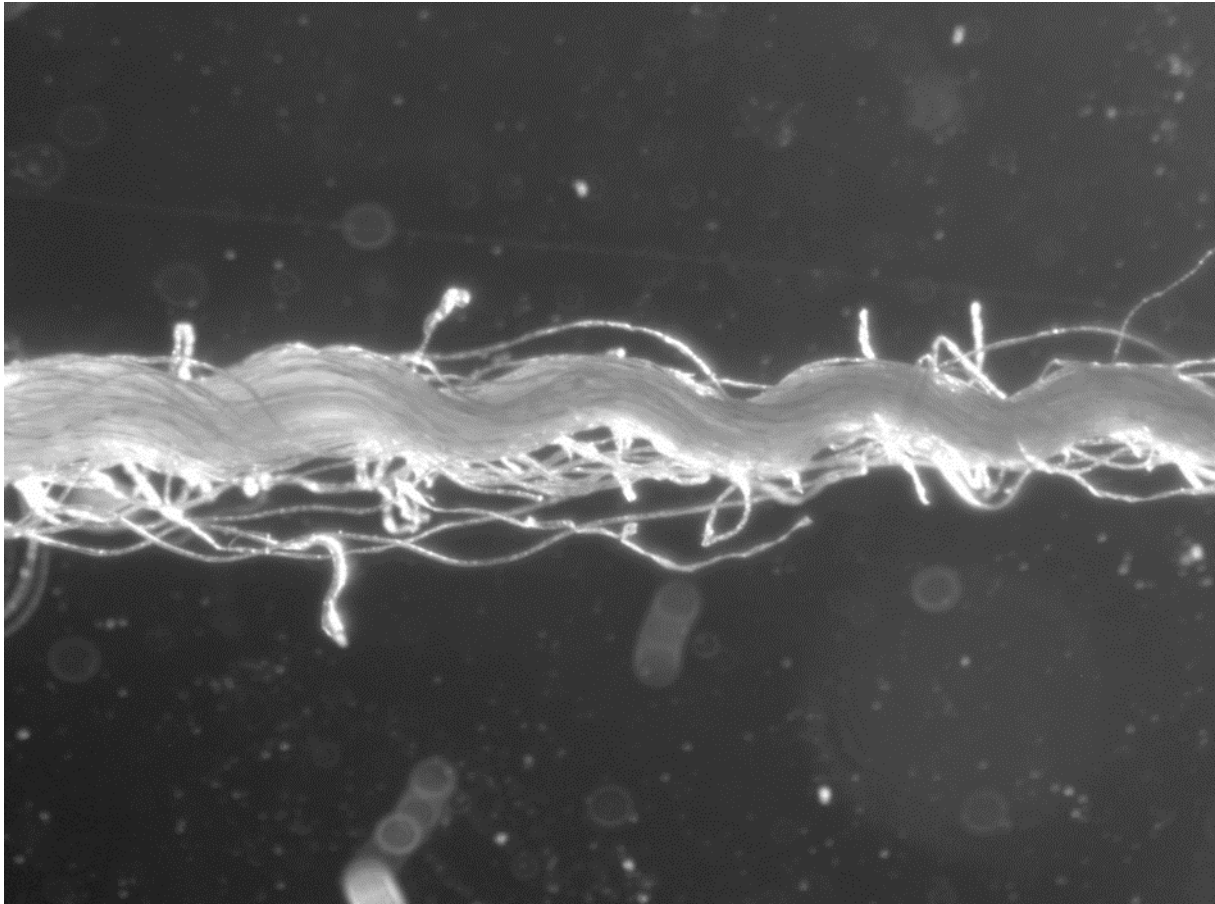




CHALMERS
UNIVERSITY OF TECHNOLOGY



Towards Recycling of Textile Fibers

Separation and Characterization of Textile Fibers and Blends

Master's thesis in Materials Chemistry and Nanotechnology

ANNA PETERSON

Department of Chemistry and Chemical Engineering
CHALMERS UNIVERSITY OF TECHNOLOGY
Gothenburg, Sweden 2015

Towards Recycling of Textile Fibers

Separation and Characterization of Textile Fibers and
Blends

ANNA PETERSON

Supervised by: Hanna de la Motte, Alexander Idström and Anna Palme

Department of Chemistry and Chemical Engineering
CHALMERS UNIVERSITY OF TECHNOLOGY
Gothenburg, Sweden 2015

Towards recycling of textile fibers

Separation and characterization of textile fibers and blends

ANNA PETERSON

© ANNA PETERSON 2015

Department of Chemistry and Chemical Engineering
Chalmers University of Technology
SE-412 96 Gothenburg
Sweden
Telephone + 46 (0)31-772 1000

Cover:
Light microscopy micrograph of a cotton/polyester thread

Abstract

Textile waste is composed of a complex matrix of materials. Textiles are often made from fiber blends, where two or more fiber types are spun together. In addition there might be buttons, zippers and seams of yet other compositions. To generate high quality recycled fibers the textile waste has to be separated into fractions of pure material. In order to introduce an efficient recycling of fibers, characterization of the fiber content as well as separation of fibers from material blends are crucial. The aim of this thesis is to increase the scientific knowledge concerning characterization and separation of post-consumer textile fibers.

Analysis of textile fibers and blends were performed using infrared (IR) and Raman spectroscopy and solid-state nuclear magnetic resonance (solid-state NMR) spectroscopy. IR and Raman spectroscopy were probed for their suitability to be used as automatic sorting techniques. Raman spectroscopy proved to be an insufficient technique in order to qualitatively characterize textile fibers at the probed excitation wavelengths, due to fluorescence emissions. IR spectroscopy revealed to be a useful technique for qualitative characterization of all types of fibers. Solid-state NMR spectroscopy was used to characterize textiles, both pure fibers and fiber blends. Its strength, to precisely resolve molecular structures was demonstrated for pure fibers. The technique also proved useful for qualitative analysis of the composition of complex fiber blends.

Separation of a polyester/cotton blended fabric by means of alkaline hydrolysis was performed. Full depolymerization of polyester under mild reaction conditions was achieved by using the phase transfer catalyst (PTC) benzyltributyl ammonium chloride. The reaction variables; NaOH concentration, PTC concentration, temperature and reaction time proved to be mutually dependent. High concentrations of PTC could facilitate almost full depolymerization in only 60 minutes at otherwise mild reaction conditions, 80 °C and 10 wt% NaOH. In the absence of PTC the yield of TPA is 23 % for 10 wt% NaOH and 67 % for 15 wt% NaOH after 100 min reaction time.

The reaction products from the separation were the pure cotton and the polyester monomers; terephthalic acid and ethylene glycol. The crystalline structure of the cotton residue was analyzed by IR spectroscopy, revealing a transformation of the crystalline structure under all reaction conditions, except when NaOH concentration was ≤ 10 wt% and temperature was ≤ 80 °C. Intrinsic viscosity measurements indicated that the reaction induced a substantial decrease of cellulose degree of polymerization.

Keywords: Textile recycling, cotton, polyester, automatic sorting, separation, infrared spectroscopy, Raman spectroscopy, solid-state nuclear magnetic resonance spectroscopy

Contents

| | |
|--|----|
| 1. Introduction..... | 1 |
| 1.1 Background..... | 1 |
| 1.2 Motivation..... | 1 |
| 1.3 Objectives..... | 2 |
| 2. Textile fibers..... | 3 |
| 2.1 Cellulose and cellulosic fibers..... | 4 |
| 2.2 Synthetic fibers..... | 6 |
| 2.3 Chemical resistance of polyester and cotton..... | 7 |
| 2.4 Characterization of textile fibers..... | 9 |
| 3. Textile recycling..... | 13 |
| 3.1 Current status of textile recycling..... | 13 |
| 3.2 Challenges in textile recycling..... | 14 |
| 3.3 Textile analysis..... | 15 |
| 3.4 Chemical separation..... | 15 |
| 4. Analytical techniques..... | 19 |
| 4.1 Vibrational spectroscopy theory..... | 19 |
| 4.2 NMR theory..... | 23 |
| 5. Materials and methods..... | 29 |
| 5.1 Materials..... | 29 |
| 5.2 Methods..... | 30 |
| 6. Results and discussion..... | 32 |
| 6.1 Textile analysis..... | 32 |
| 6.2 Separation..... | 41 |
| 7. Conclusions..... | 49 |
| 8. Outlook..... | 51 |
| Acknowledgements..... | 52 |
| Bibliography..... | 53 |
| Appendix 1..... | 58 |
| Appendix 2..... | 65 |

1. Introduction

1.1 Background

The increased awareness concerning environmental issues has alerted consumers, industry and governments on the detrimental effects on the environment from textile production. *MISTRA Future Fashion* is a research program initiated by the Swedish Foundation for Strategic Environmental Research (MISTRA) with the aim to deliver knowledge and solutions to the Swedish fashion industry and its stakeholders. This thesis is written within the framework of the MISTRA Future Fashion subproject number 5, *Reuse, Recycling and End of Life Issues*. The aim of the project is to "develop methods for collecting, handling, up-cycling and up-grading textiles, giving them a new life."

1.2 Motivation

The global demand for textile materials is steadily increasing due to world population growth and the overall improvement of living standards. The rapid change of fashion trends in combination with relatively low prices on clothing has shortened the life cycle for textile garments, generating more textile waste (Lu & Hamouda 2014). According to the Swedish Environmental Protection Agency an average Swedish person is expected to generate 12-15 kg of textile waste per year. Textile waste is still a small fraction of the total waste stream, however, seen from a lifecycle perspective textiles is one of the types of wastes associated with the heaviest climate effects. The production of new textiles generates approximately 15 kg of CO₂ per kilo textile produced and also demands high amounts of water, energy, and chemicals (Naturvårdsverket 2012). Since textile materials are generally produced in low-wage countries with insufficient environmental legislation prices can be kept down and the cost of the environmental damage is not paid by the consumer. Consequently, the utilization of virgin materials such as cotton and crude oil are more economic than recycling of textile fibers.

The recycling processes of textile fibers which are performed today are mainly down-cycling, which means a material of lower quality than the original material is produced. Post-consumer textiles are made into cleaning wipes or shredded and used as padding in for example car seats. Technology that enables the use of post-consumer waste textiles in order to generate new high quality fibers is still lacking in most of the industry. An efficient recycling chain has to meet the needs of collecting, sorting and regenerating new fibers of high quality. Existing recycling methods are either very small scaled or labor intense which makes them insufficient from an economic perspective. To be able to handle the textile waste stream, technology must be developed and the knowledge on the area must be

increased. Textile waste is composed of a complex matrix of materials. Fabrics are often made from fiber blends, where two or more types of fibers are spun together. In addition there might be buttons, zippers and seams of yet other compositions, as well as dyes and various surface treatments. To generate recycled high quality fibers the textile waste has to be separated into fractions of pure materials.

As implied above recycling of textile fibers is a challenging subject, but the environmental benefits from a working recycling chain of textile fibers are substantial. In order to introduce an efficient recycling of fibers, characterization of the fiber content as well as separation of fibers from material blends is crucial. It is thus of high interest to develop technology that enables off-line and on-line analysis of the content of material blends, as well as methods to chemically separate the fibers.

1.3 Objectives

The main objective of this thesis is to increase the scientific knowledge concerning characterization and separation of post-consumer textile fibers. The questions to be answered are:

- Are vibrational spectroscopy techniques such as infrared and Raman spectroscopy suitable characterization techniques for on-line sorting of waste textiles?
- In what ways can solid-state nuclear magnetic resonance spectroscopy be used to characterize textile fibers for recycling purposes?
- How are cellulosic and polyester fibers affected by chemical separation from a fiber blend under alkaline conditions? Parameters such as degree of polymerization and crystallinity are to be studied as well as characterization of dissolved material.

2. Textile fibers

Textile fibers are categorized as either natural or man-made. The natural fibers fall into three different chemical classes:

- Cellulosics, which origin from various parts of plants
- Protein fibers, which are obtained from wool, hair and silk
- Mineral fibers, where asbestos is the only one naturally occurring

The man-made fibers can also be divided into three sub-groups:

- Regenerated fibers, which are derived from natural sources of organic polymers
- Synthetic fibers, which are produced from non-renewable sources
- Inorganic fibers, such as glass or ceramic fibers

On the molecular level textile fibers are built up by polymer chains where the monomers and the polymer linkage are specific for each fiber type. A natural fiber is composed by many thousands of polymer chains which aggregate to form complex patterns and build up very specific layered structures accounting for much of the properties of the fiber. Natural fibers are in the length range from a few centimeters for cotton, to around one decimeter for wool up to several hundred meters for silk. Shorter fibers, as cotton and wool are spun together to form a continuous yarn. Man-made fibers are formed by extruding the melted or dissolved polymer through the small openings of a spinneret. With this process both filament yarns, in which the yarn is comprised of one infinitely long fiber or spun yarns, where the fibers are cut to shorter pieces and spun together can be produced (Mather & Wardman 2011).

Polyester and cotton are the two fiber types that have the largest production volumes globally. In 2008 the worldwide production of polyester was 30.7 million tonnes while the production of cotton was 24.4 million tonnes (Mather & Wardman 2011). However, the demand for textile fibers is constantly increasing and in 2014 the global demand for fibers was estimated to be 89.4 million tonnes (Lenzing 2015). Figure 1 gives an overview over the global fiber market in the year 2014.

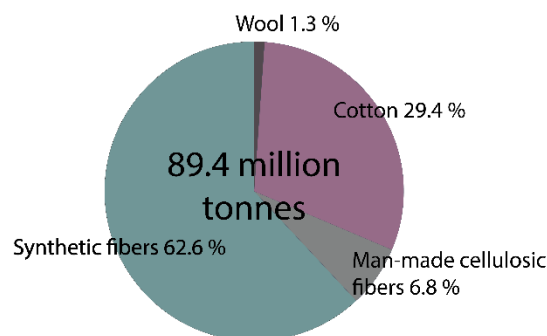


Figure 1: Global fiber market 2014. Data from Lenzing.

To gain an insight on the possibilities and challenges with textile recycling a thorough knowledge on textile fibers needs to be acquired. The following section will provide deeper knowledge on cellulosic and polyester fibers. These fiber types are emphasized since, as stated earlier, they are produced in the largest volumes and hence build up the majority of the textile waste stream. Apart from that, the separation part of this thesis work deals exclusively with a polyester/cotton (polycotton) blend. An understanding of molecular structure, crystal structure and chemical resistance of the fibers is needed in order to understand degradation processes, polymerization and depolymerization as well as possible recycling methods.

2.1 Cellulose and cellulosic fibers

Cellulosic textile fibers can both be natural, as cotton, and man-made as lyocell and viscose. This first section will provide general knowledge on cellulose, which is the polymer building up all of these fibers.

Cellulose is the most abundant polymer in nature (Zugenmaier 2001). It is a polysaccharide built up from the monomer β -D-glucopyranose also called an anhydroglucose unit (AGU). The monomers are linked by 1,4-glycosidic bonds to build up the repeating unit of cellulose, cellobiose. The cellulose polymer is terminated by one reducing and one non-reducing end. The terminal AGU in the reducing end is more reactive, it is a cyclic hemiacetal that stands in equilibrium with the aldehyde. The non-reducing end is not as reactive and always has a closed ring structure (Klemm et al. 2005).

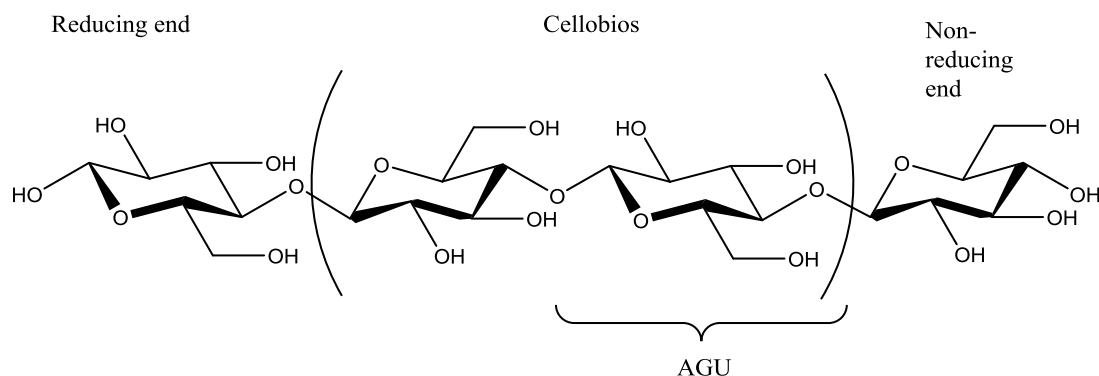


Figure 2: Molecular structure of the repeating unit of cellulose, showing the anhydroglucose unit, cellobiose and the reducing and non-reducing end.

The cellulose chains allow for close packing by adapting the chair conformation where the methyl alcohol and hydroxyl groups are in the same plane as the ring, rather than pointing in perpendicular directions. The chains are held together by hydrogen bonds between the hydroxyl groups and the oxygen atoms, both the ring and the bridging oxygen atoms. Hydrogen bonding occurs both intramolecular, within the same chain, and intermolecular, between adjacent chains. The numerous hydrogen bonds make cellulose a strong and tough polymer but also hard to dissolve (Shaw 2013). Only a few solvents have proven useful for cellulose dissolution such as ionic liquids, cold alkali, [copper(II)ethylenediamine] (Cuen), and N-Methylmorpholine N-oxide (NMMO). A recent debate within research brings up an additional source for the low solubility of cellulose; hydrophobic effects. Within this approach cellulose is regarded as an amphiphilic polymer which, due to the conformation of the polymeric chain, expresses a structural anisotropy which gives rise to hydrophobic interactions (Medronho et al. 2012).

The length of a cellulose chains is expressed as degree of polymerization (DP), an estimate of the average number of AGU's in the polymer chain.

Cellulose crystal structure

The crystal structure of cellulose is commonly described using the fringed fibrillary model in which crystalline regions of varying dimensions are mixed with non-crystalline regions. Naturally, the non-crystalline regions are more accessible and prone to reaction than the crystalline parts (Klemm et al. 2005). Cellulose exists in several polymorphs, with different crystalline structures differentiated by the way in which the cellulose molecules are packed.

Cellulose I is the native form of cellulose which can be extracted from wood, cotton, algae etc. It forms two different crystal structures, I α and I β , where I β is more thermodynamically stable. In cellulose I the chains are aligned parallel to each other with all the reducing ends pointing in the same direction which is seen in Figure 3a (Mather & Wardman 2011).

Cellulose II is the crystalline structure obtained in regenerated cellulose, after dissolution and reprecipitation of native cellulose. The transformation from cellulose I to cellulose II can also be brought about by swelling native cellulose in alkali, a process called mercerization. In cellulose II the polymer chains are oriented anti-parallel to each other which is shown in figure 3b. The chains are not lying perfectly flat but are slightly tilted which allows for better intramolecular bonding, at the expense of intermolecular bonds (Mather & Wardman 2011). The transformation between cellulose I and cellulose II is irreversible and cellulose II, because of the stronger hydrogen bonding, is thermodynamically more stable (Egal 2006).

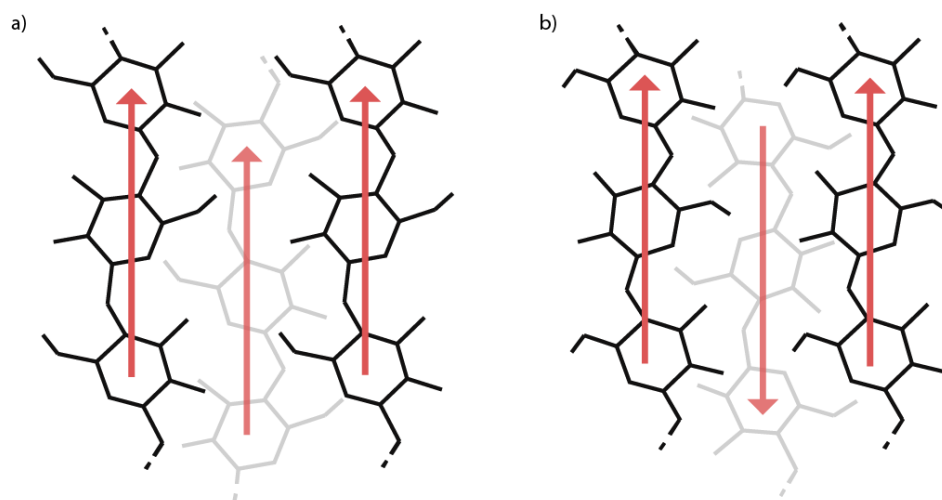


Figure 3: Schematic picture of a) cellulose I and b) cellulose II showing how the chains in cellulose I are oriented parallel to each other while the chains in cellulose II are anti-parallel (Idström 2015)

2.1.1 Cotton

Cotton is grown in many parts of the world, where the conditions are favorable i.e. warm and humid climate and a fairly sandy soil (Hatch 1993). In 1999 cotton cultivation accounted for 2.4 % of the world's arable land. It is a water demanding crop, up to 20,000 liters of fresh water is needed to produce one kilogram of cotton. Cotton production also accounts for a big share of the consumption of insecticides and pesticides, 24 % and 11 % of the global sales, respectively (Bärlocher & Holland 1999).

The main component of cotton is cellulose but the fibers also contain small amounts of pectines and proteins. The exact composition varies with the source of the cotton and growth conditions, as does the quality of the fiber, its fineness and length. The fibers of highest quality have fiber lengths between 25-65 mm whereas the lower quality cotton has fiber lengths between 10-25 mm. DP for native cotton is reported to be in the range of 6,000-10,000 (Hatch 1993) up to 15,000 (Sjöström 1981). The packing of cellulose in the cotton fibers is not uniform, but the fiber is built up by a number of layers. In the middle of the fiber there is a hollow channel, called the lumen, which is filled with sap during early stages of growth. Around the lumen several layers are spiraling along the fiber axis, the spiraling structure being the source of the inherent strength of the cotton fiber (Egal 2006).

2.1.2 Man-made cellulosic fibers

Viscose and lyocell belong to the family of regenerated textile fibers. These fibers are composed of 100 % cellulose which is extracted from cellulosic raw materials, mainly wood, which have a DP of about 10000 (Sjöström 1981). However, cellulose chains in textiles from regenerated cellulose have a DP of 400-600, much lower compared to the DP of cellulosic raw materials. The low DP is a consequence of the need to dissolve cellulose in order to produce regenerated fibers, since shorter chains dissolve more easily. The desired DP is reached by pretreatment methods and during pulping by chemical processes that generates chain cleavage, such as autoxidation and hydrolysis.

The two fibre manufacturing methods, viscose and lyocell, use different approaches to dissolve cellulose, derivatization or direct dissolution. In the viscose process cellulose is derivatized to cellulose xanthate by reaction with carbon disulfide and then dissolved in aqueous NaOH (Hatch 1993). The lyocell process uses the organic solvent NMMO to directly dissolve pure cellulose. In both methods a viscous solution is obtained which is forced through the holes of a spinneret to form continuous filaments. Subsequently the filaments are coagulated to obtain solid fibers. Viscose is coagulated in an acid bath where also the cellulose xanthate is regenerated back to pure cellulose (Hatch 1993). Lyocell is coagulated in water or dilute NMMO (Liu et al. 2001). The filaments can then be used to form filament yarns or be cut and spun to form spun yarns.

2.2 Synthetic fibers

Synthetic fibers such as polyester, elastane, acrylic and nylon are all made from organic compounds derived from crude oil (Mather & Wardman 2011). Specific monomers are reacted in order to form a polymer of the desired properties. Fiber forming is generally made by melt-spinning or dry-spinning, both techniques are based on forcing the polymer through a spinneret to form filaments. In melt-spinning the polymer is melted before extrusion and solidifies upon cooling while in dry-spinning the polymers are dissolved in a suitable solvent and solidifies when the solvent is evaporated. The filaments can then be used to form filament yarns or be cut and spun to form spun yarns (Hatch 1993).

2.2.1 Polyester

Polyesters are, according to the definition by the International Bureau for Standardization of Man-made Fibers (BISFA) “manufactured fibers in which the fiber-forming substance is any long-chain polymer composed of at least 85 % by weight of an ester of a substituted aromatic carboxylic acid including but not restricted to substituted terephthalate units.” This implies that members of the generic group polyesters can have diverse molecular structures.

The dominant type of polyester is polyethylene terephthalate most commonly known as PET (Hatch, 1993), whose repeating unit can be seen in Figure 4.

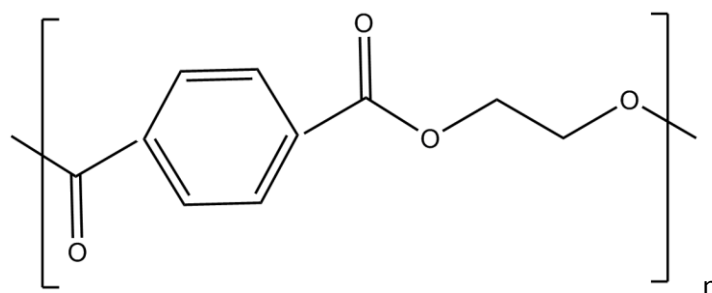


Figure 4: Molecular structure of the PET repeating unit

Polyester chains do not form intramolecular hydrogen bonds as do cellulosic fibers but are held together by the electron clouds above and below the aromatic rings. Since the chains are planar the aromatic rings can lie in close proximity to each other and dipole-dipole interactions are believed to occur. Polyester is known to be a strong and tough fiber with a high breaking tenacity and high resistance to elongation (Hatch 1993). Polyester fibers used in garments and home textiles are about 35 % crystalline and 65 % amorphous, but the degree of crystallinity can be varied for different applications. Higher crystallinity gives a stronger, but also stiffer polymer, suitable for technical textiles.

2.3 Chemical resistance of polyester and cotton

In this thesis the separation of a blended cotton/polyester fabric is part of the research performed. The method used is an alkaline hydrolysis of polyester aided by a phase transfer catalyst. The motivation for choosing this method can be read in section 3.4 and the experimental procedure is described in 5.2.7. The foundation for the implementation of this separation is that the chemical resistance to alkali differs between cotton and polyester. As can be seen in Table 1 polyester has a low resistance to hot alkali while cotton has a high resistance.

Table 1: Chemical resistance of polyester and cotton fibers (Hatch, 1993)

| PROPERTY | POLYESTER RANK | COTTON RANK |
|--|----------------|----------------|
| ALKALI RESISTANCE | | |
| - DILUTE | High | High |
| - CONCENTRATED | Low (when hot) | High (swells) |
| ACID RESISTANCE | | |
| - DILUTE | High | Low (when hot) |
| - CONCENTRATED | High | Low |
| OXIDIZING AGENT RESISTANCE | High | Medium |
| SOLUBILITY IN COMMON ORGANIC SOLVENTS | Low | Low |

2.3.1 Alkali resistance of polyester

Polyester has a low resistance to hot alkali which causes full depolymerization of the polymer by alkaline hydrolysis. The attacking hydroxide ion is not believed to diffuse into the polymer but rather act on the surface, splitting the ester bonds yielding an alcohol and a carboxylic acid (Karayannidis & Achilias 2007).

2.3.2 Alkali resistance of cotton

Cotton cellulose is readily depolymerized in acidic environments, however, its resistance to alkaline environments is higher. The fiber does not get visually damaged and though the DP is lowered cotton is not substantially depolymerized. However, as stated in section 2.1 the crystalline structure is changed by subjecting cotton cellulose to strong alkaline solutions. The treatment also reduces the overall crystallinity (Kljun et al. 2011).

The chemical processes responsible for the reduction in DP of cellulose are presented below.

Endwise peeling (beta-elimination)

Endwise peeling is the main reason for cellulose chain shortening at moderate temperatures (Mozdyniewicz et al. 2013). The reaction takes place at accessible reducing end groups of the cellulose polymer where monomers are being peeled of one by one. Reaction products are mainly isosaccharinic acid, seen in Figure 5, but also similar acids.

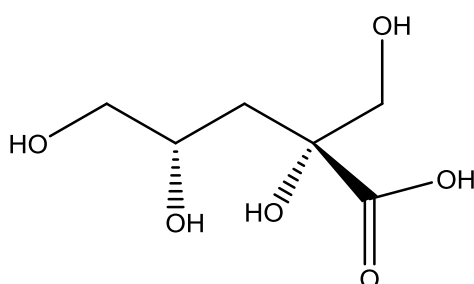


Figure 5: Molecular structure of isosaccharinic acid

In strongly alkaline environments the accessible reducing end groups of cellulose may be oxidized to carboxylic acids (Sjöström 1981). Such an oxidized end group is then transformed to an enediol via keto-enol tautomerism. In an alkaline environment the resulting 2,3 enediol is deprotonated to an enolate ion which enables β -alkoxycarbonyl elimination at the C4-carbon. The eliminated residue undergoes benzilic acid rearrangement to yield isosaccharinic acid or similar acids (Mozdyniewicz et al. 2013). The peeling reaction continues to reduce the DP of the cellulose polymer by the same mechanism until it is stopped, either by chemical or physical stopping. Chemical stopping is achieved when the reactive aldehyde terminated end group is reacted to the alkali-stable metasaccharinic acid by β -hydroxy elimination (Sjöström 1981). Physical stopping is achieved upon reaching a crystalline region of the fiber which is less prone to reaction than the amorphous parts. The over-all rate of chain shortening is dependent on the rates of the peeling versus stopping reactions (Mozdyniewicz et al., 2013). For cellulose with high DP the number of accessible reducing end groups is limited, hence only a minor number of peeling reactions can be initiated. Thus, for high DP celluloses, peeling does not have a substantial effect on DP.

Alkaline hydrolysis

Hydrolysis of the 1,4-glycosidic bond is causing a rapid decrease in DP, compared to endwise peeling, since the polymeric chain is cleaved at random positions rather than only at end groups. While cellulose is easily hydrolyzed in acidic environments it has a stronger resistance towards alkali and alkaline hydrolysis does usually not occur on a detectable scale below 140 °C (Mozdyniewicz et al. 2013). Cleavage of the chain introduces new reducing end groups which are accessible to secondary peeling, which leads to further chain shortening.

Autoxidation/Oxygen induced homolytic degradation pathways

Uptake of oxygen is accompanied by random degradation of the cellulose polymer by chain scissioning, chain cleavage at random positions. The degradation is proceeding via the formation of alkali labile oxycelluloses, carbonyl containing oxidized celluloses. However, the detailed mechanism is not clear (Knill & Kennedy 2003). Pure, neutral cellulose in air at room temperature is stable towards oxidation, but elevated temperatures and moisture or additives such as dyestuffs sensitizes cellulose towards autoxidation (Entwistle et al. 1949).

Some prerequisites for autoxidation of cellulose in an alkaline environment are (Mattor 1963):

- Strong alkali.

At least 1 M NaOH is needed to start autoxidation. A peak in reaction rate can be seen at NaOH concentrations between 6 and 8 M.

- Specific cellulose concentration

Cellulose is most susceptible to autoxidation in its pressed state, at a ratio of about 1:2 of cellulose to alkali solution. Completely dry alkali cellulose is stable to oxygen, as is low concentrations of cellulose in strong alkali solutions.

Sixta et al. have investigated the influence of air exclusion on yield loss during steeping of dissolving pulp. Typical steeping conditions, as it occurs in the viscose process is 18 wt% NaOH at 50 °C with a pulp to liquid ratio of 1:60. The authors concluded that at short steeping times, in the range of a few hours, the difference between oxygen containing and oxygen free atmospheres is negligible. Only at times of ten hours or more a notable difference in yield loss could be seen between the samples steeped in oxygen free and oxygen containing atmospheres, respectively.

2.4 Characterization of textile fibers

The names of textile fibers do not imply a finite molecular structure but rather are generic terms. The naming of textile fibers is a question of legislation rather than chemistry. In the European Union the European commission works close with *the International Bureau for Standardization of Man-made Fibers, BISFA*. BISFA establishes the terminology of man-made fibers, provides technical rules for fibers and yarns and establishes internationally agreed procedures and test methods. The rules of BISFA are mandatory for all members of the association (BISFA 2014). Elastane can be used as an example. According to BISFA rules elastane is a: "Fibre composed of at least 85 % by mass of a segmented polyurethane and which, if stretched to three times its unstretched length, rapidly reverts substantially to the unstretched length when the tension is removed." The manufacturer hence has a great freedom

in choice of what monomers to use to build the polymer but the final products can still legally be called elastane without further specification.

To be able to qualitatively discriminate between textile fibers knowledge is needed on their distinguishing attributes, which is commonly the polymer linkage or the functional groups attached to the polymer backbone. Examples of these are the ester linkage in polyester, the amide linkage in polyamide and the nitrile group in acrylic. A summary of the distinguishing attributes for some common textile fibers is given in Table 2.

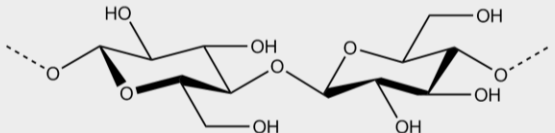
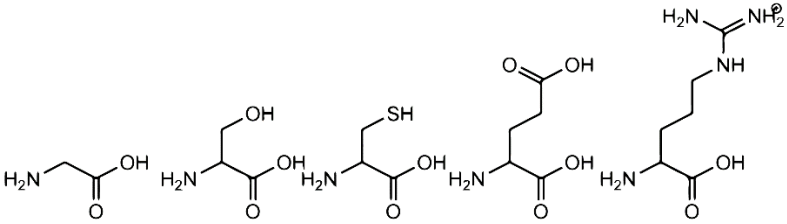
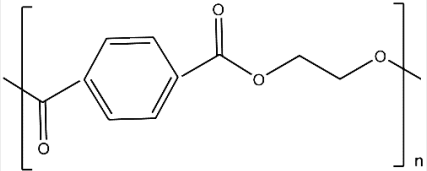
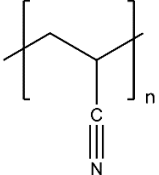
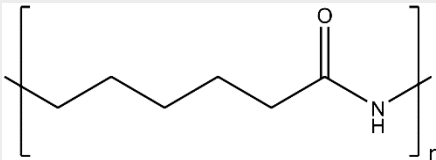
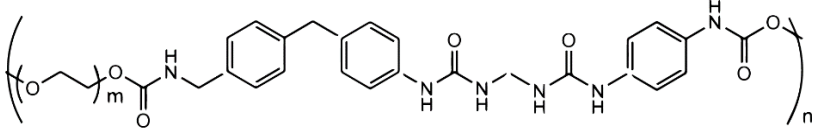
| Fiber | BISFA description | Example of molecular structure of repeating unit | Distinguishing attribute |
|------------------|--|---|---|
| Cotton | None, natural fiber |  | <ul style="list-style-type: none"> Alcohols, primary and secondary O-glycosidic bond |
| Wool | None, natural fiber Wool is built up from amino acids and the composition varies. |  | <p>Including but not restricted to:</p> <ul style="list-style-type: none"> Alcohol Carboxylic acid Thiol Amide Guanidino group |
| Polyester | Fibre composed of linear macromolecules having in the chain at least 85 % by mass of an ester of a diol and terephthalic acid |  | <ul style="list-style-type: none"> Ester Benzene ring |
| Acrylic | Fibre composed of linear macromolecules having in the chain at least 85 % by mass of acrylonitrile repeating units. |  | <ul style="list-style-type: none"> Nitrile |
| Polyamide | Fibre composed of linear macromolecules having in the chain recurring amide linkages, at least 85 % of which are joined to aliphatic cycloaliphatic units |  | <ul style="list-style-type: none"> Amide |
| Elastane | Fibre composed of at least 85 % by mass of a segmented polyurethane and which, if stretched to three times its unstretched length, rapidly reverts substantially to the unstretched length when the tension is removed |  | <ul style="list-style-type: none"> Urethane Benzene ring (commonly but not mandatory) |

Table 2: Compilation of common textile fibers, their BISFA description, molecular structure of repeating unit and distinguishing attribute of each fiber.

3. Textile recycling

3.1 Current status of textile recycling

The current status of textile recycling and reuse in the world has been surveyed by J. Lu and coworkers (Lu & Hamouda 2014). Their data show that 10 % of the fiber waste in China, 12-13 % in Japan and 15 % of the fiber waste in the US is reused or recycled. In Europe, Germany is one of the pioneer countries where as much as 66 % of the projected textile fiber turnover is collected and recycled or reused according to a report from bvse, the German federal organization for secondary raw materials and disposals (Bvse 2008).

The pathways for textile recycling is summarized schematically in Figure 6. The two areas of textile recycling which are in focus of this thesis work are highlighted, namely sorting of textiles and chemical recycling.

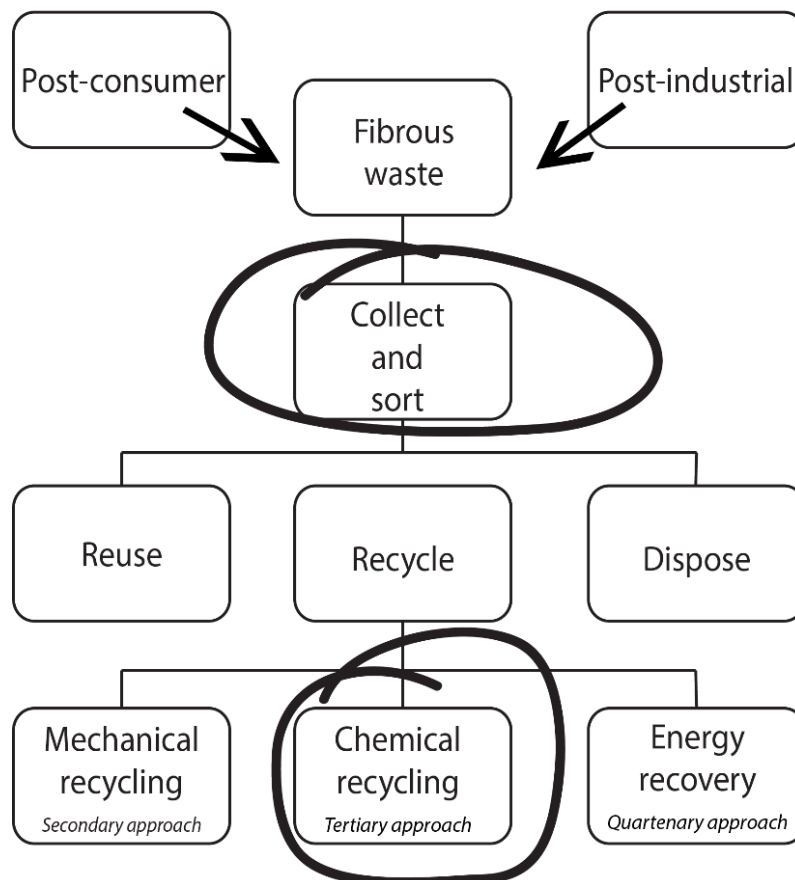


Figure 6: Pathways for fibrous waste

The sorting of textile waste today is mainly done manually, both in developing and developed countries. There are some solutions proposed for automating the process such as tagging all manufactured clothes with an radio frequency identification (RFID) that specifies the fiber composition of the item, or using spectroscopic techniques such as near-infrared spectroscopy (NIR) that can distinguish between textile fibers and blends based on their chemical composition (Palm et al. 2014).

Recycling technologies are commonly divided into four different approaches based on the raw material used and the products obtained at the end of the process (Karayannidis & Achilias 2007). *The primary approach* is using industrial scraps to produce products of equal value as the waste. Almost all textiles that are sold as “made from recycled fibers” today are produced from industrial scraps according to the primary approach. *The secondary approach* is mechanical processing of post-consumer products. Mechanical recycling is possible for thermoplastic polymers that can be melted and re-extruded, such as polyester and nylon. To obtain a polymer of equal value as the raw waste material the contamination of waste has to be very low. This approach is used for example in making fleece clothing from recycled PET-bottles (Vadicherla & Saravanan 2014). Mechanical recycling also applies for cotton and wool which may be combed and spun into new threads. *The tertiary approach* is chemical recycling in which the polymers are fully or partly depolymerized. The monomers or oligomers can then be used as feedstock to produce new polymers. The Japanese company Teijin is one of the pioneers in this field and has developed a closed-loop system for recycling of polyester textile fibers by depolymerization to dimethyl terephthalate and subsequent re-polymerization to textile fibers (Teijin 2015) *The quarternary approach* is energy recovery which aims to recover the energy content of the fiber. Currently incineration and utilization of the heat produced is the most effective method (Karayannidis & Achilias 2007).

3.2 Challenges in textile recycling

Textiles are complex materials. First of all many textiles are composed of fiber blends to obtain the desired properties. If the textiles are colored, there are dyes strongly attached to the fibers. The textiles may also be treated with certain chemicals to induce properties such as fire proofing or water resistance. The manufacturing process of textiles is chemical intense and residues from processes might stay in the textile. The thread used for seams is often of a different fiber type than the fabric in general. Buttons, zippers and prints introduce yet other materials to the product.

During the use phase the textile fibers are degraded. The most evident degradation of textiles comes from mechanical stress during use and laundering. However, the fibers are also subjected to other degrading processes. Physical aging cause an increase in ordering of non-crystalline polymer chains, which decreases the molecular mobility of the polymer. This causes a stiffer and more brittle material, with larger tendencies to permanently deform or break upon stress (Bresee 1986). Chemical aging cause changes in molecular bonds and includes thermal degradation, hydrolysis and various oxidation reactions. Chemical aging generally cause chain scissioning of the polymer chain, which causes a rapid decrease of the degree of polymerization. The net decrease in molecular weight causes a decrease in tensile strength and elasticity of the fiber and also may affect its chemical reactivity by introducing more sites of reaction (Hawkins 1984).

To produce new high value textiles from textile waste there is a need for development of automatic technology for sorting of textile wastes and for separation of fiber blends into pure fiber fractions. Degraded textile fibers needs to be upgraded to high-quality fibers. The specific methods chosen to accomplish recycling of textile materials into high value textiles has to be optimized to each fiber type.

3.3 Textile analysis

To develop the textile analysis area, methods for on-line as well as off-line characterization of textiles are needed. As was explained in Section 3.1 sorting of textile waste is currently done manually. To scale up textile recycling, automatic on-line characterization techniques are needed. To be useful as an analytical technique for automatic sorting of textile materials some characteristics have to be met:

- Ability to qualitatively distinguish between the fibers
- Ability to quantitatively analyze fiber blends
- High throughput

Spectroscopic techniques are considered interesting for automating sorting purposes. Spectroscopy is based on interaction of electromagnetic radiation with materials, a process that induces certain energetic transitions which can be detected and used for sample identification. There are several spectroscopic techniques that has a limited or no sample preparation and the possibility to provide rapid and accurate analysis.

Thorough analysis of textile materials may be performed off-line. Thorough characterization of textiles is of importance to elucidate molecular structures of fibers and to quantify the fiber content in fiber blends.

In this work infrared (IR) spectroscopy, Raman spectroscopy and solid state nuclear magnetic resonance (solid-state NMR) spectroscopy were chosen for further investigation. The aim was to build a spectral library of common textile fibers and to deduce their respective ability to be used for qualitative analysis of textile fibers.

Vibrational spectroscopy techniques such as Near-infrared (NIR), IR and Raman are already used on-line in the industry to for example monitor reactions and determine moisture content (Bakeev 2004) (Chaves et al. 2014). Solid-state NMR spectroscopy on the other hand is not a suitable on-line technique due to the setup of the instrument, the need for sample preparation and the time frame for analysis. Solid-state NMR spectroscopy is interesting for textile recycling purposes due to its ability to precisely resolve molecular structures. Hence, the technique may be used to build a textile fiber spectral library which could be used as a reference for other analytical techniques.

3.4 Chemical separation

Polycotton blends are some of the most common fiber blends and are used both in apparel and home textiles such as curtains and bed sheets (Hatch 1993). In the service textile area, comprising for example bed sheets in hotels and hospitals, polycotton blends are dominating. The large volumes of blended textiles of this kind motivates a deeper study on feasible methods to separate the used fibers

into pure fractions in order to enable subsequent recycling. In this study, an alkaline hydrolysis of polyester aided by a phase transfer catalyst was the method chosen. The following section will provide a background to this choice.

Separation of cotton and polyester can be done with several approaches and methods, giving a range of final products. A schematic survey of the different separation methods are presented in Figure 7.

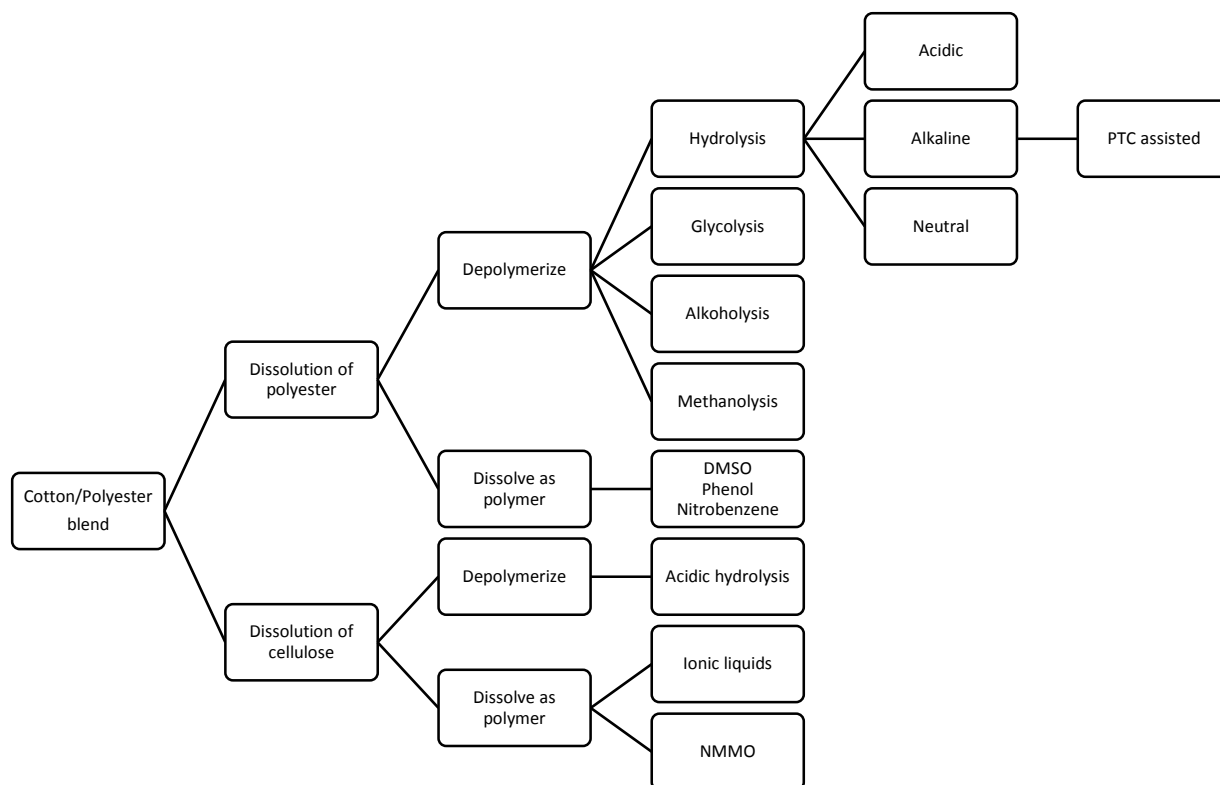


Figure 7: Schematic of the different separation methods possible for polycotton blends.

Recent articles on the subject mainly uses the approach of dissolving the cellulosic fiber in order to separate the polycotton blends (Jeihanipour et al. 2010, Negulescu et al. 1998, De Silva et al. 2014, Ouchi et al. 2009). Cellulose is hard to dissolve, hence specific and expensive solvents such as NMMO or ionic liquids are used. Dissolved cellulose chains can be processed into regenerated cellulose fibers such as viscose and lyocell. Depolymerization of cellulose, on the other hand, gives glucose monomers which cannot be re-polymerized into cellulose polymers. Hence, new cellulosic fibers cannot be made using this approach but the glucose can be used for other purposes such as fermentation into biofuels (Jeihanipour et al. 2010).

Dissolution of polyester in organic solvents have been conducted by Serad (Serad 1994) using a sulfone solvent and Everhart and coworkers (Everhart et al. 1998) using phthalates. Polyester has a low solubility in common organic solvents, hence specific solvents are needed, just as for cellulose. Dissolved polymeric chains can be respun into polyester fibers, however, there are issues with impurities such as dyestuffs. Depolymerization of polyester yields monomers which can be purified and re-polymerized. There are a number of routes to depolymerize polyester including hydrolysis, glycolysis, alcoholysis and methanolysis, which are visualized in Figure 7. The reaction products vary with depolymerization route and polyester type. Considering PET, which is the most common type of

polyester fiber, hydrolysis is the method of choice to produce the monomers currently most used as feedstock to produce virgin PET, terephthalic acid (TPA) and ethylene glycol (EG) (Karayannidis & Achilias 2007).

Hydrolysis of PET can be carried out under acidic, alkaline or neutral reaction conditions. In the context of separation of a polycotton textile for recycling purposes, neither acidic nor neutral conditions is feasible since an acidic environment would depolymerize the cotton fibers and neutral conditions requires high temperatures and pressures, which would degrade the cotton fibers severely. Alkaline hydrolysis, however, is suitable since cotton has high resistance to alkaline conditions at moderate temperatures, see Table 1.

Normally, alkaline hydrolysis of PET is a harsh and energy demanding process involving strong alkalis, temperatures of above 200 °C and reaction times of several hours (Achilias & Karayannidis 2004). Such a treatment would cause severe degradation of the cotton residue. To accomplish heterogeneous hydrolysis under milder circumstances phase transfer catalysts (PTC) can be used. PTCs are molecules which facilitate the transport of reagents between two immiscible phases, in this case the aqueous NaOH-solution and the hydrophobic, solid PET. There are several classes of PTCs, such as quaternary ammonium and phosphonium salts, crown ethers and cryptands, of these the quaternary ammonium salts are the cheapest and most widely used (Selvi et al. 2012). Depending on the nature of the ligands the hydrophobic/hydrophilic properties of the PTC can be tuned. For alkaline hydrolysis of PET it has been shown that the PTC has to have a high lipophilicity to be active but still be small enough to not induce steric hindrance (Kosmidis et al. 2001). The proposed mechanism for the alkaline hydrolysis is a phase transfer of the hydroxide anion from the aqueous phase to the polymer surface facilitated by the cationic part of the PTC. In this way the ester linkages of the polymer strands on the surface of PET can easily be attacked by the OH^- which causes depolymerization. The terephthalate anion produced in the reaction returns to the aqueous phase where its disodium salt is formed with Na^+ while the other reaction product ethylene glycol remains in the organic phase. The PTC returns to the aqueous phase from where it could hopefully be recovered (López-Fonseca et al. 2009). By acidifying the reaction solution TPA-Na_2 is converted to TPA and precipitated.

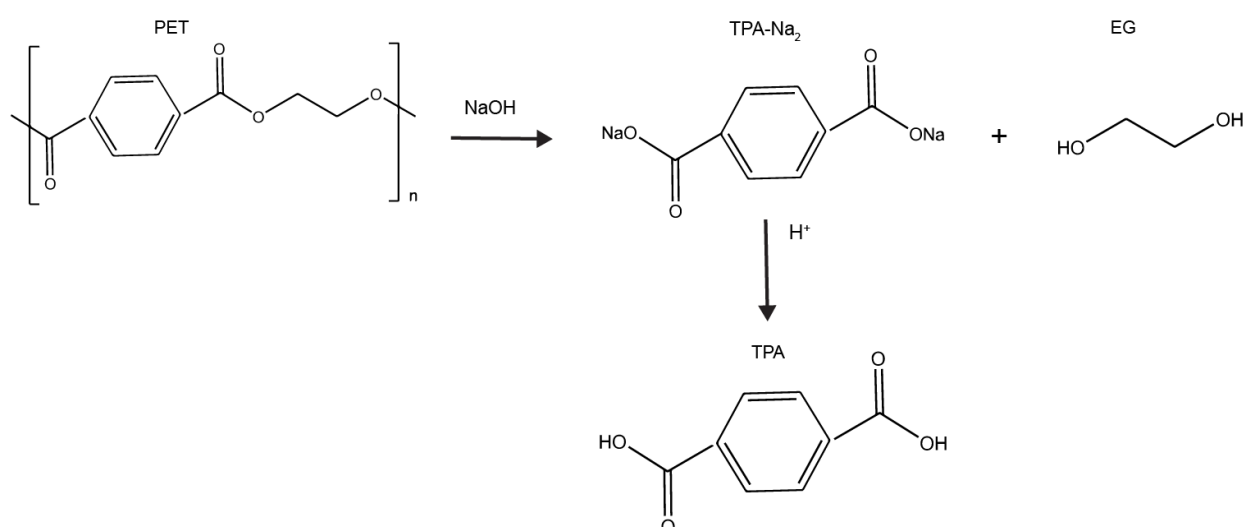


Figure 8: Alkaline hydrolysis of PET

The phase transfer catalyst (PTC) used in this study is benzyltributyl ammonium chloride (BTBCl), the molecular structure can be seen in Figure 9. It fulfills the requirements of having a high lipophilicity, while still being small enough to not induce steric hindrance. Furthermore, BTBCl has no reported aquatic toxicity nor is it persistent, bioaccumulative or toxic (Sigma-Aldrich 2013).

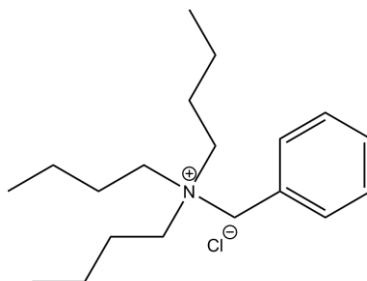


Figure 9: Molecular structure of BTBCl

Generation of new textiles from the separated products

The products from alkaline hydrolysis of polycotton textiles are terephthalic acid (TPA), ethylene glycol (EG) and cotton. TPA is in the form of a solid precipitate while EG is present as an organic component in the aqueous phase and needs to be extracted in order to be recovered. To use the obtained TPA and EG as feedstock in the polymerization of new PET, purification is needed. Contaminants that affect the polymerization include acids and moisture; which both catalyze the hydrolysis of the ester bonds, dyes; which gives unwanted color, and metal ions; which promote transesterification and polycondensation reactions, leading to chemical heterogeneity of the recycled PET (Park & Kim 2014).

The cotton residue may be recycled into man-made cellulosic fibers, with dissolution as the first step. In order to facilitate dissolution, DP of cotton is ideally to be 400-600. The crystalline structure of cellulose may have an influence on the dissolution mechanism, due to differences in thermodynamical stability. Literature studies performed in the present work, however, could not find any published articles on the matter. However, since cellulose II is more thermodynamically stable than cellulose I, dissolution of this polymorph may be harder. Hence it may be beneficial to obtain the cotton residue as cellulose I rather than cellulose II.

4. Analytical techniques

For this study three analytical techniques were chosen, solid-state NMR, IR and Raman spectroscopy. Solid-state NMR spectroscopy was used to build a spectral library of textile fibers since the technique can provide detailed structural information on samples. IR and Raman spectroscopy was evaluated on their ability to be used as on-line sorting techniques. The basis upon why they were chosen can be read in section 3.3.

In this chapter the general basics on these analytical techniques will be discussed, as well as their specific application in textile characterization.

Spectroscopic techniques

Spectroscopic techniques all rest on the foundation that, under certain conditions, molecules absorb or emit energy. Subjecting a material to electromagnetic radiation of the right wavelength will induce certain energetic transitions in the material. Different spectroscopic techniques rely on different kinds of transitions as is schematically presented in Figure 10. For IR and Raman spectroscopy the radiation is in the infrared range and causes vibrational and rotational excitations. For NMR spectroscopy the transitions are nuclear spin transitions, brought about by low energy radio frequency waves.

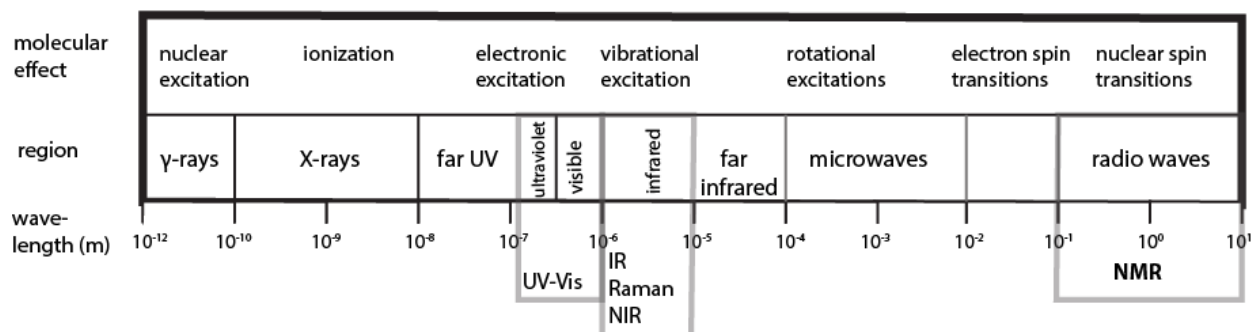


Figure 10: Schematic representation of the frequency ranges where spectroscopic techniques operate.

4.1 Vibrational spectroscopy theory

Vibrational spectroscopy includes several techniques where mid-infrared (IR), near-infrared (NIR) and Raman spectroscopy are the most important. These spectroscopic techniques are used to study a wide range of parameters, from simple identification tests to in-depth information on molecular structure, dynamics and environment. All vibrational techniques are based on the interaction of matter with electromagnetic waves in the infrared region, where absorption of light causes excitation of the vibrational and rotational states of the molecule. The frequencies at which the molecule absorbs light

is specific for each molecule and depends on the constituting atoms, their geometrical arrangements and the strength of the bonds (Larkin 2011).

4.1.1 Instrumentation

There are two principal kinds of spectrometers for vibrational spectroscopy, dispersive spectrometers and interferometric spectrometers. In a dispersive spectrometer the light falling on the detector is monochromatic; hence the transmittance of one wavelength at a time is analyzed. This results in a rather slow scanning process since a broad spectrum of wavelengths is to be scanned through. The use of interferometric spectrometers allows all wavelengths to be measured at the same time, hence analysis time is shortened. An interferometer produces a unique kind of signal, an interferogram, which has all the infrared frequencies encoded into it. This is done by splitting and recombining the beam in a way that causes both constructive and destructive interferences. Mathematical manipulation by Fourier transformation of the signal then gives the regular absorption versus wavelength spectrum (Pavia et al. 2009).

4.1.2 IR

Mid-infrared spectroscopy, or IR spectroscopy as it is often referred to, operates in the $4000\text{--}400\text{ cm}^{-1}$ frequency region. The technique measures the absorbance of light of a sample and the spectrum is a plot of the transmittance of light versus wavelength. The sample absorbs photons of frequencies that match its natural vibrational frequencies; the resulting energy gain serves to increase the amplitude of the vibration. To be able to interact with the infrared light and hence be IR active the vibrational motion of a bond has to generate a dipole moment. When frequencies are matched, see Figure 11, the electric dipole is changing direction at the same frequency as the sinusoidally changing electromagnetic field of the incoming radiation, these can couple and energy is transferred (Pavia et al. 2009).

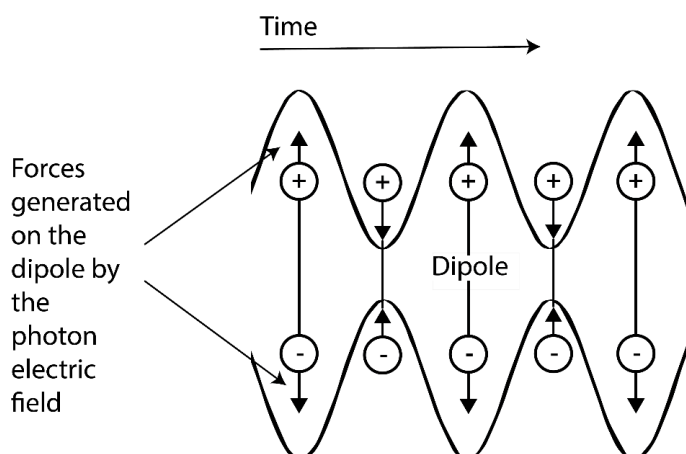


Figure 11: Match in frequencies between the oscillations of the dipole and the oscillating electric field generated by the photon.

The infrared light is produced by a hot wire made from a material that emits radiation in the desired frequency region. In a dispersive instrument the light is passed through a monochromator whose grating is rotated to let light of one wavelength at a time reach the sample. In an interferometric spectrometer the light is passed through a beam splitter to produce an interferogram which is directed at the sample. The transmittance of light through the sample is sensed by the detector, the signal amplified at the resulting spectrum produced (Pavia et al. 2009).

Attenuated total reflectance

The main obstacles in IR spectroscopy of solids and liquids are the need for sample preparation and the subsequent spectral reproducibility issues (Piketech 2011). The use of attenuated total reflectance (ATR) eliminates the need for sample preparation and hence gives faster sampling with high reproducibility. The key feature of ATR is the internal reflection element; a crystalline material of high refractive index in which the infrared beam is internally reflected. The sample is kept in tight contact with the crystal in order to let the evanescent wave formed at the interface penetrate into the sample. The depth of penetration is dependent on the angle and wavelength of the incident light, and the refractive index of the crystal and the sample, respectively. Normally the depth of penetration is between 0.5-5 μm . (Piketech 2011). In the regions of the spectrum where there is absorption of light the evanescent wave will be altered generating an energy difference of the reflected IR beam which is read by the detector. A schematic representation of the ATR setup is shown in Figure 12.

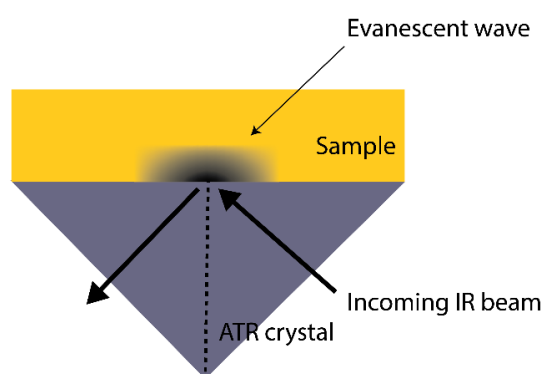


Figure 12: Schematic representation of a Single Reflection ATR

4.1.3 Raman spectroscopy

Raman spectroscopy is based on scattering of photons, rather than absorption. The origin of light scattering is interactions between incoming radiation and oscillating dipoles induced in the sample by the electromagnetic fields of the same incoming radiation. These interactions are visualized in Figure 13. To be Raman active the molecule has to be polarizable, i.e. the electron cloud has to be easily deformed by the incoming radiation to produce dipoles (Pavia et al. 2009).

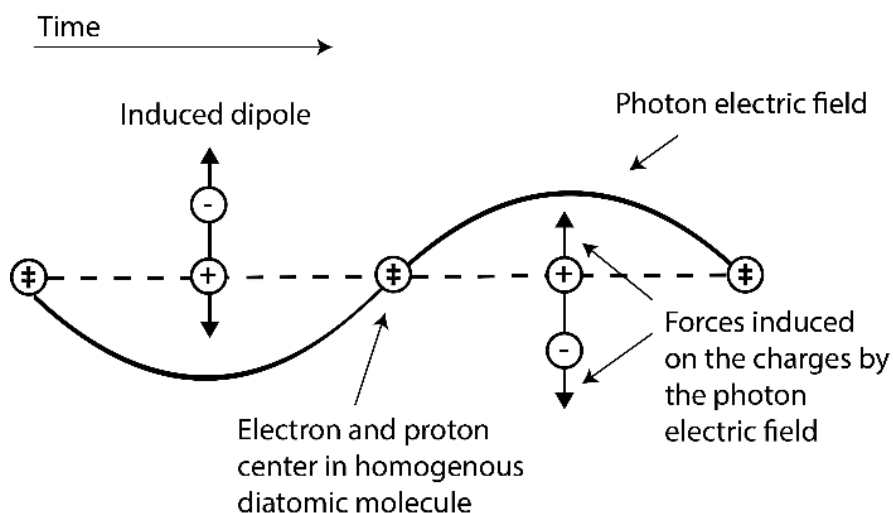


Figure 13: Induced dipole moment in a homonuclear diatomic molecule originating from the photon electric field

The most prominent type of scattered light is the elastically scattered Rayleigh scattering. However, what is detected in Raman spectroscopy is the Raman scattering whose intensity is at least three orders of magnitude lower than the intensity of Rayleigh scattering. Raman scattering is an inelastic type of scattering and comes in two types, Stokes and anti-Stokes. In Stokes Raman scattering the absorbing molecules are in the ground state whereas in anti-Stokes the absorbing molecules are in a vibrationally excited state. At thermal equilibrium the relative intensity of the lines are described by the Boltzmann distribution, hence at ambient temperatures, where more molecules are in the ground state, the Stokes Raman scattering is of higher intensity (Pavia et al. 2009).

The light source in Raman spectroscopy is a laser producing monochromatic light which is used to irradiate the sample. In a dispersive spectrometer the light which is scattered by the sample is entering a monochromator which only lets light of a certain wavelength pass and reach the detector. By rotating the grating in the monochromator different wavelengths are allowed to pass. Rayleigh scattering, being of the same wavelength as the incident light is filtered out and not allowed to reach the detector. In an interferometric spectrometer the scattered light is sent through a beam splitter rather than a monochromator, allowing for faster analyses since all wavelengths can be detected at the same time (Pavia et al. 2009).

One of the central problems in Raman spectroscopy is fluorescence. If the intensity of the incoming photons is close to the transition energy between two electronic states of the molecule the light may be absorbed rather than scattered. Fluorescence is the emission of a photon of longer wavelengths than the absorbed one and the phenomenon produces very broad peaks that are interfering with the spectrum. The effect reaches from modest changes of the baseline to totally hiding the peaks from Raman scattering. (Yang & Akkus 2013)

There are some different strategies to address the problem of fluorescence. The most common and efficient way is to utilize lasers of longer wavelengths, red light of 785 nm has been the standard but now there are working systems with light of even longer wavelengths, in the near infra-red region at 1064 nm. The problem with using lower energy lasers is that the intensity of the Raman scattering decreases. Another strategy is to use photobleaching, in which the sample is subjected to prolonged exposure of laser light. This process destructs the fluorophores responsible for fluorescence but is time consuming and may damage the sample (Yang & Akkus 2013).

4.1.4 Textile analysis by vibrational spectroscopy techniques

Vibrational spectroscopy techniques are powerful tools for distinguishing between similar materials such as textiles since each molecular vibration ends up on a specific wavelength. The so called "fingerprint region" below 1500 cm^{-1} in IR and Raman spectroscopy contains a massive range of absorption bands which is specific for each molecule.

There are numerous publications on the use of Raman spectroscopy for textile characterization. In forensic sciences it is a common technique to identify fibers (Miller & Bartick 2001) (Cho 2007) and to discriminate between dyes in colored fibers (Jochem & Lehnert 2002)(Buzzini & Massonnet 2013). It is also used in archeology to date ancient textiles (Edwards & Wyeth 2005). IR spectroscopy have been suggested for classification of textiles aided by chemometric techniques (Pumure et al. 2015) and for polycotton blend analysis (Pancholi et al. 1988).

In principle both Raman and IR spectroscopy could be used for on-line characterization of textiles. They offer analysis on the timescale of seconds to minutes, no sample preparation is needed and spectrophotometers can even be made into portable units (Murray 2012). The timescale for analysis could be shortened if each fiber type contained a marker, a non-overlapping peak specific for each textile fiber.

While Raman spectra often has fewer and less overlapping bands than the respective IR spectra of the same polymer (Cho 2007) the technique suffers from fluorescence. Cotton is highly fluorescing at lower wavelengths of the incoming laser and excitement in the near-infrared region at 1064 nm is generally needed to reduce fluorescence and obtain acceptable spectra. Further, many dyes are organic and comprises aromatic rings whose vibrations are not detected by IR spectroscopy but produces either fluorescence or additional peaks in Raman spectrum (Jochem & Lehnert 2002).

An interesting vibrational spectroscopy technique not studied in this work is near-infrared spectroscopy (NIR). NIR is the vibrational technique that is most commonly utilized for on-line analysis and it is used in a range of applications including monitoring fermentation reactions, moisture determination in pharmaceuticals and particle size determination of nanoparticles (Bakeev 2004). NIR is also used within the textile environment; textiles4textiles which is an automated textile sorting installation, not yet commercially available, uses NIR as the detection technique and claims a scanning rate of one second per textile garment (Palm et al. 2014).

4.2 NMR theory

NMR spectroscopy is a spectroscopic technique where the energy transition in question is the nuclear spin transition. To be detected with NMR a nucleus has to possess a magnetic moment (μ). The magnetic moment is related to the spin quantum number (I) according to Equation 1: (Keeler 2010)

$$\mu = \gamma I \quad (1)$$

where γ is the gyromagnetic ratio, a constant specific for each kind of nucleus. All nuclei possess a spin quantum number and nuclei that have an odd number of either or both protons and neutrons have a non-zero spin quantum number and hence possess a magnetic moment. (Pavia et al. 2009) Nuclei with spin quantum number $\frac{1}{2}$ are the most frequently studied in NMR since the tensor of these nuclei are spherical in shape and have convenient magnetic properties. Spin $\frac{1}{2}$ nuclei include the most abundant isotopes of hydrogen and phosphorus; ^1H and ^{31}P , as well as the less abundant isotopes of carbon and nitrogen; ^{13}C and ^{15}N (Levitt 2008).

In the absence of an external magnetic field the quantum states of the spins all have the same degenerate energy and the magnetic moments are randomly oriented, see Figure 14a. When placed in a strong external magnetic field this degeneracy is removed. For the simplest nuclei, spin $\frac{1}{2}$, there are two energy levels which represent alignment with or against the applied field (Jacobsen 2007). There will always be a preference for the energetically lower case, hence a higher population of spins will be directed with the magnetic field and the net magnetization of the sample will be aligned with the external magnetic field at equilibrium, as seen in Figure 14b.

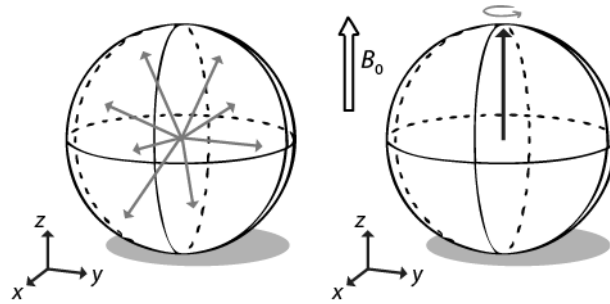


Figure 14: Vector model showing a) the magnetic moments randomly oriented in the absence of an external field and b) net magnetization directed with the external magnetic field, precessing around the z-axis. (Idström 2015)

In NMR the external magnetic field is denoted B_0 and directed in the z-direction. The net magnetization vectors of the magnetic moments will rotate about the z-axis at a constant rate, a motion called precession. The frequency of the precession is called Larmor frequency (ν_0) and is dependent on the gyromagnetic ratio and the strength of the field as shown in Equation 2: (Keeler 2010)

$$\nu_0 = \frac{\gamma B_0}{2\pi} \quad (2)$$

The NMR-signal is measured in a selected direction of the xy-plane. To tip the net magnetization vector away from the z-direction short radio-frequency (RF) pulses are used. The RF pulse produces a second oscillating magnetic field, B_1 , which is perpendicular to the static magnetic field, B_0 . If the frequency of the oscillating field matches the Larmor frequency of the studied nucleus a force is applied on the net magnetization vector, tipping it away from the z-axis. The net magnetization vector is still precessing around the z-axis, but now it also has a direction in the xy-plane. As soon as the applied force from the RF-pulse is removed the magnetization returns to its equilibrium, alignment with the z-axis. This is done while still precessing around the z-axis, forming the spiraling movement seen in Figure 15 (Keeler 2010).

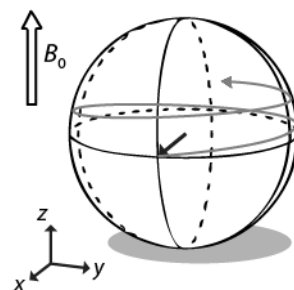


Figure 15: Magnetic moment precessing round z-axis back to equilibrium (Idström 2015)

The moving, decaying xy-component of the magnetization vector is inducing an oscillating voltage in detector coils situated along one or two directions in the xy-plane. This signal is called a Free Induction Decay (FID) and applying a Fourier transform on the FID gives the NMR spectrum (Keeler 2010). The process is visualized in Figure 16.

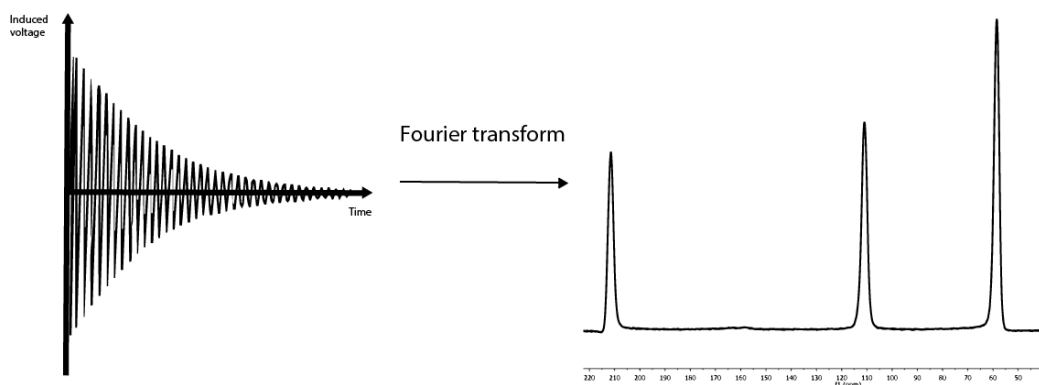


Figure 16: The free induction decay signal is Fourier transformed into a NMR spectrum

In an NMR spectrum the position of the peaks is dependent on the Larmor frequency of the spin that give rise to the peak. However, the positions of the peaks are not reported with their absolute frequencies since the Larmor frequency is dependent on the strength of the magnetic field, see equation 2. To facilitate accurate comparisons between absorption frequencies obtained at spectrometers of different magnetic strengths the chemical shift scale with the unit ppm is used. The conversion between absolute frequencies and ppm is mathematically expressed as

$$\delta(\text{ppm}) = 10^6 * \frac{\nu - \nu_{ref}}{\nu_{ref}} \quad (3)$$

where ν is the frequency of the NMR-line in question and ν_{ref} is the frequency of the line of the reference compound. The position of the line of the reference compound is used to define zero on the chemical shift scale. For ^1H and ^{13}C NMR the reference compound is agreed to be TMS (Keeler 2010).

4.2.1 Solid state NMR

To understand the difference, the possibilities and difficulties with solid-state NMR compared to solution state NMR, knowledge is needed on the nature of the solid state and the various factors affecting an NMR spectrum. The most evident factor that influences solid-state NMR is the anisotropic effects which will be explained in more detail in the coming passage.

The energy of a spin ensemble

The total energy of an ensemble of spins E_{NMR} , is comprised of several terms, where some refer to interaction between the spins and the applied forces and some to internal interactions between the spins. This is true both for the solid and the liquid state (Apperley et al. 2012).

$$E_{NMR} = E_Z + E_{RF} + E_S + E_J + E_D \quad (4)$$

The Zeeman energy (E_Z) is the potential energy possessed by a magnetized body in an external magnetic field. In NMR this is generally the biggest contributor to the energy of the spins and for an individual spin (ignoring shielding) it is expressed as:

$$E_Z = \frac{\gamma_j}{2\pi} \hbar m_j B_0 \quad (5)$$

where \hbar is Planck's constant, γ_j is the gyromagnetic ratio of the nucleus concerned and m_j is the spin component quantum number of nucleus j .

E_{RF} is the force from the radio frequency pulse which perturbs the B_0 magnetic field and makes the spins change the direction of their magnetic vector.

The internal interactions are the shielding (E_S), the indirect coupling (E_J) and the dipolar coupling (E_D). For systems that are paramagnetic or quadrupolar, i.e. has a nuclei of spin quantum number $> \frac{1}{2}$, terms according for these effects has to be included (Apperley et al. 2012).

Anisotropic effects

All the internal interactions in NMR are tensor properties, they are direction dependent. In liquids the rapid tumbling of molecules averages out any directional dependency but the relative lack of molecular motion in solid matter makes the anisotropic effects come into play.

The shielding electron cloud (E_S) around a given nucleus is generally not spherically distributed but are either slightly elongated or contracted along the axis of symmetry. This gives rise to the tensor property called chemical shift anisotropy. Depending on the angle (θ) between the local symmetry axis and the B_0 field the magnitude of shielding, and hence the Larmor frequency of the nucleus, will vary, causing broad and asymmetric peaks.

The indirect coupling (E_J), often referred to as J-coupling, is also a tensor property. However, the anisotropic contribution from this term is generally small and hence neglected.

The dipolar coupling (E_D) between spins is a magnetic interaction that is dependent on the strength of the individual magnetic moments and their distance from each other. In a polycrystalline sample there is a huge variety of internuclear distances and orientations causing extensive line broadening. The coupling constants are commonly in the range of 1-30 kHz (Apperley et al. 2012).

4.2.2 Pulse sequences

Pulse sequences are series of RF-pulses and delays that are applied to the spins of the sample in order to manipulate the magnetization in a chosen way. In solid-state NMR the Cross-Polarization/Magic Angle Spinning (CP/MAS) pulse sequence is routinely used and it is also the pulse sequence utilized in this master thesis. The use of this pulse sequence is aiming to increase the output signal from ^{13}C nuclei by cross polarization and broadband decoupling, to reduce line broadening by magic angle spinning and to shorten the recycle delay which is also achieved by cross polarization. More details on the respective techniques are given below.

Magic angle spinning

The anisotropic effects addressed in earlier sections give rise to extensive line broadening in solid-state NMR. By using magic angle spinning (MAS) the lines can be narrowed since it removes the effects of chemical shift anisotropy and reduce the effects of heteronuclear dipolar coupling (Duer 2008). The aim is to resemble an isotropic case by rapid physical spinning of the sample that averages out the

anisotropic effects. This is achieved by rapid rotation of the sample while tilted 54.74 degrees with respect to B_0 , the direction of the external magnetic field. If the spinning is sufficiently fast, a factor 3 to 4 greater compared to the linewidth of the anisotropic effect in question, the anisotropy will be set to zero. Spinning rates of 3-30 kHz is normally sufficient to remove the chemical shift anisotropy but faster spinning rates are needed to average out homonuclear couplings or for nuclei with a large number of electrons. Too slow spinning results in a set of spinning sidebands separated by a frequency equal to the spinning rate that are equally spaced around the isotropic peak (Duer 2008).

Cross polarization

Cross polarization transfers magnetization from an abundant spin to a less abundant spin. The abundant spin is most commonly ^1H and the dilute spin any other spin $\frac{1}{2}$ nucleus. There are two main advantages with this method:

1. The recycle delay is shortened. Since the magnetization originate from ^1H rather than a more slowly relaxing nucleus the longitudinal relaxation time is substantially shortened which means that the pulse sequence can be repeated more rapidly.
2. There is a signal enhancement due to magnetization transfer from the more abundant spin. The initial magnetization of a sample is proportional to the population of a given spin and to its gyromagnetic ratio. ^1H and ^{13}C can be used as an example, where $\gamma^{1\text{H}} = 4 \gamma^{13\text{C}}$ and the theoretical increase in magnetization of ^{13}C hence is a factor 4.

Magnetization is transferred by simultaneously applying radio frequency pulses of matching strength to the different spins. The RF pulses have to be designed in a way that the Hartmann-Hahn condition, Equation 6, is fulfilled.

$$\gamma^{\text{H}} B_1^{\text{H}} = \gamma^{\text{X}} B_1^{\text{X}} \pm (n * \nu_{\text{MAS}}) \quad (6)$$

where γ^i is the gyromagnetic ratio of the spin, B_1^i is the amplitude of the RF pulse applied to the spin and ν_{MAS} is the frequency of the MAS rotation (Duer 2008).

As stated above the initial magnetization of a sample is proportional to the strength of the external magnetic field, to the population of the studied spin and to its gyromagnetic ratio. However, manipulations of the magnetization as transfer of magnetization between spins, changes the initial magnetization. Therefore, the signal intensity of the observed spin in the output spectra may no longer be proportional to the population of the spin but to the density of protons in the vicinity of the spin. This makes the use of cross polarization spectra for quantitative applications complex.

Decoupling

High-power decoupling is used to remove the effects of heteronuclear dipolar coupling. There are two types of dipolar couplings as mentioned above, direct dipolar coupling and indirect dipolar coupling. Direct dipolar coupling is causing line broadening and when observing a dilute spin, e.g. ^{13}C in the presence of an abundant spin, e.g. ^1H the heteronuclear couplings are making the already weak spectrum from ^{13}C hard to interpret. J-coupling induces peak splitting which makes the spectrum harder to interpret and distributes the intensity of a peak to a multiplet instead of a singlet. By continuously irradiating the abundant spin with a high power during acquisition of the spectrum both effects are suppressed; line broadening is decreased and the splitting is removed (Duer 2008).

4.2.3 Textile analysis by solid-state NMR spectroscopy

Solid-state NMR spectroscopy is sparsely used in textile characterization although it is a non-destructive technique with high accuracy and the ability to precisely resolve molecular structures. However, the equipment and maintenance are expensive and sample preparation and insertion in the instrument is work intensive compared to Raman and ATR-IR spectroscopy. Moreover, in order to obtain a good signal to noise ratio the experiment has to be repeated several times, giving analysis times of at least minutes but more commonly hours (Colletti & Mathias 1988).

Although sparsely used solid-state NMR spectroscopy may provide detailed information of textiles such as molecular structure, segment mobility and adsorption of water (Colletti & Mathias 1988) or characterization of surface modifications (Princi et al. 2005).

In the framework of this thesis NMR spectroscopy is being evaluated on its ability to resolve molecular structures and characterize fiber blends in order to be used as a library and a reference for other analytical techniques.

5. Materials and methods

5.1 Materials

5.1.1 Textile analysis

The textile fiber types selected for the textile analysis survey are presented in Table 3. The selection is based on the most used textile fibers in the textile industry today as well as upcoming fiber types that are claimed to have an environmental profile such as lyocell and polylactic acid (PLA). No sample preparation was done to the samples prior to analytical evaluation.

Table 3: Textile fibers surveyed in the present study

| FABRICS/THREADS COMPOSED OF A SINGLE FIBER TYPE | FABRICS/THREADS COMPOSED OF FIBER BLENDS |
|--|---|
| Cotton | Cotton/Polyester (50/50) |
| Viscose | Cotton/Elastane (92/8) |
| Lyocell | |
| Linen | |
| Polyester | |
| Elastane | |
| Polyamide (nylon) | |
| Acrylic | |
| Polylactic acid (PLA) | |
| Polypropylene | |
| Wool | |

Apart from pure fibers and two-part blends a fraction called complex blends was also analyzed. These blends are composed of shredded clothes from a textile recycling facility where they have been sorted manually. Two fractions were analyzed, shreds from jeans manually sorted as 100 % cotton and shreds from pullovers manually sorted as 100 % cotton. To obtain representative samples the shreds were defibrated in a Wiley mill (<1mm).

5.1.2 Chemical separation

The materials used in the chemical separation part are presented in Table 4.

Table 4: Materials used in the separation part of the present study

| MATERIAL | MANUFACTURER |
|--|-----------------------|
| Polycotton bedsheets 50 % polyester, 50 % cotton | Textilia |
| NaOH pellets | Fisher scientific |
| Benzyltributyl ammonium chloride | Sigma-Aldrich |
| Glass microfiber filter GF/A | Whatman GE Healthcare |

5.2 Methods

5.2.1 Analytical techniques

Attenuated Total Reflectance Fourier-Transform Infrared Spectroscopy (ATR FT-IR)

IR spectra were recorded using a PerkinElmer FT-IR spectrophotometer with the diamond ATR attachment GladiATR from Pike Technologies. Scanning was conducted from 4000-400 cm^{-1} with 16-64 repetitious scans. Resolution was 2 cm^{-1} , and interval scanning was 0,5 cm^{-1} . Measurements were conducted at 298 K in air. Spectra were displayed using the IgorPro 6.36 software and peaks were assigned with aid from KnowItAll® Informatics System 2014, a software package provided by Bio-Rad Laboratories.

Nuclear magnetic resonance spectroscopy (NMR)

Solid-state NMR experiments were performed on a Varian Inova-600 operating at 14.7 T and equipped with a 3.2 mm solid state probe. Measurements were conducted at 298 K at a MAS spinning rate of 15 kHz. A Cross-Polarization Magic-Angle Spinning (CP/MAS) pulse sequence was used on all samples. The number of acquisitions for each spectrum were 16384. Prior to analysis the textile samples were cut into small pieces, approximately 5*2 mm.

Solution-state NMR experiments were performed on a Varian Inova-400 operating at 9.4 T and equipped with a 5mm broadband probe and a sample changing robot. Measurements were performed at 298 K, shimming and tuning of the magnet was done automatically. A 90° (x) pulse was used on all samples. For proton spectra 8 acquisitions were recorded. For ^{13}C spectra 256 acquisitions were recorded under continuous irradiation on the proton channel. TPA samples were dissolved in DMSO- d_6 while filtrate samples were analyzed as water-solutions with 10 % D_2O added.

All NMR spectra were processed by MestreNova 8.1 software. First order polynomial baseline correction were used in all spectra, manual phase correction and no apodization, unless otherwise indicated.

Light microscopy

Micrographs were obtained on a Zeiss Discovery V.12 optical microscope equipped with a Linkam PE120 cooling stage. Polycotton sheet samples were objected to hydrolysis at 80 °C during light microscopy analysis in order to visually analyze the reaction.

Raman Spectroscopy

Raman spectra were recorded using an InVia Reflex Renishaw spectrometer. The 785 or 532 nm line of a diode laser were used as the excitation sources. The spectral resolution was 2 cm^{-1} . Recorded spectra were accumulated by 5 scans. Measurements were conducted at 298 K in air. Spectra were displayed using the IgorPro 6.36 software.

Intrinsic viscosity

The intrinsic viscosity of the cellulose samples was measured after dissolution in Cuen [copper(II)ethylenediamine] according to the SCAN-C 15:99 method.

Quantitative chemical analysis

Quantitative data on the composition of the polycotton bed sheets were obtained according to the European standard *Mixtures of cellulose and polyester fibres (method using sulphuric acid)* (ISO 1833 -11:2006).

5.2.2 Chemical separation

Chemical separation of polyester and cotton was performed on 50/50 % polycotton sheets. The method of choice was an alkaline hydrolysis aided by a PTC to obtain total depolymerization of polyester.

The experimental procedure was adapted from Das et al. Reaction parameters were varied according to Table 5. Prior to separation the sheets were defibrated in a Wiley mill (<1mm) to increase the contact area.

Table 5: Reaction parameters

| REACTION PARAMETER | RANGE |
|---------------------------|------------------------------------|
| CONCENTRATION NAOH | 1.5-15 wt% |
| CONCENTRATION PTC | 0.005-1 mol/mol repeating unit PET |
| TEMPERATURE | 80-90°C |
| TIME | 15-240 min |

NaOH was heated with BTBCl to the selected temperature in a shaking bath. The defibrated fabric sample was added and the mixture was allowed to react for the selected time at constant temperature. The reaction was quenched by immersing the reaction vessel in an ice bath. The products were separated into solid and liquid phases using vacuum filtration through a glass microfiber filter. The cotton residue was collected and dried in air. The aqueous phase was acidified to pH 2-3 with H₂SO₄ in order to precipitate the TPA. The precipitate was washed using vacuum filtration through a glass microfiber filter, and dried in an oven at 105°C, weighed after drying.

After separation, the cotton residue of some samples were subjected to regeneration of alkaline cellulose, for viscosity determination. The experimental procedure was adapted from Mattor.

The cotton residue was placed in an Erlenmeyer flask together with acetic acid (5 wt%) in excess. The flask was stoppered and shaken for approximately 2 minutes in order to disperse any lumps. The slurry was filtered through a glass microfiber filter, washed with distilled water until neutral, then washed with acetone, and allowed to air dry.

6. Results and discussion

6.1 Textile analysis

As stated in section 3.3, three analytical techniques were chosen for textile analysis; solid-state NMR, IR and Raman spectroscopy. In a future application, qualitative as well as quantitative analysis of the fiber composition of post-consumer textiles are desirable. However, the research described in this thesis was focused on qualitative analyses of textile fibers and blends. The quantitative capacity of each analytical technique will be briefly summarized in a literature study, see section 6.1.2. To perform rapid and adequate analyses it is preferable that each fiber type expresses a “marker”, a non-overlapping peak specific for each fiber type. Identification of textile fibers hence would be aided since the presence of a marker in a specific region of the spectrum would indicate for a certain fiber type. The hypothesis was that it would be possible to find such markers since textile fibers are chemically diverse and contain different functional groups as is summarized in Table 2.

6.1.1 Qualitative analysis of textile fibers

IR spectroscopy

ATR-IR spectroscopy was applied to all textile fibers and blends seen in Table 3. IR analysis of textile fibers shows that peaks from different fiber types overlap severely throughout the IR spectrum, with acrylic as the only exception, see Figure 17.

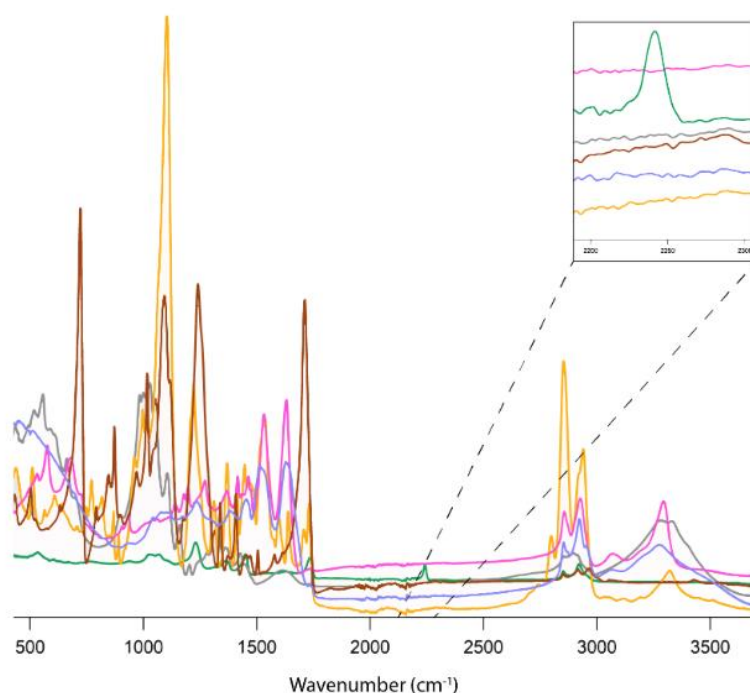


Figure 17: ATR-IR spectra pure textile fibers. Polyamide (pink trace), cotton (grey trace), elastane (orange trace), polyester (brown trace), acrylic (green trace). As is accentuated in the scale-up, acrylic is the only fiber that exhibits a marker.

Characterization on behalf of markers is hence unachievable and to identify the fiber a full spectrum has to be acquired and matched with a spectral library. Such a spectral library is provided in this thesis and can be found in Appendix 1. Future work within this area could include development of proper search algorithms.

Table 6 accentuates how different fiber types exhibit absorption bands in the same region. Acrylic is the only fiber type that shows a marker, a peak with absorbance in a distinct region of the spectrum without interference from other peaks.

Table 6: Typical IR band frequencies for common textile fibers. Knowitall, Bio-Rad Laboratories

| BAND FREQUENCY (CM⁻¹) | TYPE OF VIBRATION | FIBER TYPE |
|---|---------------------------------|-----------------------|
| 3700-3200 | O-H stretch (free and bonded) | Cellulosics |
| 3500-3200 | N-H stretch | Polyamides, elastane |
| 2930-2840 | C-H stretch | Most fibrous polymers |
| 2260-2240 | C≡N stretch (saturated nitrile) | Acrylics |
| 1740-1715 | C=O stretch (ester) | Polyesters, acrylics |
| 1670-1630 | C=O stretch (amide) | Polyamide, wool |
| 1650-1590 | N-H deform (primary amine) | Wool, polyamide |
| 1570-1515 | N-H deform (secondary amine) | Wool, polyamide |
| 1250-1150 | C-O stretch (ester) | Polyester, acrylic |
| 1100-1000 | C-O stretch (alcohols) | Cellulosics |
| 730-650 | C-H (aromatic) | Polyester |

Raman spectroscopy

Raman spectra of the textile samples have been acquired using lasers of either 532 or 785 nm as the excitation sources. Raman spectroscopy revealed to be an insufficient technique in order to qualitatively characterize textile fibers under present circumstances, due to fluorescence. As can be seen in Figure 18 several fiber types suffers from broad fluorescence peaks that cover the peaks from Raman scattering. Cotton (grey trace), wool (blue trace) and elastane (orange trace) exhibits broad fluorescence peaks. Polyester (brown trace) and polyamide (pink trace) gives acceptable spectra while the baseline of acrylic (green trace) is clearly altered by fluorescence.

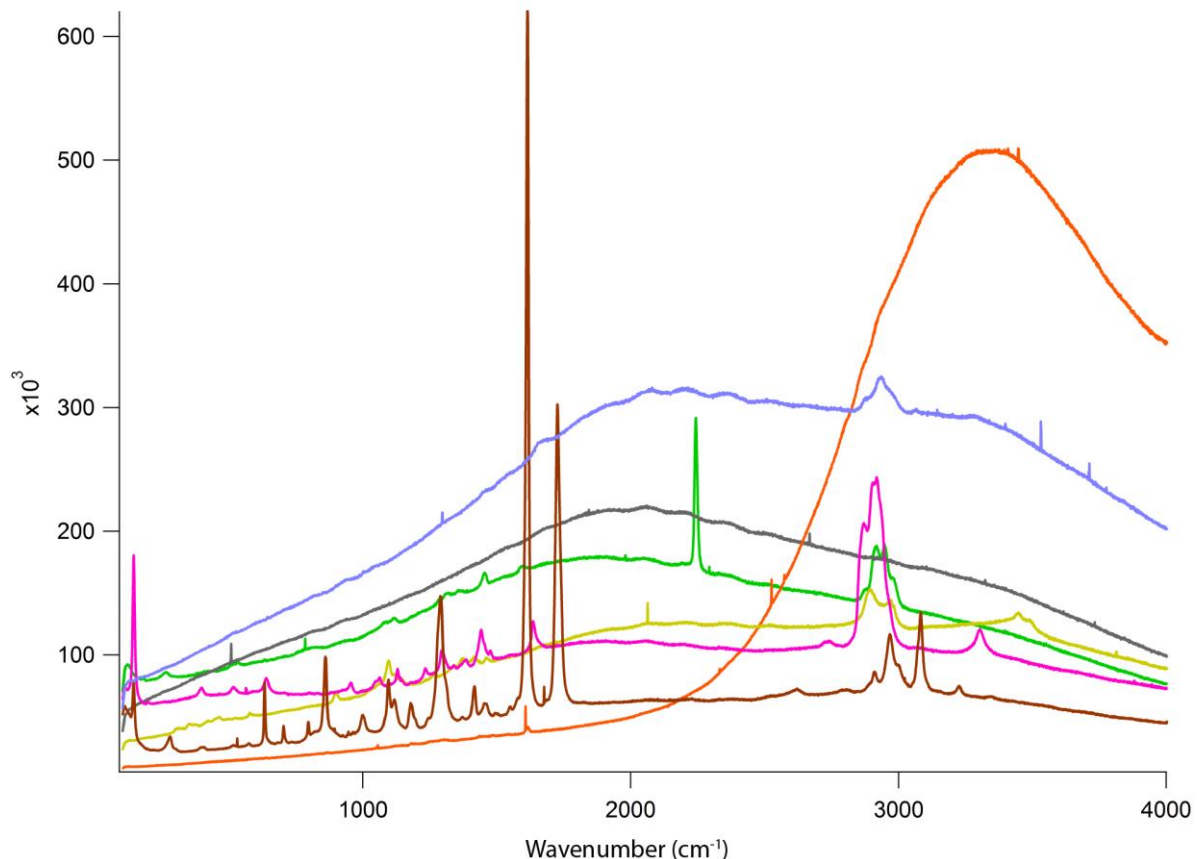


Figure 18: Raman spectra of textile fibers, excitation source 532 nm diode laser. Traces represent cotton (grey), wool (blue), elastane (orange), polyester (brown), polyamide (pink), acrylic (green).

A shift to even higher wavelengths, in the infrared region at 1064 nm could give acceptable spectra. However, since the intensity of Raman scattering decreases with lower energy of the incoming light there might be a problem in distinguishing peaks from the background. Hence, the choice was made not to proceed with Raman measurements at higher wavelengths.

Solid-state NMR spectroscopy

Solid-state NMR spectroscopy was applied to all textile fibers and blends seen in Table 3. The NMR spectral library of fibers and blends is found in Appendix 2.

NMR signals from common functional groups of textile fibers are seen at a rather narrow shift range. Amides, esters, carboxylic acids and urethanes are all found at shifts ranging from 150-185 ppm according to literature. Spectra acquired in this thesis confirms that signals from the urethane group

in elastane is found at 156-158 ppm while the ester in polyester is found at higher shifts, 163-168 ppm. These groups can hence be identified as is seen in figure 19a. Signals from carboxylic acid, the amide link from polyamide and the ester group from acrylic co-monomers are all found at shifts around 170-178 ppm and cannot be distinguished from each other, see figure 19b.

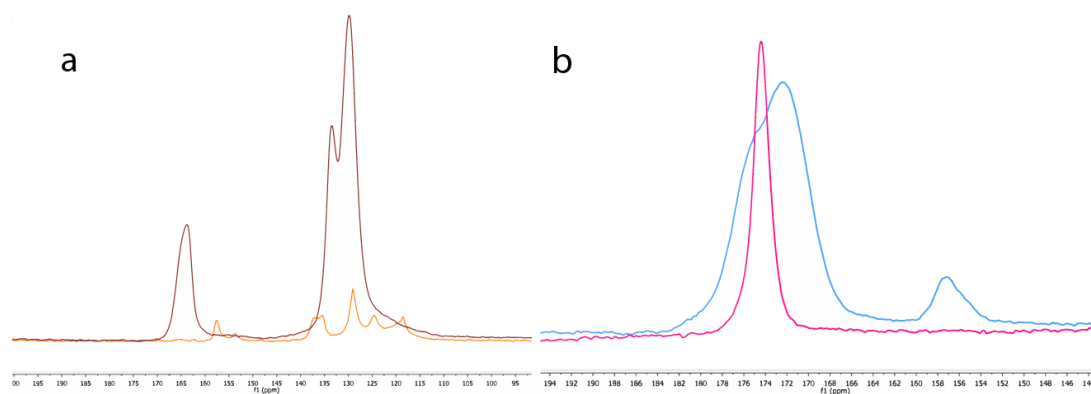


Figure 19: ^{13}C Solid-state NMR spectra of a) aromatic peak, urethane peak and ester peak for polyester (brown) and elastane (orange) and b) carboxylic acid peak and amide peak for wool (blue) and polyamide (pink). Exponential apodization of 40 Hz.

Typical ^{13}C chemical shifts for common textile fibers, from literature and present experiments are presented in Table 7.

Table 7: ^{13}C chemical shifts for common textile fibers, from literature and present experiments

| ^{13}C CHEMICAL SHIFT LITERATURE (PPM) | ^{13}C CHEMICAL SHIFT EXPERIMENTAL (PPM) | FUNCTIONAL GROUP | FIBER |
|---|---|------------------|---------------------|
| 110-130 (Ning 2011) | 122 | Nitrile | Acrylic |
| 110-150 (Ning 2011) | 125-138 | Aromatic ring | Polyester, elastane |
| 157-158 (Reich 2015) | 156-158 | Urethane | Elastane |
| 165-175 (Ning 2011) | 163-168 | Ester | Polyester |
| | 171-174 | Ester | Acrylic |
| 167-170, non-saturated | 174 | Amide | Polyamide |
| 173-178, saturated (ul Hasan 1980) | | | |
| 172-185 (Ning 2011) | 169-178 | Carboxylic acid | Wool |

Solid-state NMR spectroscopy can be used to precisely assign the molecular structure of a fiber. This is shown in Figure 20 for a polyester sample, where all peaks have been assigned. As stated in section 2.2.1 polyester is a generic group with a great diversity in possible members. Interpretation of the spectrum concludes that the textile fiber in Figure 20 is comprised by pure PET.

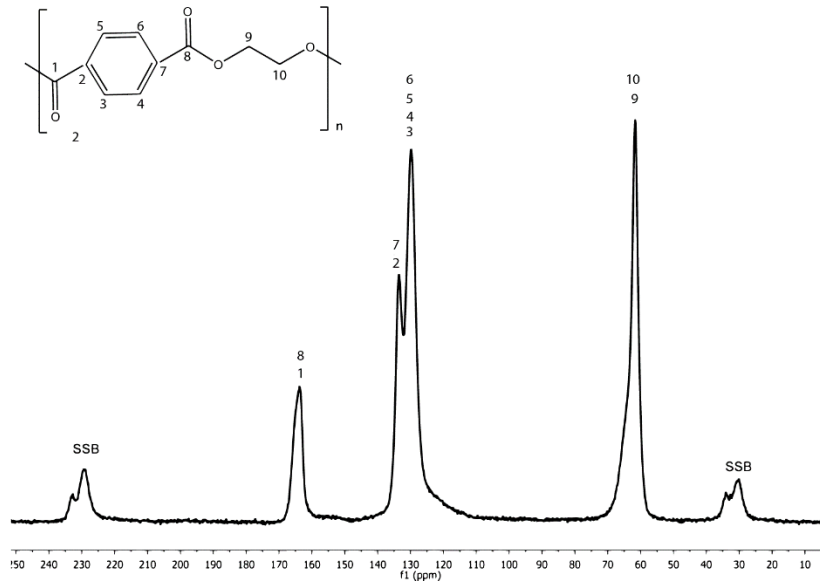


Figure 20: ^{13}C solid-state NMR spectrum of PET, with assignments. SSB is short for spinning side band, artefacts from MAS-spinning

Evaluation of complex blends

The complex blend samples are comprised of a multipart matrix of fibers with cotton being the predominant fiber type.

The pink traces represent the pullover sample while the blue traces represents the jeans sample, duplicate samples are made. A trace from pure cotton (black) is included as a guide for the eye. It is evident from both IR (21.a) and NMR (21.b) spectra that the jeans sample has a higher cotton content than the pullover sample since it resembles the black cotton trace more closely.

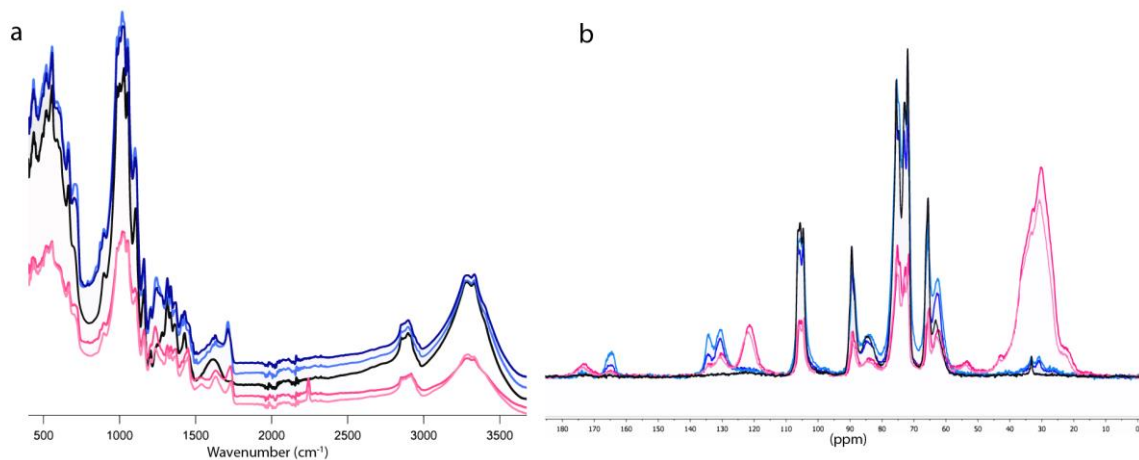


Figure 21: Spectra of complex blend samples a) ATR FT-IR, b) ^{13}C solid-state NMR. Pullover samples (pink), jeans samples (blue), cotton (black), duplicate samples are shown for the jeans and pullover sample.

The knowledge acquired on the positions of peaks of textile fibers in IR and NMR spectra was used to do an evaluation of the complex blends. Below are presented assignments of peaks to the respective fiber type.

ATR FT-IR spectrum of the pullover sample is shown in Figure 22. Three fiber types may be identified with certainty from the spectrum; cotton, polyester and acrylic. Cotton absorbance peaks are dominating the spectrum, giving it its overall shape. Apart from the cotton peaks the characteristic peak from C≡N stretch in acrylic is seen at 2242 cm^{-1} while the C=O stretch at 1727 cm^{-1} as well as the C-O stretch at 1235 cm^{-1} stems from polyester and from comonomers present in acrylic.

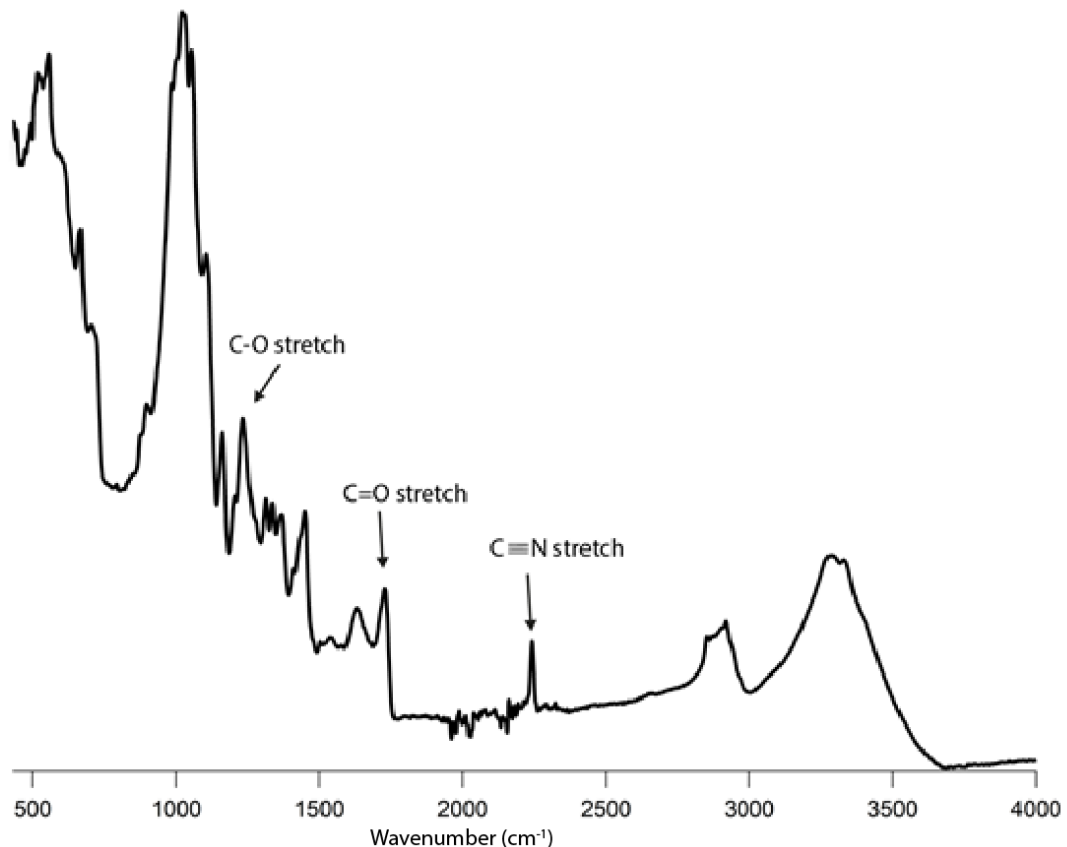


Figure 22: ATR FT-IR spectrum of complex blend, pullover sample, with assignments

As is mentioned in section 4.1.4 the fingerprint area, situated below 1500 cm^{-1} in IR spectroscopy, is useful for identification of specific molecules. However, in a blends such as the pullover sample where several textile fibers are present it is not possible to tell the fibers apart in this area due to the massive range of absorption bands. For a matrix of textile fibers this is true not only for the region below 1500 cm^{-1} but also for the $1800\text{-}1500\text{ cm}^{-1}$ region. As is demonstrated in Table 6 and Figure 17 in this section, peaks from different fiber types overlap even throughout this region making identification of individual fiber types difficult.

The NMR spectrum of the pullover sample, Figure 23, confirms the findings of cotton, acrylic and polyester fibers. Wool and polyamide are also possible fiber candidates. The spectrum shows a high alkyl peak centered at 30 ppm which is mainly from alkanes present in acrylic, and it also expresses the typical nitrile peak at 122 ppm stemming from acrylic. The peaks from aromatic rings at 125-137 ppm are assigned to polyester as well as the ester peak at 165 ppm. The peak at 173 ppm is corresponding to carboxylic acids, amides and high shift esters which are present in wool, polyamide and acrylic respectively.

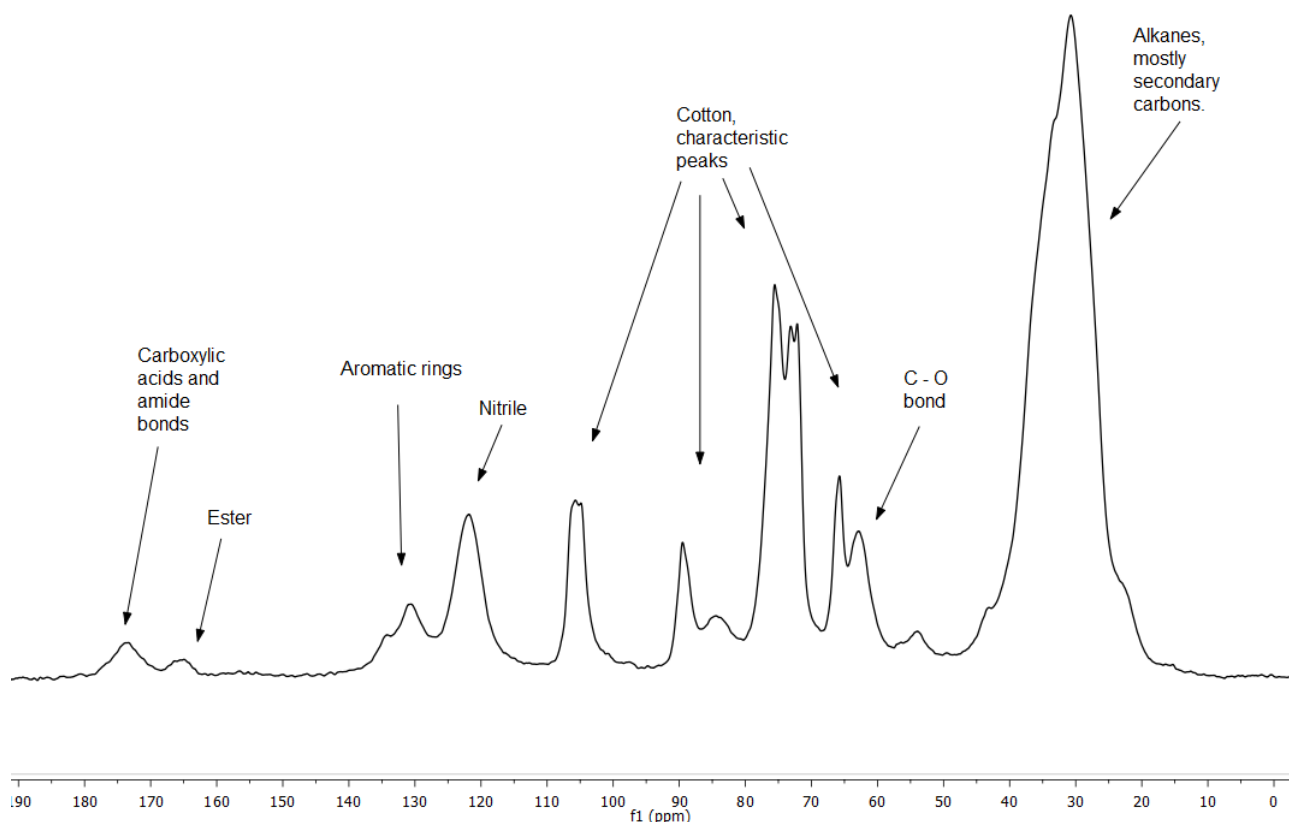


Figure 23: ^{13}C solid-state NMR spectrum of complex blend, pullover sample, with assignments. Exponential apodization of 70 Hz.

The alkyl peak

The alkyl peak, centered at 30 ppm in the pullover sample, appears as if it has a very high intensity compared to the rest of the peaks. However, this is an effect of the CP/MAS pulse sequence explained in section 4.2.2. Using a cross polarization pulse the signal intensity of the observed spin in the output spectra will no longer be proportional to the population of the spin but to the density of protons in the vicinity of the spin. Carbons in secondary alkanes have a high proton density in the vicinity giving the peak a high intensity contrasted to other spins. A closer look at the peak shows that its shape closely resembles the shape of the pure acrylic sample in the same region, bringing evidence that the pullover sample has a high acrylic content. The peak shapes for some common textile fibers in the alkyl area are shown in Figure 24.

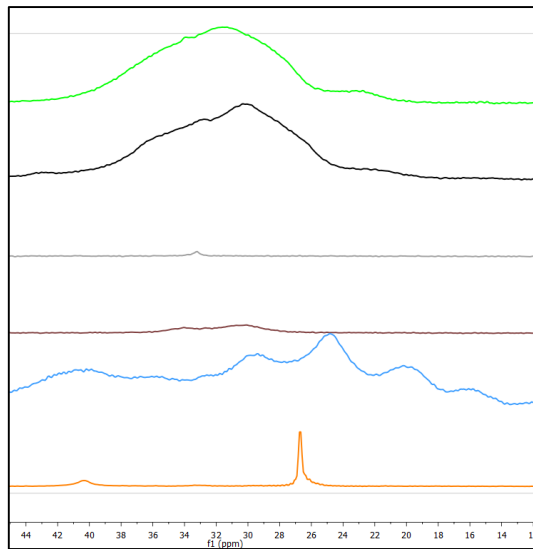


Figure 24: ^{13}C solid-state NMR spectra of the alkyl peak area. Traces represent acrylic (green), complex blend (black), cotton (grey), polyester (brown), wool (blue), elastane (orange),

NMR spectrum of the jeans sample is seen in Figure 25. Cotton is evidently the largest part while the peaks not stemming from cotton resembles polyester most closely. Characteristic polyester features are the ester link at 164 ppm, the aromatic rings at 125-140 ppm and the C-O bond that is accentuating the cotton peak at 71 ppm. Elastane is a common co-fiber in stretch jeans, but cannot be detected in the sample, since it is missing the peak at 157 ppm stemming from the urethane link.

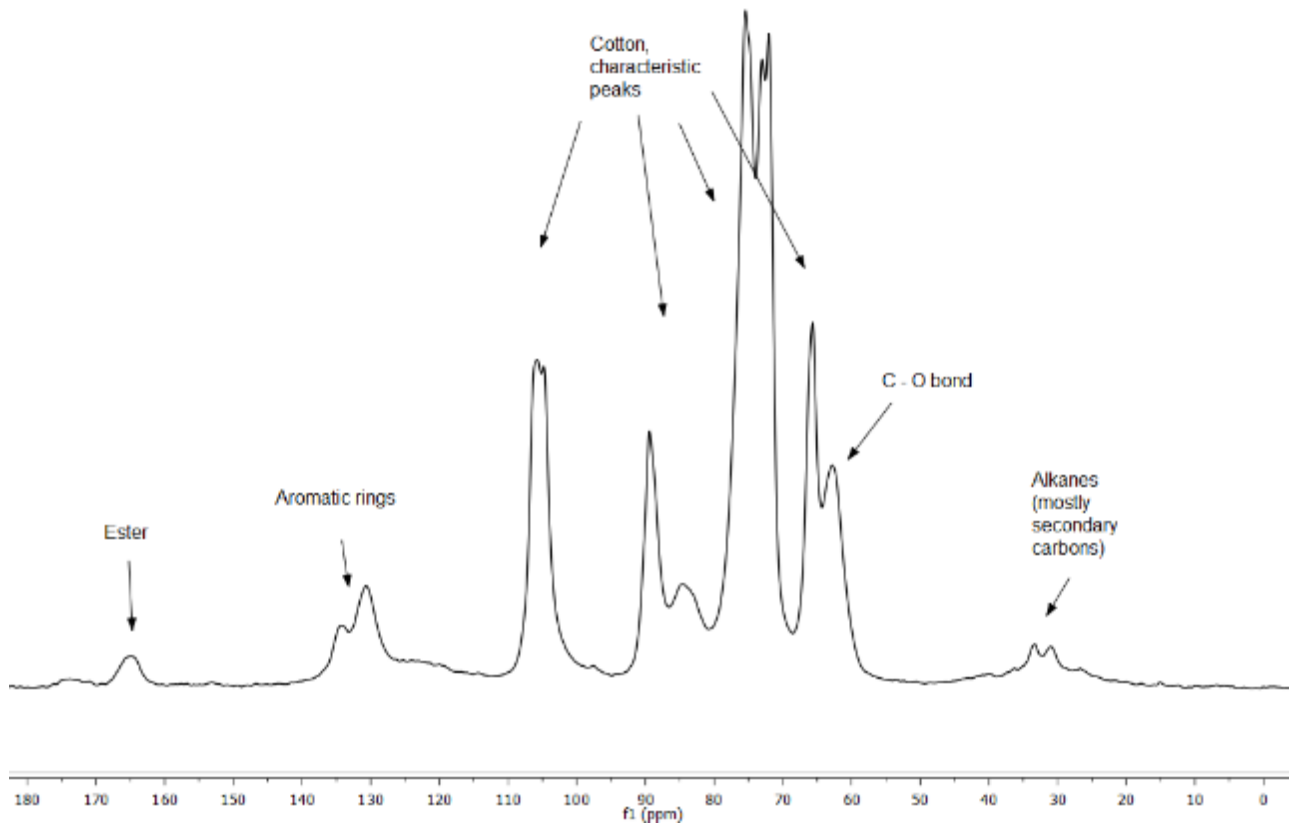


Figure 25: ^{13}C Solid-state NMR spectrum of complex blend, jeans sample, with assignments. Exponential apodization of 70 Hz.

Blend analysis – comparison between IR and NMR spectroscopy

The complex blends analyzed in this section were comprised of complex matrices, the pullover sample even more so than the jeans sample. Both IR and NMR spectroscopy could with certainty identify cotton, acrylic and polyester in the pullover sample. NMR spectroscopy also indicated for the presence of wool and/or polyamide and confirmed acrylic to be the major fiber type next to cotton. None of the techniques could exclude the presence of fiber types not detected in the spectrum. For both techniques peaks are overlapping, meaning peaks could be “hidden” behind each other and the signal to noise ratio could be improved to not lose small peaks in the background noise.

Characterization of textile fibers in this thesis has been performed by considering the intensity of characteristic bands. In IR spectroscopy the peaks from different fiber types overlap throughout the spectrum making identification of individual fiber types difficult. In NMR spectroscopy, peaks from textile fibers are overlapping as well, but not to the same extent. Hence, for this type of characterization of textile fibers NMR spectroscopy is superior to IR spectroscopy.

6.1.2 Quantitative analysis of textile fibers

Vibrational spectroscopy

Direct quantification from vibrational spectra is not possible since the amount of energy absorbed by different vibrations is not equal; hence there is no direct correlation between peak area and the quantity of molecules causing the vibration. To extract quantitative information chemometric methods such as principal component analysis (PCA) and partial least squares (PLS) are used. Chemometrics is the science of extracting relevant information about chemical systems from data produced in chemical experiments and analysis. The main objectives of chemometric methods is data reduction, grouping and modelling of relationships between variables. By such statistical analyses it is possible to extract quantitative information and resolve otherwise overlapping peaks (Wold 1995). The use of chemometric methods is inevitable in the interpretation of NIR spectra since the peaks are severely overlapping and rarely can be interpreted by visual means (Nørgaard et al. 2012) The general use of chemometric methods to interpret NIR spectra has made it the most popular quantitative method of the vibrational spectroscopy techniques. However, PCA and/or PLS are used to extract quantitative data in all vibrational spectroscopy techniques in a range of fields reaching from wine quality (Ieuwoudt et al. 2004) to medical science (González-Solís et al. 2014) and inorganic synthesis control (Chaves et al. 2014).

NMR spectroscopy

In direct-polarization NMR experiments the magnetization of a sample is proportional to the population of the studied spin and to its gyromagnetic ratio. Since the magnetization of a spin is directly proportional to the peak area in the spectrum conclusions about the relative quantities can be drawn. The CP-pulse used in the present research however, manipulates the magnetization, as explained in section 4.2.2. Therefore, the signal intensity of the observed spin in the output spectra will no longer be proportional to the population of the spin but to the strength of the dipolar couplings and the density of protons in the vicinity of the spin. In a homogenous sample this effect can be circumvented by choosing the right set of parameters for the pulse sequence. However, the samples of interest are often comprised of several fiber types which makes it difficult to choose parameters that provide quantitative data for all fibers in a single experiment.

6.2 Separation of polycotton textiles

Alkaline hydrolysis was performed on polycotton sheets in order to separate polyester and cotton into pure fractions. The reaction course is visualized in section 6.2.2. The reaction parameters; NaOH concentration, PTC concentration, temperature and time, were varied according to Table 5. An evaluation of the influence of reaction parameters on yield is given in section 6.2.3. The reaction products; the cotton residue, TPA and EG have been analyzed and the result is discussed in section 6.2.4.

6.2.1 Characterization of starting material

A quantitative chemical analysis according to the European standard (ISO 1833-11:2006) was performed on the bed sheets. The result, with a confidence limit of ± 1 for the confidence level of 95 % was that the sheets contain 47.9 % cotton and 52.1 % polyester.

Solid-state NMR spectrum of the untreated bed sheet showed the characteristic peaks of cotton and PET. The chemical formula of the polyester fiber hence was confirmed to be pure PET, this information was needed in order to calculate the reaction yield.

6.2.2 Course of reaction

The course of reaction was followed by light microscopy using a cooling stage accessory. Reaction was conducted at 80 °C in 15 wt% NaOH at a high PTC concentration. Figure 26 visualizes hydrolysis of polyester as well as swelling of cotton. After 600 s reaction time the polyester fiber is completely depolymerized.

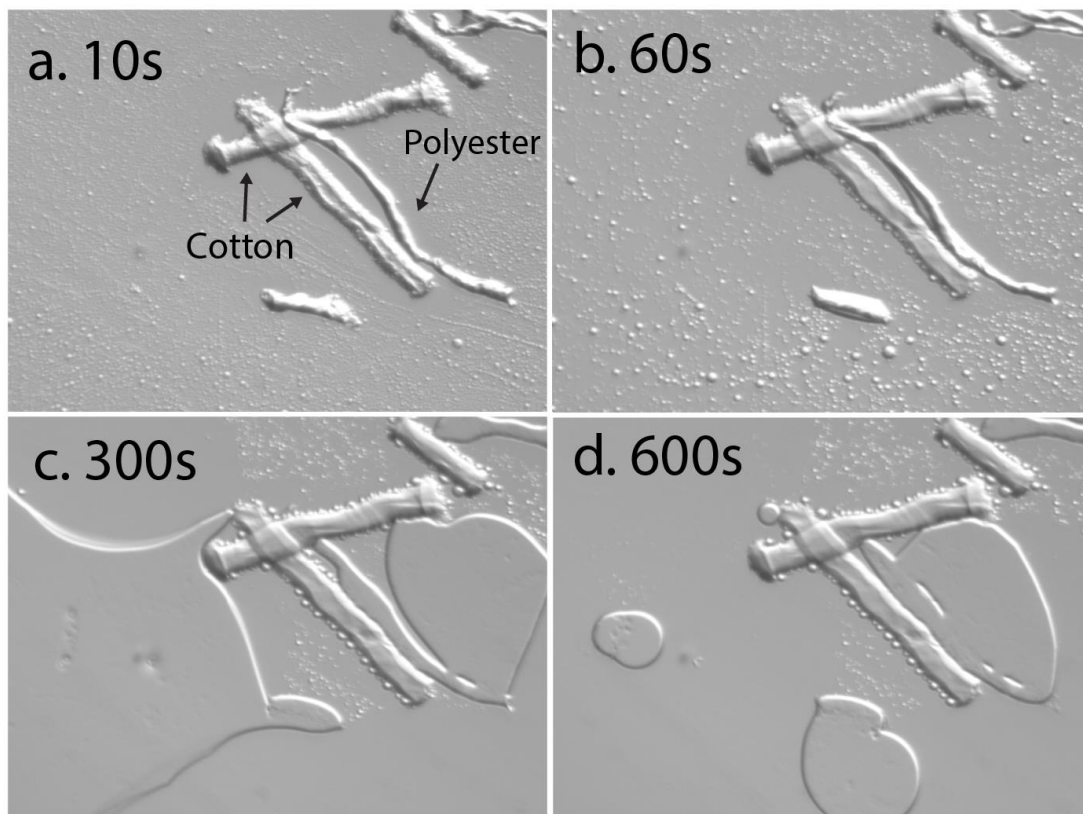


Figure 26: Course of reaction followed by light microscopy.

6.2.2 Influence of reaction parameters

To optimize the yield of the reaction the reaction parameters; NaOH concentration, PTC concentration, temperature and time, were varied according to Table 5. The result presented below indicates that reaction parameters were mutually dependent on each other. For example, as seen in Figure 28, an increased temperature could facilitate full depolymerization of PET at a lower PTC concentration, compared to what was needed to obtain full depolymerization at a lower temperature.

Both NaOH concentration and PTC concentration reached a limiting value. Above this value additional increase of the concentration of NaOH/PTC only had a minor influence on the yield of TPA. This is seen in Figure 27 where the dependence of yield on NaOH concentrations levels off above 10 wt%. The limiting value of 10 wt% NaOH has also been found in literature (Kosmidis et al. 2001).

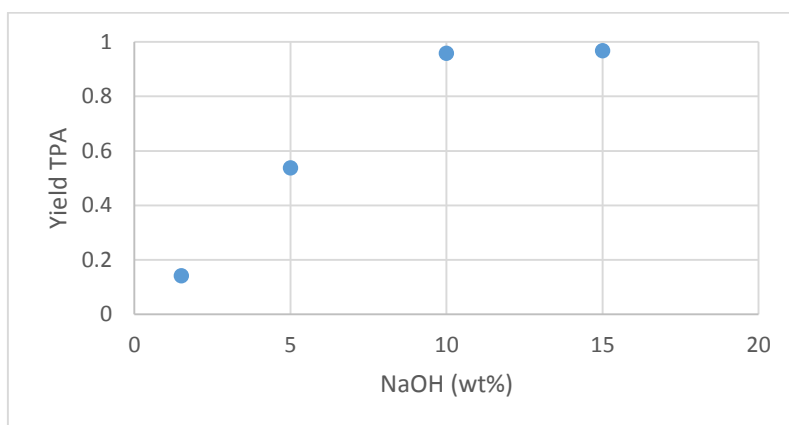


Figure 27: Yield of TPA at different NaOH concentrations. 90 °C, 0.1 mol PTC/mol repeating unit PET, 100min reaction time

A similar pattern were seen for PTC concentration, presented in Figure 28. The effect of PTC concentration was seen to be co-varying with temperature. At 90 °C already low concentrations of PTC gave high yields; 0.005mol PTC/mol PET repeating unit gave 45 % yield at 80 °C and 82 % yield at 90°C. The difference between the yield at 80 °C and 90 °C was decreasing with increasing PTC to PET ratio.

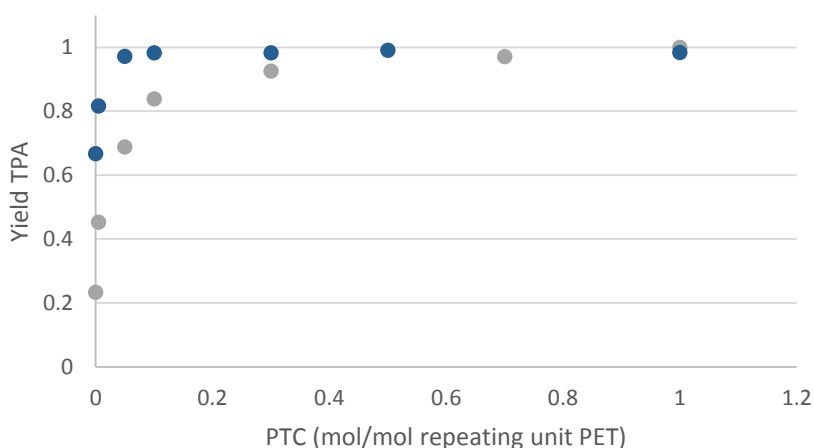


Figure 28: Yield of TPA at different ratios of PTC to repeating unit PET at different temperatures. Grey bullets 80 °C, blue bullets 90 °C. 10 wt% NaOH, 100min reaction time.

Compared to research on depolymerization of PET bottles found in the literature (Das et al. 2007, Kosmidis et al. 2001), a higher PTC to PET ratio was required in the experiments on polycotton textiles. Previous experiments on alkaline hydrolysis of pure PET in the same temperature and time range as the present study is reaching full conversion of PET at PTC concentrations about two orders of magnitude lower than the results obtained in this thesis. Cotton is not competing with PET for the lipophilic part of the PTC. Thus, the most probable explanation for the high PTC concentration needed to obtain full conversion is that PTC adhered to the polypropylene reaction vessels. The PTC used is highly surface active, due to its molecular structure. The hypothesis was verified when vessels used in earlier reactions were reused and uncharacteristically high yields were obtained. Hence, the PTC concentrations reported are initial PTC concentrations rather than bulk concentrations actually available in the reaction solution.

The dependence on time at high PTC concentrations and 80 °C is shown in Figure 29. High conversions were obtained in 15 wt% NaOH solution after only 30 min of treatment. Almost full conversion was obtained in both 10 wt% and 15 wt% NaOH after 60 minutes reaction time under present conditions.

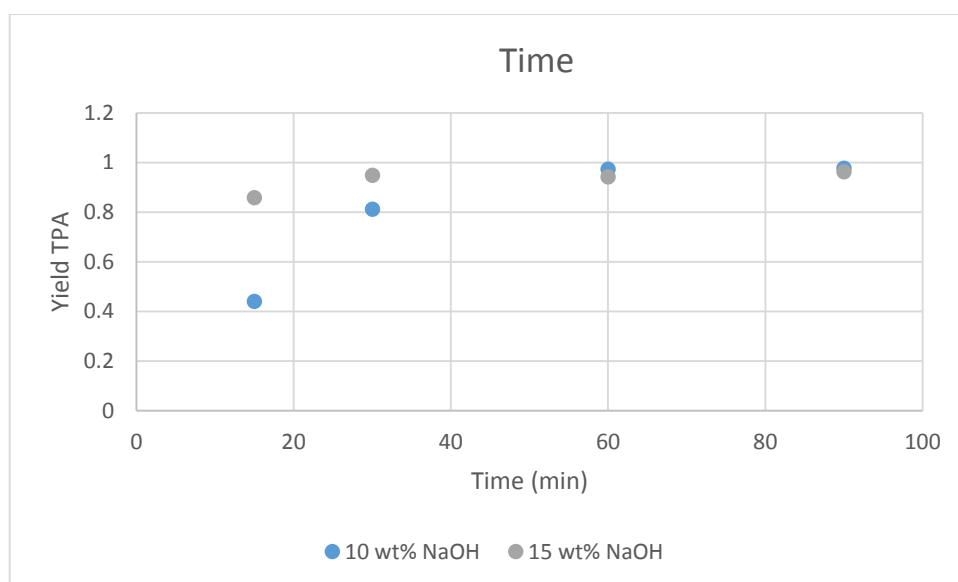


Figure 29: Yield of TPA as a function of time at different NaOH concentrations. Blue bullets 10 wt% NaOH, grey bullets 15 wt% NaOH. 80 °C, 1 mol PTC/mol repeating unit PET.

The reaction rate was found to be limited by mass transfer. This was evident from trials where different modes of shaking, orbital or linear, was applied in the shaking bath. The dependence of shaking modes leveled off at higher PTC concentrations where enough PTC was present to facilitate the transport between the aqueous phase and the plastic surface regardless of the mode of shaking.

6.2.3 Characterization of separation products

Cotton residue

Pure cotton was obtained when reaction conditions are strong enough to depolymerize polyester completely. This was confirmed by gravimetric analysis of the obtained TPA and ATR FT-IR analysis of the cotton residue.

Crystalline structure

ATR FT-IR spectra revealed a shift in crystal lattice from cellulose I in native cotton to cellulose II. However, all reaction conditions did not induce crystalline transformation to the same extent. Results showed that after reaction at NaOH concentration of 10 wt% or lower and temperatures of 80 °C or lower the dominant polymorph was still cellulose I. This is evidenced by ATR FT-IR spectroscopy as can be seen in Figure 30. As stated in section 2.1 cellulose II is the more thermodynamically stable polymorph of cellulose which indicates that it is maybe harder to dissolve. It might thus be favorable to obtain cellulose I as the reaction product, since it might dissolve more easily, which is beneficial for the subsequent steps of textile recycling.

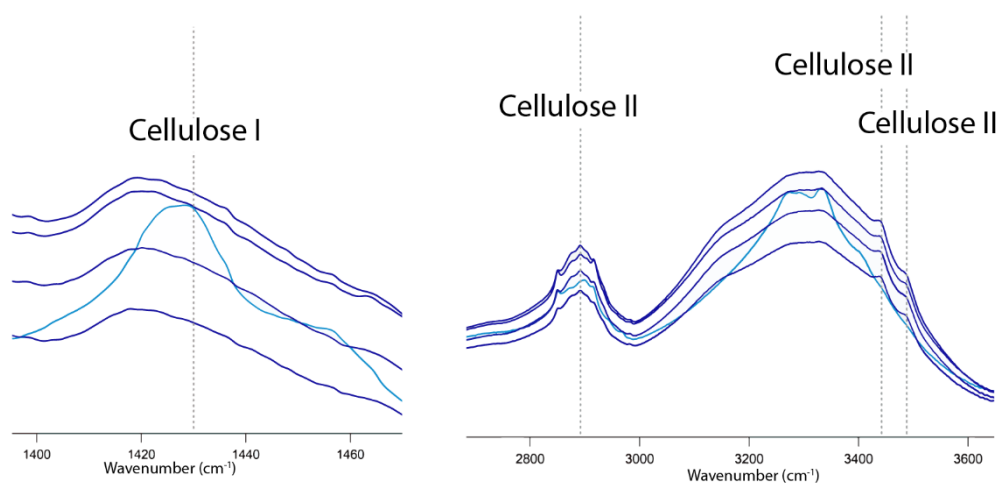


Figure 30: ATR FT-IR spectrum of the cellulose residue after reaction under different conditions, accentuating the transformation between cellulose I and cellulose II. The light blue trace shows cellulose that mainly exhibits absorbancies typical for cellulose I while the darker traces mainly exhibits absorbancies typical for cellulose II. The dashed lines provides a guide for the eye to frequencies where cellulose I and II, respectively, show specific absorbance.

Intrinsic viscosity

The intrinsic viscosity of cellulose is closely related to the degree of polymerization. Numerous researches have tried to establish relationships between DP and intrinsic viscosity and several standards are in use such as the one by Immergut et al, 1953 and Harland, 1952. However, no consensus exists on this subject, hence this thesis will refer to the intrinsic viscosities of samples rather than convert to DP. Here, intrinsic viscosity readings are used to probe the difference in DP between samples, rather than evaluate absolute chain lengths.

Intrinsic viscosities for the cotton residue from separation of polycotton sheets are shown in Table 8. Reaction parameters were varied between the runs to elucidate how intrinsic viscosity depends on the respective reaction parameter. Results showed that NaOH concentration was the parameter with the greatest influence on the intrinsic viscosity, since reaction in 10 wt% NaOH gave an intrinsic viscosity

of 1402 cm³/g while 15 wt% NaOH gave an intrinsic viscosity of 1140 cm³/g. Temperature did not show any effect on intrinsic viscosity. Kinetic studies on pure cellulose in alkaline solutions from literature have shown that the degradation of cellulose has a high dependence on temperature (Haas et al. 1967, Shaw 2013). This was not reflected in the present study, however, the temperature span was quite narrow, only 10 °C, which might be an explanation.

Table 8: Intrinsic viscosities for cellulose separated from polycotton sheets.

| Sample ID | Temperature (°C) | NaOH (wt%) | PTC (mol/mol PET repeating unit) | Reaction time (min) | Intrinsic viscosity (cm ³ /g) |
|-----------------|------------------|------------|----------------------------------|---------------------|--|
| NaOH conc A | 80 | 10 | 1 | 90 | 1402 |
| NaOH conc B | 80 | 15 | 1 | 90 | 1140 |
| Temp A | 80 | 15 | 1 | 100 | 1178 |
| Temp B | 90 | 15 | 1 | 100 | 1169 |
| Time A (Temp B) | 90 | 15 | 1 | 100 | 1169 |
| Time B | 90 | 15 | 1 | 150 | 1124 |

Intrinsic viscosity was also determined for pure cotton samples (bedsheets, 100 % cotton) which were treated under similar reaction conditions as the polycotton sheet. The reaction parameters; time, NaOH concentration and PTC concentration were varied according to Table 9. However, these samples were neutralized in 5 % acetic acid prior to intrinsic viscosity measurements, according to the procedure from Mattor. The acidic treatment is intended to neutralize the highly alkaline cellulose. However, for sample C and D the acid is believed to have induced hydrolysis and hence a decrease in intrinsic viscosities. During the neutralization step these samples were highly swelled and hard to filter. Hence, samples were heated, in the presence of acid, in order to enable filtering. This treatment is considered being the reason for the drastically lowered intrinsic viscosity readings for these samples. The highly swelled state of sample C and D is not believed to be a consequence of the low PTC concentration but rather of the temperature of samples when filtered. These samples were the last filtered and consequently had longer time to equilibrate to the temperature of the ice bath. NaOH acts more efficiently on cellulose at lower temperatures causing increased swelling (Egal 2006).

Table 9: Intrinsic viscosities for cellulose from pure cotton

| Sample | Temperature (°C) | NaOH (wt%) | PTC (mol/mol PET repeating unit) | Reaction time (min) | Intrinsic viscosity (cm ³ /g) |
|--------|------------------|------------|----------------------------------|---------------------|--|
| A | 80 | 10 | 1 | 90 | 1170 |
| B | 80 | 15 | 1 | 90 | 1128 |
| C | 80 | 10 | 0.1 | 90 | 701 |
| D | 80 | 15 | 0.1 | 90 | 979 |
| E | 80 | 10 | 1 | 30 | 1083 |
| F | 80 | 15 | 1 | 30 | 1086 |

The lower PTC concentration in samples C and D, compared to samples A, B, E and F, is not believed to have any effect on the intrinsic viscosity of cotton. The viscosity reading in Table 9 can neither confirm nor contradict this statement since sample C and D were hydrolyzed during processing. However, a study on cotton fibers in an alkaline system in the presence of a quaternary ammonium base, similar to the PTC used in the present work, have been performed by Vigo et al., 1969. They discovered synergistic effects between the hydroxide ion and the quaternary ammonium cation where the bulky cation is believed to induce swelling and decrease the crystallinity of cotton by a combination of electrostatic and steric effects. This was observed for high concentrations (25-35 %) of the quaternary ammonium base with additions of 1-16 % NaOH. In the present work NaOH is present in much higher concentrations than the quaternary ammonium ions, hence the effect of the PTC is assumed to be negligible.

A comparison of the effect of NaOH concentration on intrinsic viscosity between Table 8 and Table 9 gives that cotton from the blended sample seem to have a dependency on NaOH concentration, while for the pure cotton sample this dependency is lacking. These inconclusive results cannot be explained without further research. It is reasonable to believe that NaOH concentration affects the intrinsic viscosity of cellulose. Entwistle et al. reported a peak in reaction rate of autoxidation of cellulose at concentrations of 6-8 M NaOH. 10 wt% NaOH corresponds to approximately 3M NaOH, hence autoxidation rate is expected to increase from 10 wt% (3M) to 15 wt% (4.4M).

Viscosity reduction appeared to be a fast reaction since 30 or 90 minutes reaction time, samples E, F and A, B, respectively, do not influence the viscosity. This is consistent with the results for cellulose from fiber blends where 100 or 150 min reaction time did not have a notable effect on the viscosity. The discrepancy where samples E and F, reacted for 30 min have a lower intrinsic viscosity than A and B reacted for 90 min is believed to be due to natural fluctuation in the readings of the viscosity.

Earlier studies on the same bedsheets (100 % cotton) have been performed by Palme et al., 2014. Their results include an intrinsic viscosity of approximately 2200 cm³/g for the untreated bedsheets. As can be seen in Table 9 the viscosity results from the present study was in the range of 1100 cm³/g, which corresponds to a notable decrease of DP.

As described in section 2.3.2 there are three main mechanisms causing decrease of cellulose DP. Alkaline hydrolysis and autoxidation produce large reductions in DP since they cause chain scissioning. However, these mechanisms are not supposed to be particularly active under present reaction conditions, higher temperatures and/or longer reaction times are needed to activate these mechanisms according to literature. Peeling is the mechanism that is reported to be most active and responsible for cellulose degradation at present reaction conditions. However, intrinsic viscosity readings of pure cotton are reduced to about half after heating in alkali as is evident from Table 9. The same reaction yielded a weight loss from cotton of only about 3 %. If peeling was the main mechanism causing decrease in DP the weight loss would be larger. Further, NMR spectra of the obtained TPA and of the filtrate from the separation reaction showed no detectable amount of the cellulose peeling products isosaccharinic acid or its derivatives. These results suggests that peeling only accounted for a minor part of cellulose chain shortening and that autoxidation and subsequent chain scissioning accounted for the major part. However, only a minor number of fulfilled autoxidation reactions are needed to reduce the intrinsic viscosity to half, since the mechanism causes chain cleavage at random positions.

Terephthalic acid

The purity of TPA was analyzed with ATR FT-IR spectroscopy and solution state NMR spectroscopy. Depolymerization of PET gives EG and TPA, the reaction is shown in Figure 8, section 3.4. ATR FT-IR spectra of the samples show that pure TPA was obtained regardless of reaction conditions which can be seen in Figure 31. This was also confirmed by NMR spectroscopy.

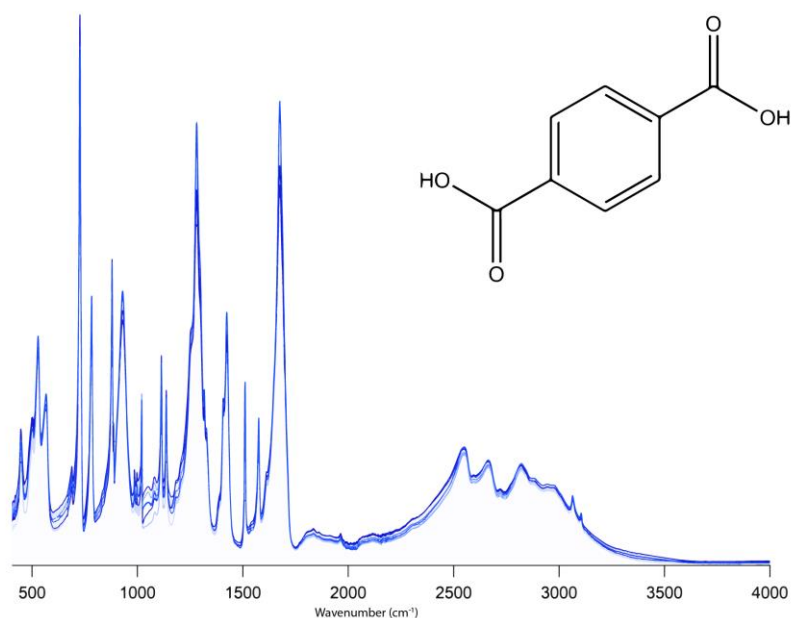


Figure 31: ATR FT-IR spectra of TPA obtained at temperatures between 80-90°C, NaOH concentration between 10-15 wt%, reaction times between 90-150 min and with or without PTC.

A zoom in on the baseline of the $^1\text{H-NMR}$ spectrum of the obtained TPA reveals minor impurities, see Figure 32. The shifts do not match neither with residual PTC nor with isosaccharinic acid, the main degradation product of cellulose assuming that peeling is the major degradation mechanism. $^1\text{H-NMR}$ spectrum of 98 % TPA purchased from Sigma-Aldrich shows impurity peaks of a similar pattern, hence it is assumed that the impurities are either residues from TPA manufacturing such as isophthalic acid or present in the solvent.

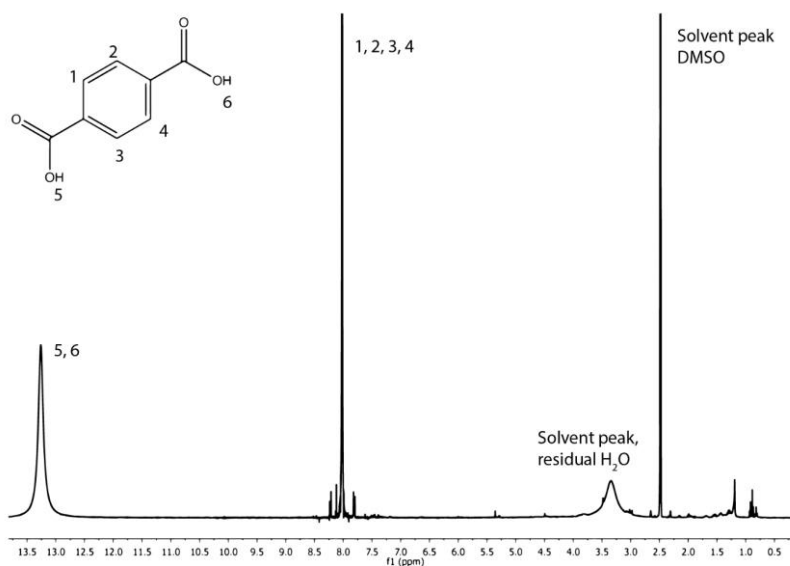


Figure 32: $^1\text{H-NMR}$ spectrum of TPA, with assignments

Filtrate

^{13}C NMR and ^1H NMR spectroscopy on the filtrate gave unanimous result. No hydrocarbons were present in the filtrate in a detectable quantity except PTC and EG as is seen in Figure 33. As for the NMR spectrum of TPA, no isosaccharinic acid was detected.

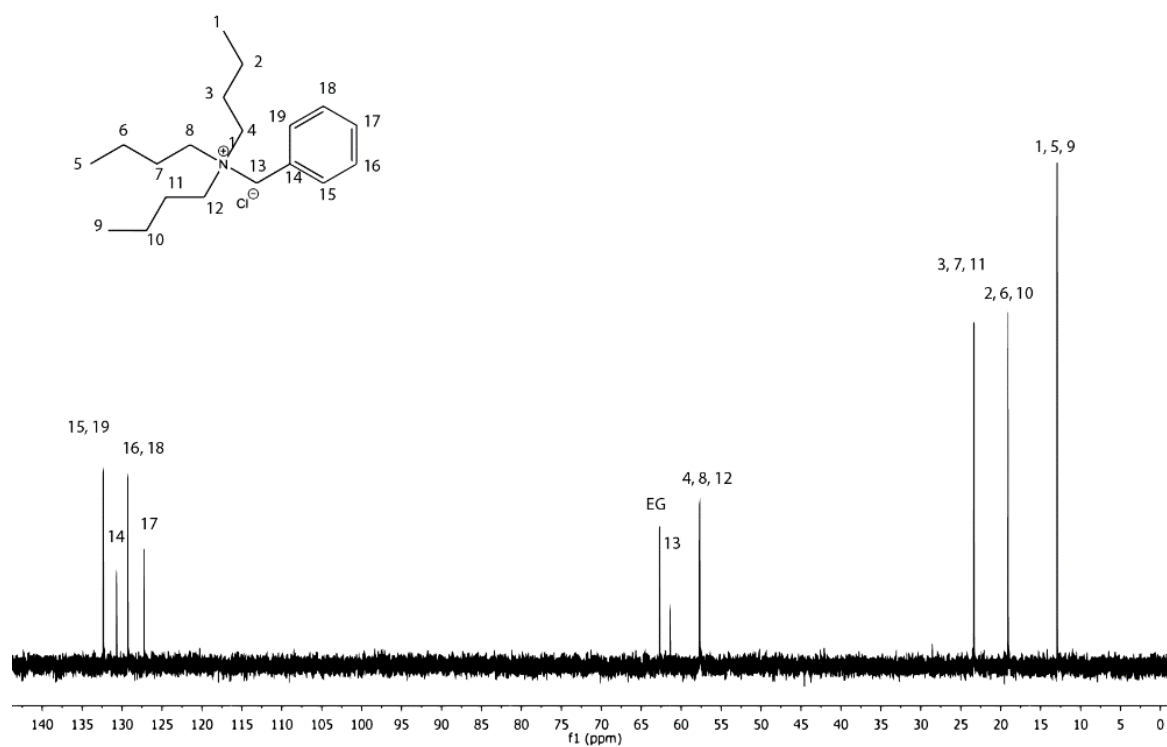


Figure 33: ^{13}C NMR spectrum of filtrate, showing peaks from PTC and EG

7. Conclusions

Today the technology to use post-consumer waste textiles as raw material to produce high quality fibers is lacking in most of the industry. In order to introduce efficient recycling of textile fibers, characterization of fiber content as well as separation of fibers from material blends are essential.

The vibrational spectroscopy techniques; IR and Raman, were probed for their suitability to be used as automatic sorting techniques. Raman spectroscopy proved to be an insufficient technique in order to qualitatively characterize textile fibers under present circumstances due to fluorescence. ATR FT-IR spectroscopy revealed to be a useful technique for all types of fibers. However, peaks from different fiber types overlap severely throughout the IR spectrum and characterization cannot be made on behalf of *markers*, characteristic, non-overlapping peaks distinct for each fiber type. Instead the full spectrum has to be acquired and matched with a spectral library to identify the fiber which prolongs analysis time. Solid-state NMR spectroscopy was used to characterize textiles, both pure fibers and fiber blends. Its strength, to precisely resolve molecular structures was demonstrated for pure fibers. The technique also proved useful for qualitative analysis of the composition of fiber blends, confirming the presence of cotton, acrylic and polyester. ATR FT-IR spectroscopy was used for qualitative analysis of the same blends, however interpretation was more difficult due to overlapping of peaks.

None of the surveyed spectroscopic techniques can provide direct quantification of the fiber content in fiber blends. Chemometric techniques such as principal component analysis or partial least squares may be coupled to each technique to provide quantitative results. To be suitable for automatic sorting purposes a technique has to accurately perform qualitative as well as quantitative characterization. Of the techniques surveyed in this study IR spectroscopy has the largest potential, since it is applicable to types of textile fibers and provides rapid analysis with no sample preparation.

Separation of a polyester/cotton blended fabric by means of alkaline hydrolysis have been successfully performed. Mild reaction conditions were generated by using the phase transfer catalyst benzyltributyl ammonium chloride. Full depolymerization of polyester was achieved when reaction conditions were optimized. The variables; NaOH concentration, PTC concentration, temperature and reaction time proved to be mutually dependent. High concentrations of PTC can facilitate almost full depolymerization in only 60 minutes at otherwise mild reaction conditions, 80 °C and 10 wt% NaOH. In the absence of PTC the yield of TPA is 23 % for 10 wt% NaOH and 67 % for 15 wt% NaOH after 100 min reaction time at 80 °C.

The reaction products from the separation were pure TPA and EG which was confirmed by ATR FT-IR and NMR spectroscopy. The crystalline structure of the cotton residue was analyzed by ATR FT-IR spectroscopy, revealing that a transformation of the crystalline structure was obtained under all reaction conditions except when NaOH concentration was ≤ 10 wt% and temperature was ≤ 80 °C. This might be of importance for the subsequent steps of textile recycling. Intrinsic viscosity measurements on the cotton residue were inconclusive. The dependence of DP on NaOH concentration could not be verified, neither the effect of PTC concentration. However, a substantial decrease of DP could be

confirmed by intrinsic viscosity readings. Since cellulose degradation products, such as isosaccharinic acid and similar acids, could not be detected as reaction products it was concluded that the main reaction mechanism for cellulose chain shortening is rather proceeding by chain scissioning than by peeling.

The products from alkaline hydrolysis are intended to be used for production of new textile fibers. Purification of the obtained PET monomers and subsequent re-polymerization could generate new polyester fibers. The cotton residue can be dissolved and used to produce man-made cellulosic fibers. There and then, recycling is done according to the tertiary approach and a material of equal value as the recycled one is obtained. Further research may tell us how to get there.

8. Outlook

The results presented in this master thesis have given rise to further questions. Suggestions of interesting continuations of this project are presented below.

- ❖ For the automatic sorting part it would be interesting to broaden the knowledge on possible analysis techniques and data utilization by:
 - Include NIR as a vibrational spectroscopy technique explored for the purpose of automatic sorting of textile fibers.
 - Evaluate the use of chemometric techniques for each analysis technique to extract more information from the obtained data.

- ❖ For the separation part more knowledge on the separation process could be gained by:
 - Apply a factorial design on the separation experiments in order to conclude how the reaction parameters depend on each other.
 - Scale-up of the separation experiment.

- ❖ The products from separation could be further characterized and utilized by:
 - Continue investigation of the dependence of cellulose chain length on NaOH concentration.
 - Further characterization of the cotton residue by techniques such as scanning electron microscopy and molecular weight distribution
 - Investigate methods to extract and purify ethylene glycol and PTC from the filtrate.
 - Repolymerize PET using the obtained monomers.

Acknowledgements

This work has been carried out within the framework of Mistra Future Fashion in cooperation with SP Technical research Institute of Sweden and Chalmers University of Technology. These organizations are gratefully acknowledged for giving me the opportunity to work with an interesting subject.

A special thanks is directed towards;

- My examiner, Lars Nordstierna.
- All of my supervisors; Hanna de la Motte, Alexander Idström and Anna Palme. For support and inspiration, and for the opportunity to do a very interesting thesis.
- The Swedish School of textiles for kindly providing me with fabrics and threads for the textile analysis study.
- SOEX group for providing post-consumer textiles from their recycling facility.
- Textilia for providing bed sheets for the separation study.
- The Swedish NMR Centre for letting me use their equipment. Special thanks to Diana Bernin for advice on solid-state NMR spectroscopy.
- Anna Martinelli for tutorials on IR and Raman spectroscopy.
- Negin Yaghini for her helpfulness considering Raman and Igor, and inspiration on hiking in Iran.
- Gunnar Westman group for letting me use the shaking bath, repeatedly.
- Helena Wedin, SP, for interesting talks on the textile industry and recycling.
- The amazing present and post members of Lars Nordstierna group, Jonatan Bergek, Lorenz Bock, Alexander Idström and Lisa Åkerlund. Thanks for group activities, “group activities” lunches, laughs and pep-talks.
- All other friends and colleagues at TYK.
- Friends and family.

Bibliography

- Achilias, D.S. & Karayannidis, G.P., 2004. The Chemical Recycling of PET in the Framework of Sustainable Development. *Water, Air, & Soil Pollution: Focus*, 4(4/5), pp.385–396.
- Apperley, D.C., Harris, R.K. & Hodgkinson, P., 2012. *Solid state NMR: Basic principles and practice*, Momentum press.
- Bakeev, K.A., 2004. Near-Infrared Spectroscopy as a Process Analytical Tool. *Spectroscopy*, 19(1), pp.39–42.
- Bärlocher, C. & Holland, R., 1999. *The impact of cotton on fresh water resources and ecosystems*, WWF Background Paper
- BISFA, 2014. <http://www.bisfa.org/WHATISBISFA.aspx>. [Accessed October 20, 2014].
- Bresee, R.R., 1986. General effects of ageing on textiles. *Journal of the American Institute for Conservation*, 25(1), pp.39–48.
- Buzzini, P. & Massonnet, G., 2013. The discrimination of colored acrylic, cotton, and wool textile fibers using micro-Raman spectroscopy. Part 1: in situ detection and characterization of dyes. *Journal of forensic sciences*, 58(6), pp.1593–600.
- Bvse, 2008. *Textilrecycling in Deutschland*, Available at: http://bvse.de/356/6043/Zahlen_zur_Sammlung_und_Verwendung_von_Altkleidern_in_Deutschland. [Accessed April 23, 2015].
- Chaves, T.F., Soares, F. L. F., Cardoso, D, Carneiro, R. L., 2014. Monitoring of the crystallization of zeolite LTA using Raman and chemometric tools. *The Analyst*, 140 (3), pp 354-359.
- Cho, L., 2007. Identification of textile fiber by Raman microspectroscopy. *Forensic Science Journal* , 6(1), pp.55–62.
- Colletti, R.F. & Mathias, L.J., 1988. Solid state C-13 NMR characterization of textiles: Qualitative and quantitative analysis. *Journal of Applied Polymer Science*, 35(8), pp.2069–2074.
- Das, J., Halgeri, A. B., Sahu, V., Parikh, P. A., 2007. Alkaline hydrolysis of poly (ethylene terephthalate) in presence of a phase transfer catalyst. *Indian Journal of Chemical Technology*, 14(1), pp.173–177.
- Duer, M.J., 2008. *Solid State NMR Spectroscopy : Principles and Applications*, Oxford: Blackwell Science.
- Edwards, H.G.M. & Wyeth, P., 2005. Case study: Ancient textile fibers. *RSC Analytical Spectroscopy Monographs*. pp. 304–324.
- Egal, M., 2006. *Structure and properties of cellulose/NaOH aqueous solutions, gels and regenerated objects*. Ecole des Mines de Paris.

- Entwistle, D., Cole, E.H. & Wooding, N.S., 1949. The Autoxidation of Alkali Cellulose. *Textile Reserach Journal*, 19(9), pp.527–546.
- Everhart, W., Makar, K. & Rudolph, R., 1998. Recovery of polyester from contaminated polyester waste. US Patent.
- González-Solís, J.L. Martínez-Espinosa, J. C., Salgado-Román, J. M., Palomares-Anda, P., 2014. Monitoring of chemotherapy leukemia treatment using Raman spectroscopy and principal component analysis. *Lasers in medical science*, 29(3), pp.1241–9.
- Haas, D.W., Hrytfjord, B.F. & Sarkanen, K. V, 1967. Kinetic study on the alkali degradation of cotton hydrocellulose. *Journal of Applied Polymer Science*, 11, pp.1573–1576.
- Harland, W.G., Cumberbirch, R., 1958. Relation between Intrinsic Viscosity and Degree of Polymerization. *Journal of the Textile Institute Transactions*, 49(12), pp 679-686
- Hatch, K.L., 1993. *Textile Science*, St. Paul, MN: West Publishing Company.
- Hawkins, W.L., 1984. Polymer Degradation. In *Polymer Degradation and Stabilization*. Berlin: Springer Berlin Heidelberg.
- Idström, A., 2015. *Investigating cellulose structure using solid-state NMR spectroscopy*. Chalmers University of Technology.
- Ieuwoudt, H., Rior, B., Retorius, I., Anley, M., Auer, F., 2004. Principal Component Analysis Applied to Fourier Transform Infrared Spectroscopy for the Design of Calibration Sets for Glycerol Prediction Models in Wine and for the Detection and Classification of Outlier Samples. *J. Agric. Food Chem.*, 52, pp.3726–3735.
- Immergut, E.H., Schurz, J. & Mark, H., 1953. The intrinsic viscosity-molecular weight relationship for cellulose and investigations of nitrocellulose in various solvents. *Monatsheft fur Chemie*, 84(2), pp.219–249.
- Jacobsen, N.E., 2007. *NMR Spectroscopy Explained: Simplified Theory, Applications and Examples for Organic Chemistry and Structural Biology*, Hoboken, New Jersey: John Wiley & Sons.
- Jeihanipour, A. et al., 2010. A novel process for ethanol or biogas production from cellulose in blended-fibers waste textiles. *Waste management*, 30(12), pp.2504–9.
- Jochem, G. & Lehnert, R., 2002. On the potential of Raman microscopy for the forensic analysis of coloured textile fibres. *Science and Justice*, 42, pp.215–221.
- Karayannidis, G.P. & Achilias, D.S., 2007. Chemical Recycling of Poly(ethylene terephthalate). *Macromolecular Materials and Engineering*, 292(2), pp.128–146.
- Keeler, J., 2010. *Understanding NMR Spectroscopy*, Chichester, South Sussex: Wiley.
- Klemm, D. et al., 2005. Cellulose: Fascinating biopolymer and sustainable raw material. *Angewandte Chemie - International Edition*, 44, pp.3358–3393.

- Kljun, A., Benians, T., Goubet, F., Meulewaeter, F., Knox, J., Blackburn, R. S., 2011. Comparative analysis of crystallinity changes in cellulose i polymers using ATR-FTIR, X-ray diffraction, and carbohydrate-binding module probes. *Biomacromolecules*, 12, pp.4121–4126.
- Knill, C.J. & Kennedy, J.F., 2003. Degradation of cellulose under alkaline conditions. *Carbohydrate Polymers*, 51(3), pp.281–300.
- Kosmidis, V. a., Achilias, D.S. & Karayannidis, G.P., 2001. Poly(ethylene terephthalate) Recycling and Recovery of Pure Terephthalic Acid. Kinetics of a Phase Transfer Catalyzed Alkaline Hydrolysis. *Macromolecular Materials and Engineering*, 286(10), p.640.
- Larkin, P., 2011. Basic Principles. In *Infrared and Raman Spectroscopy: Principles and Spectral Interpretation*. Elsevier Science and Technology Books, Inc., pp. 7–25.
- Lenzing, 2015. The Global Fiber Market in 2014. *Company web page*. Available at: <http://www.lenzing.com/en/investors/equity-story/global-fiber-market.html>. [Accessed April 23, 2015].
- Levitt, M.H., 2008. *Spin Dynamics: Basics of Nuclear Magnetic Resonance, Second Edition*, Chichester, South Sussex: John Wiley & Sons.
- Liu, R., Shen, Y., Shao, H, Wu, C., Hu, X., 2001. An analysis of Lyocell fiber formation as a melt – spinning process. *Cellulose*, 8, pp.13–21.
- López-Fonseca, R., González-Marcos, M. P., González-Velasco, J. R., Gutiérrez-Ortiz, J. I., 2009. A kinetic study of the depolymerisation of poly(ethylene terephthalate) by phase transfer catalysed alkaline hydrolysis. *Journal of Chemical Technology & Biotechnology*, 84(1), pp.92–99
- Lu, J.J. & Hamouda, H., 2014. Current Status of Fiber Waste Recycling and its Future. *Advanced Materials Research*, 878, pp.122–131.
- Mather, R.R. & Wardman, R.H., 2011. *Chemistry of textile fibers*, Cambridge: Royal Society of Chemistry.
- Mattor, J.A., 1963. *A study of the mechanism och alkali cellulose autooxidation*. Lawrence College.
- Medronho, B. Romano, A., Miguel, M., Stigsson, L., Lindman, B., 2012. Rationalizing cellulose (in)solubility: Reviewing basic physicochemical aspects and role of hydrophobic interactions. *Cellulose*, 19(3), pp.581–587.
- Miller, J. V & Bartick, E.G., 2001. Forensic Analysis of Single Fibers by Raman Spectroscopy. *Applied Spectroscopy*, 55(12), pp.1729–1732.
- Mozdyniewicz, D.J., Nieminen, K. & Sixta, H., 2013. Alkaline steeping of dissolving pulp. Part I: Cellulose degradation kinetics. *Cellulose*, 20, pp.1437–1451.
- Murray, H., 2012. *Overview and comparison of portable spectroscopy techniques: FTIR, NIR and Raman*, analytikLtd: Whitepaper

- Naturvårdsverket, 2012. *Avfallsstatistik för bättre miljöarbete*, Rapport 6536
- Negulescu, I., Kwon, H., Collier, B., Collier, J., Pendse, A., 1998. Recycling cotton from cotton/polyester fabrics. *Textile Chemist and Colorist*, 30(6), pp.31–35.
- Ning, Y., 2011. Interpretation of Organic Spectra. In *Interpretation of 13C NMR spectra*. Singapore: John Wiley and Sons, pp. 39–51.
- Nørgaard, L., Bro, R. & Engelsen, S.B., 2012. *Principal Component Analysis and Near Infrared Spectroscopy*, FOSS: Whitepaper.
- Ouchi, A., Toida, T., Kumaresan, S., Ando, W., Kato, J., 2009. A new methodology to recycle polyester from fabric blends with cellulose. *Cellulose*, 17(1), pp.215–222.
- Palm, D., Elander, M., Watson, D., Kiörboe, N., Salmenperä, H., et. al., 2014. *Towards a Nordic textile strategy - collection, sorting, reuse and recycling of textiles*, The Nordic Region: Report
- Palme, A. Idström, A., Nordstierna, L., Brelid, H., 2014. Chemical and ultrastructural changes in cotton cellulose induced by laundering and textile use. *Cellulose*, 21, pp.4681–4691.
- Pancholi, B.S., Talele, A. B., Rao, M. V. S., Gandhi, R S., 1988. Blend analysis by conventional infra-red spectrophotometry. Part 1 - polyester/ cotton blends. *Journal of Society of Dyers and Colorists*, 104(March), pp.135–138.
- Park, S.H. & Kim, S.H., 2014. Poly (ethylene terephthalate) recycling for high value added textiles. *Fashion and textiles*, 1(1), pp.1–17.
- Pavia, D. Lampman, G., Kriz, G., Vyvyan, J., 2009. *Introduction to spectroscopy*, Belmont, CA: Brooks/Cole.
- Piketech, 2011. *Application Note ATR – Theory and Applications*. Pike Technologies: Whitepaper
- Princi, E., Vicini, S., Proietti, N., Capitani, D., 2005. Grafting polymerization on cellulose based textiles: A 13C solid state NMR characterization. *European Polymer Journal*, 41(6), pp.1196–1203.
- Pumure, I., Ford, S., Shannon, J., Kohen, C., Mulcahy, A., Frank, K., Sisco, S., Chaukura, N., 2015. Analysis of ATR-FTIR Absorption-Reflection Data from 13 Polymeric Fabric Materials Using Chemometrics. *American Journal of Analytical Chemistry*, 6, pp.305–312.
- Reich, H.J., 2015. C 13 Chemical Shifts. *University of Wisconsin*. Available at: <http://www.chem.wisc.edu/areas/reich/handouts/nmr-c13/cdata.htm>. [Accessed November 3, 2014].
- Selvi, S., Nanthini, R. & Sukanyaa, G., 2012. The Basic Principle of Phase-Transfer Catalysis , Some Mechanistic Aspects and Important Applications. *International Journal of Scientific & Technology Research Volume 1*, 1(3), pp.61–63.
- Serad, S., 1994. Polyester dissolution for recycling from the fabric blends with polyester and cotton. US Patent

- Shaw, P.B., 2013. *Studies of the Alkaline Degradation of Cellulose and the Isolation of Isosaccharinic Acids*. University of Huddersfield.
- Sigma-Aldrich, 2013. MSDS Benzyltributylammonium chloride. *Materials Safety Data Sheet*. Available at:
<http://www.sigmaaldrich.com/MSDS/MSDS/PleaseWaitMSDSPage.do?language=&country=SE&brand=ALDRICH&productNumber=193771&PageToGoToURL=http://www.sigmaaldrich.com/catalog/product/aldrich/193771?lang=en®ion=SE> [Accessed May 20, 2015].
- De Silva, R., Wang, X. & Byrne, N., 2014. Recycling textiles: the use of ionic liquids in the separation of cotton polyester blends. *RSC Advances*, 4(55), p.29094.
- Sjöström, Ee., 1981. *Wood Chemistry - Fundamentals and Applications*, Helsinki: Academic Press.
- Teijin, 2015. Eco Circle Fibers. Available at:
(http://www.teijin.com/products/advanced_fibers/poly/specifics/ecopet-plus.html) [Accessed May 5, 2015].
- ul Hasan, M., 1980. NMR Spectra of some Amides and Imides. Effect of Inductive and Mesomeric Interactions, Cyclization and Hydrogen Bonding on ¹³C NMR Chemical Shifts. *Organic Magnetic Resonance*, 14(6), pp.447–450.
- Vadicherla, T. & Saravanan, D., 2014. Textiles and Apparel Development Using Recycled and Reclaimed Fibers. In *Roadmap to Sustainable Textiles and Clothing*. Textile Science and Clothing Technology. Singapore: Springer, pp. 139–160.
- Vigo, T.L. et al., 1969. Synergistic Effect of Mixed Bases in the Conversion of Cotton Cellulose I to Cellulose II The Role of Cations as Cocatalysts for Crystal Lattice Rearrangement. *Textile Research Journal*, 39(4), pp.305–316.
- Wold, S., 1995. Chemometrics ; what do we mean with it , and what do we want from it? *Chemometrics and Intelligent Laboratory Systems*, 20, pp.109-115.
- Yang, S. & Akkus, O., 2013. *Fluorescence Background Problem in Raman Spectroscopy: Is 1064 nm Excitation an Improvement of 785 nm?*, Wasatch Photonics: Report
- Zugenmaier, P., 2001. Conformation and packing of various crystalline cellulose fibers. *Progress in Polymer Science (Oxford)*, 26(9), pp.1341–1417.

Appendix 1

ATR FT-IR spectra of textile fibers

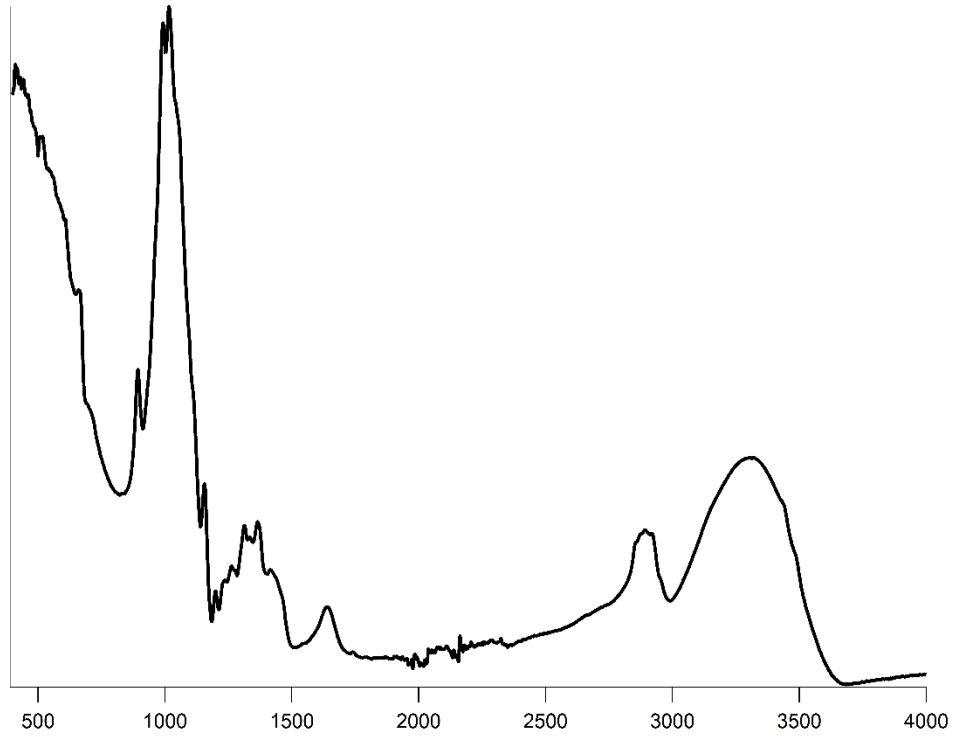


Figure 1: Viscose

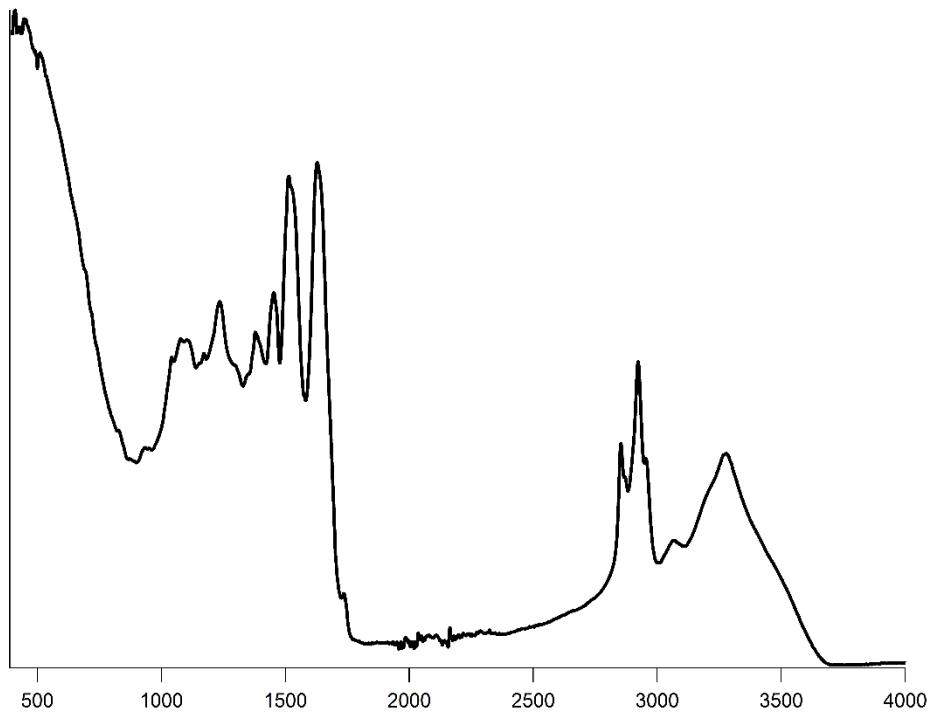


Figure 2: Wool

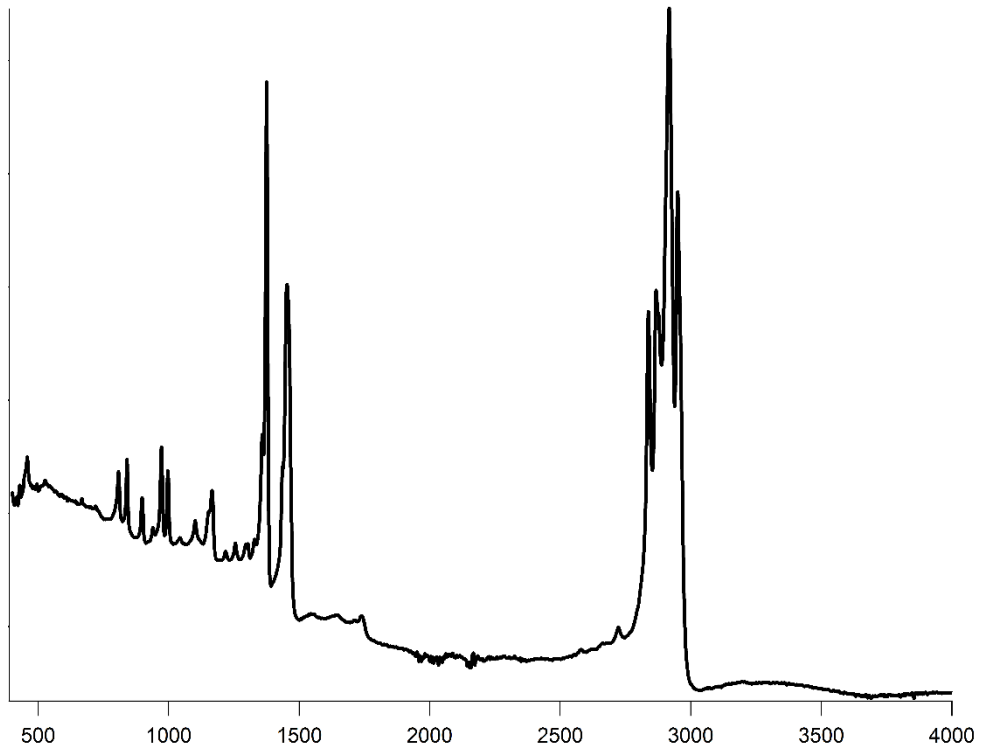


Figure 3: Polypropylene

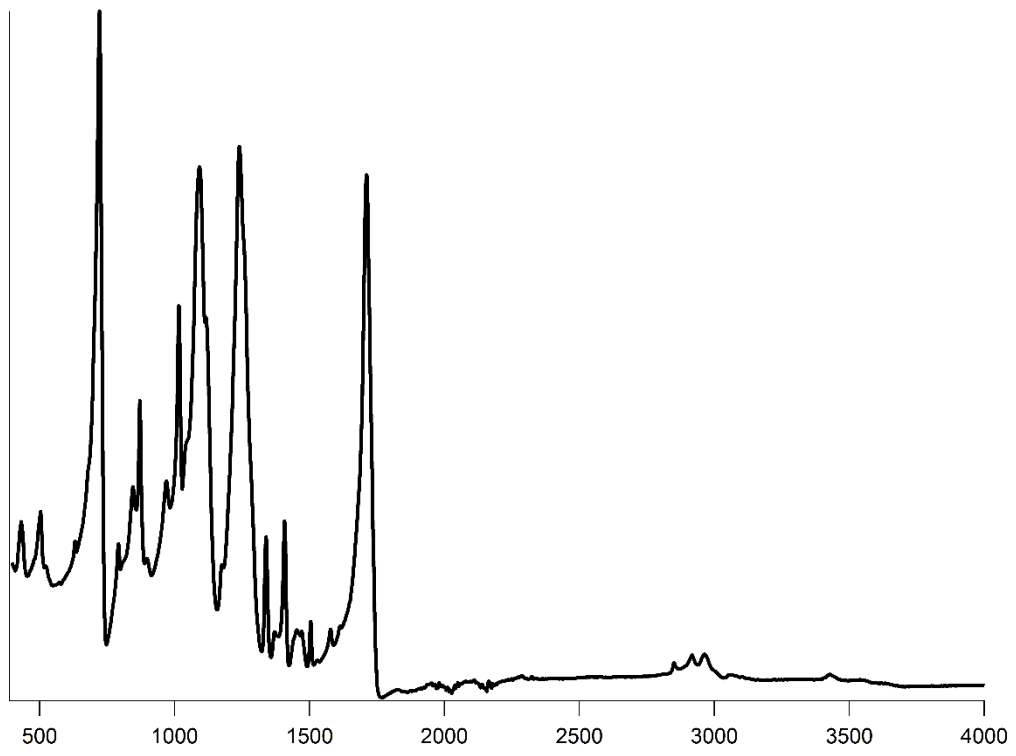


Figure 4: Polyester

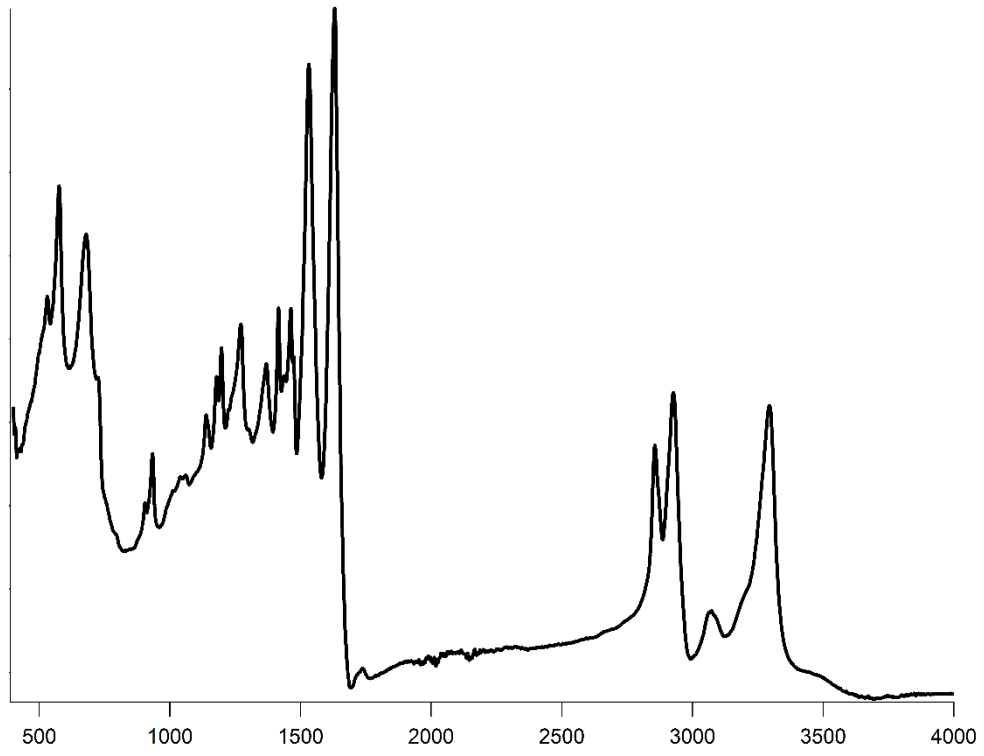


Figure 5: Polyamide

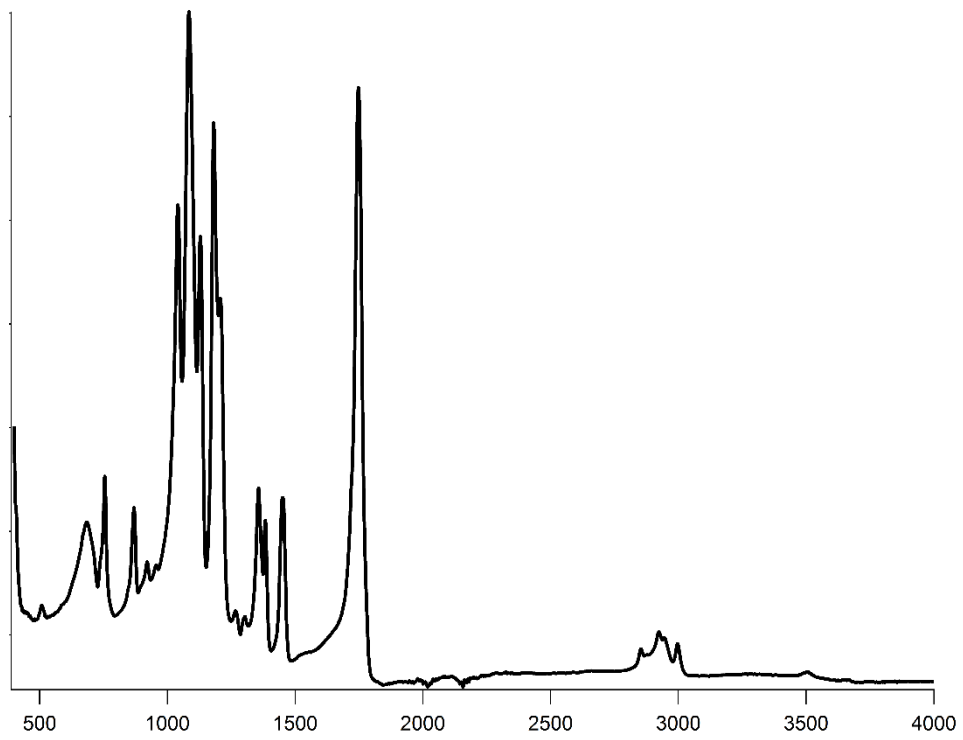


Figure 6: Polylactic acid

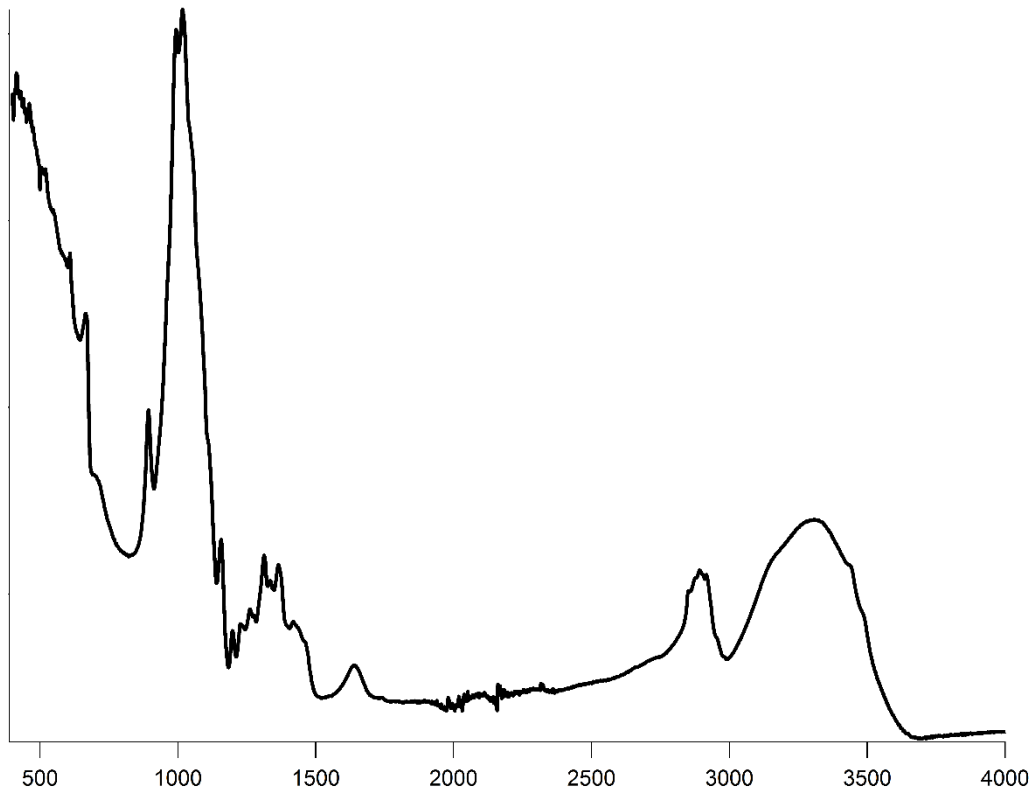


Figure 7: Lyocell

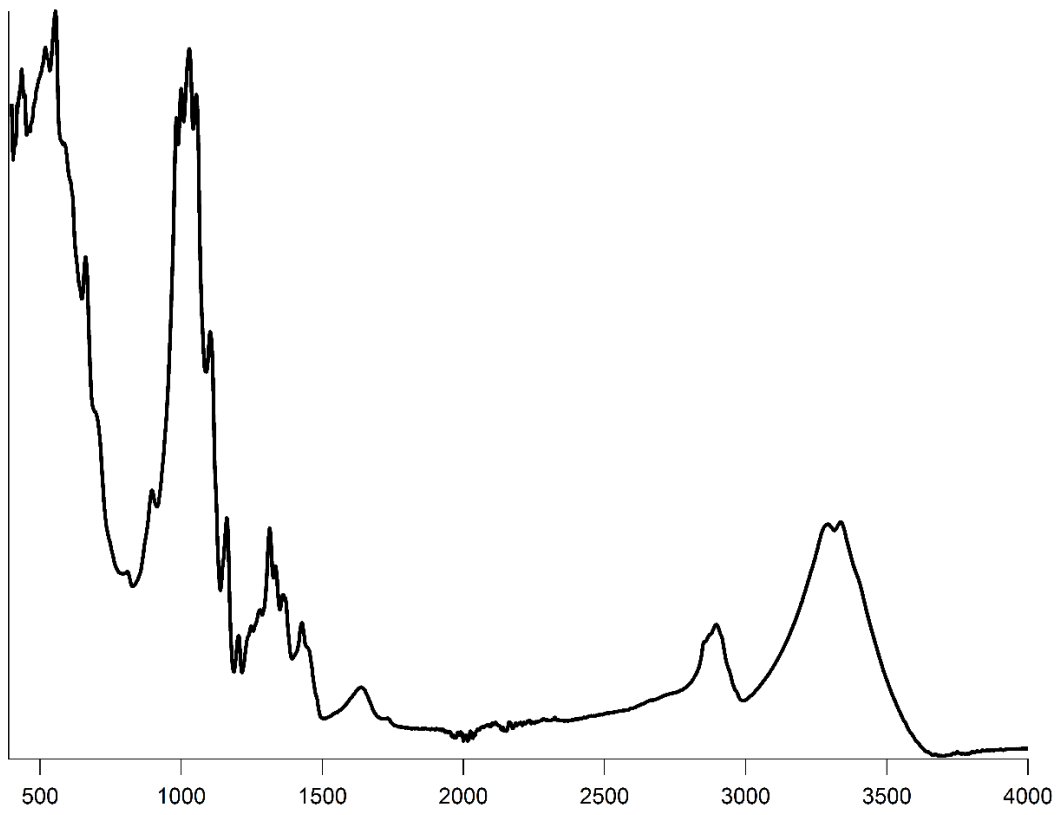


Figure 8: Linne

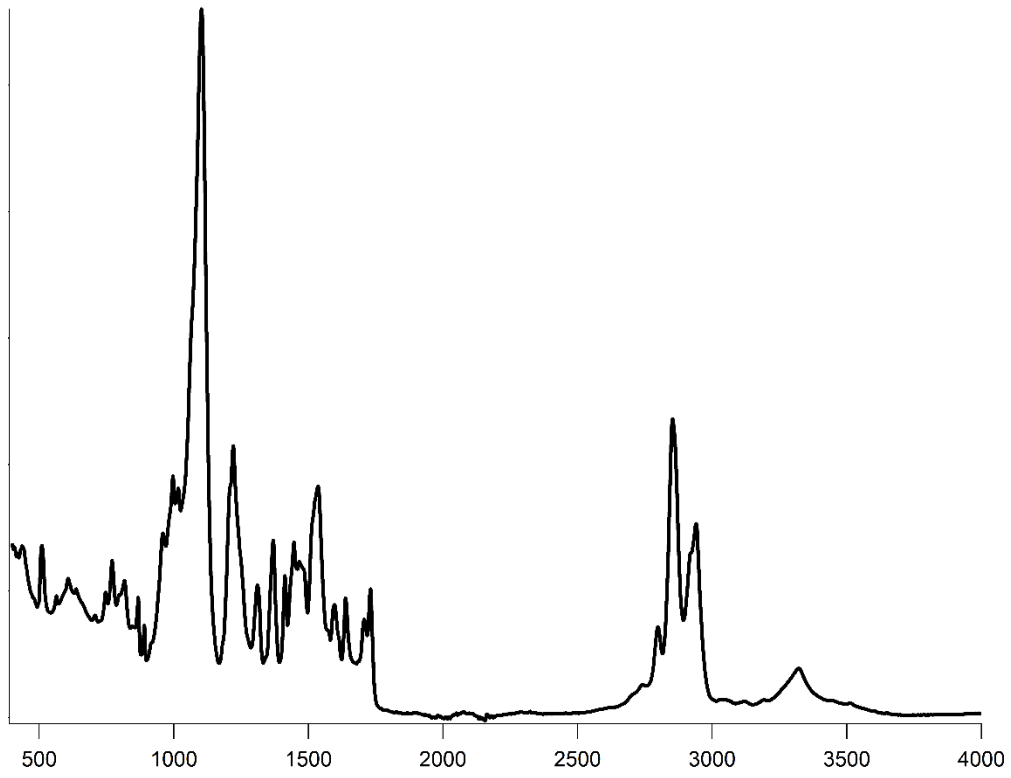


Figure 9: Elastane

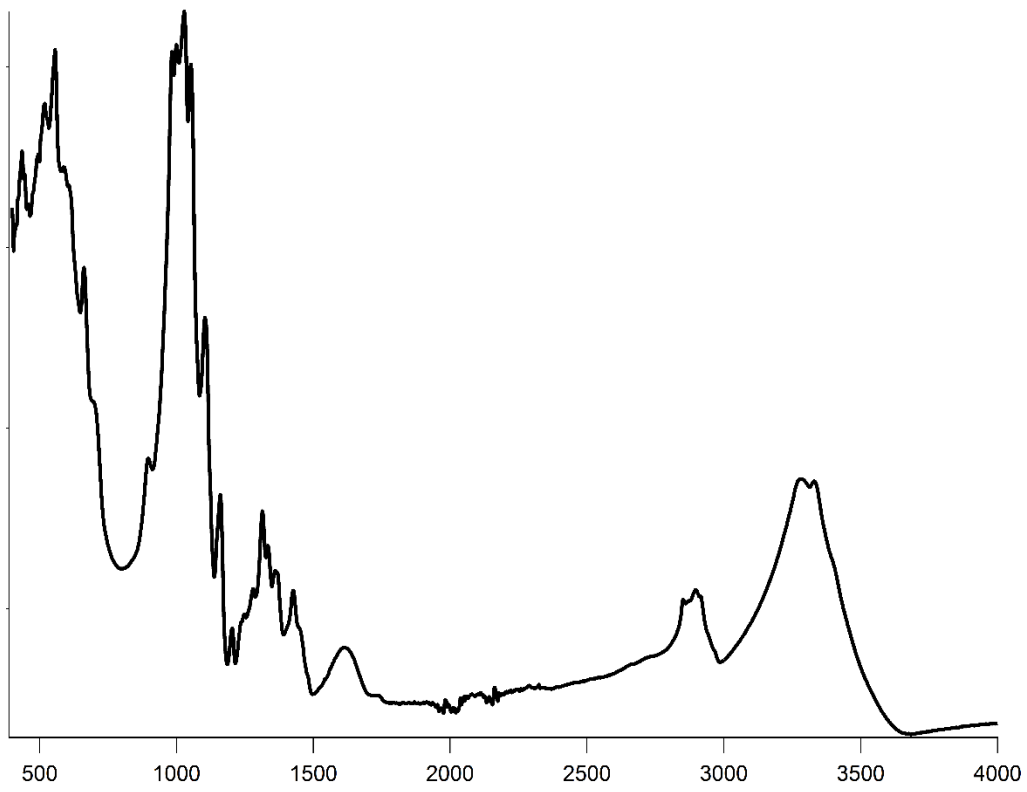


Figure 10: Cotton

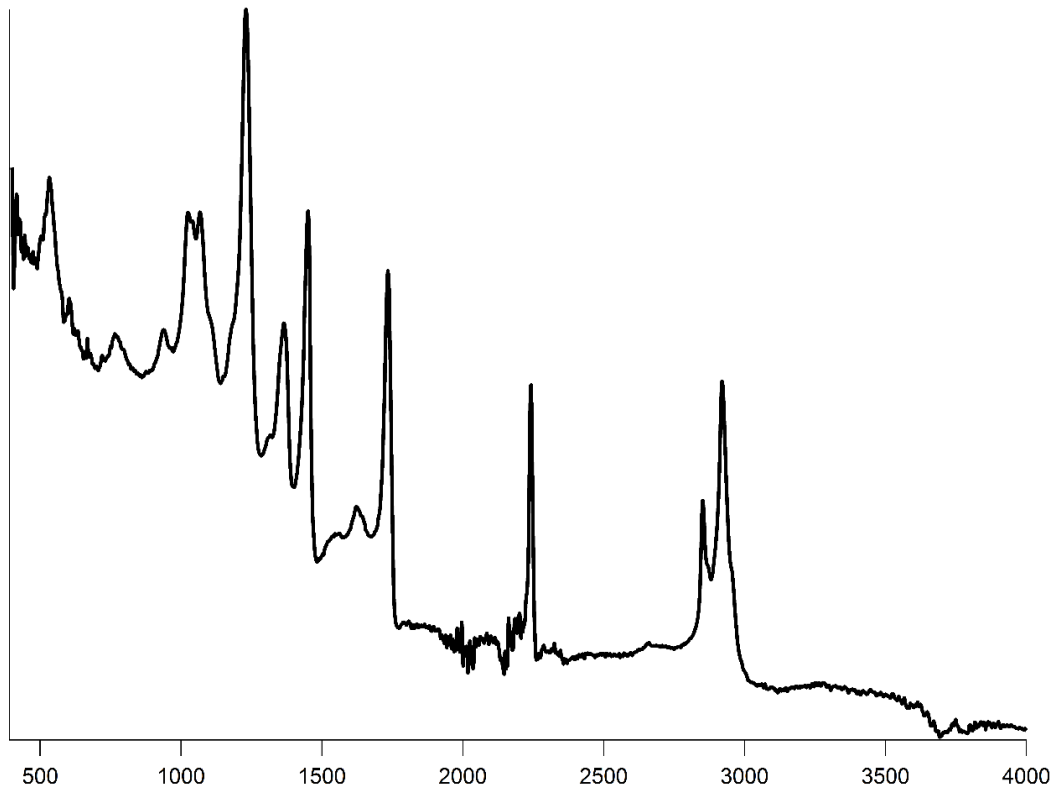


Figure 11: Acrylic

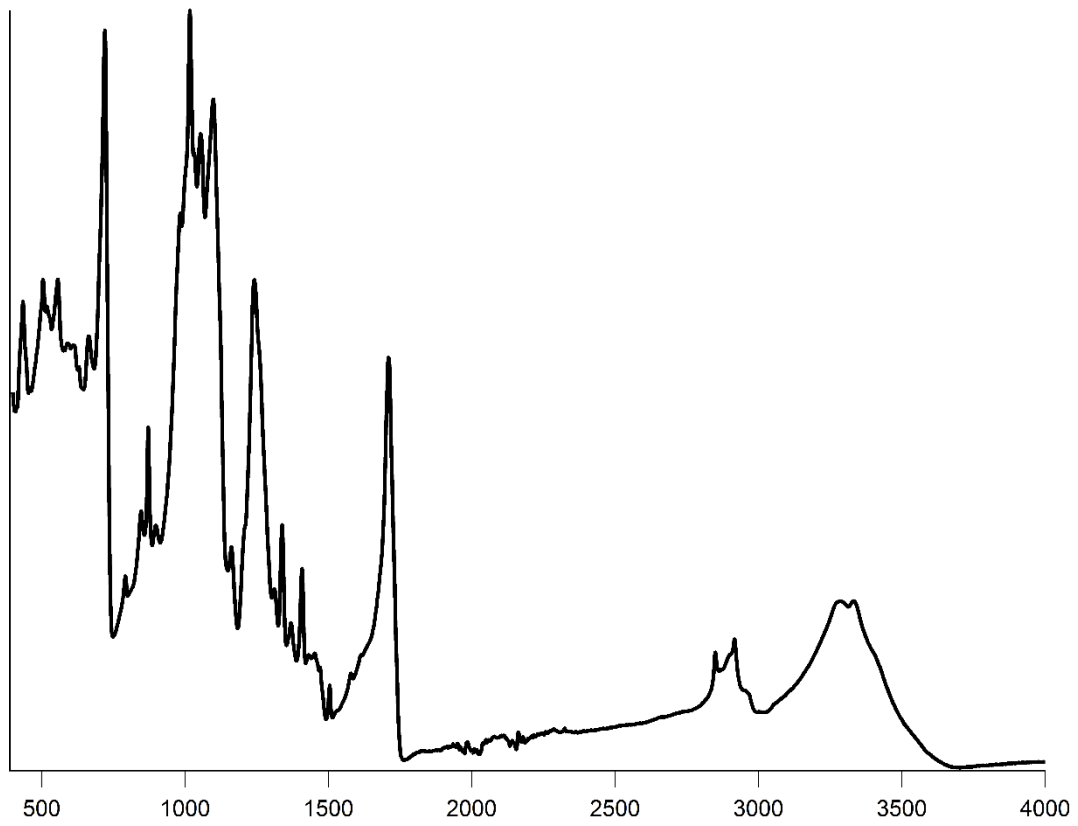


Figure 12: Cotton/Polyester 50/50

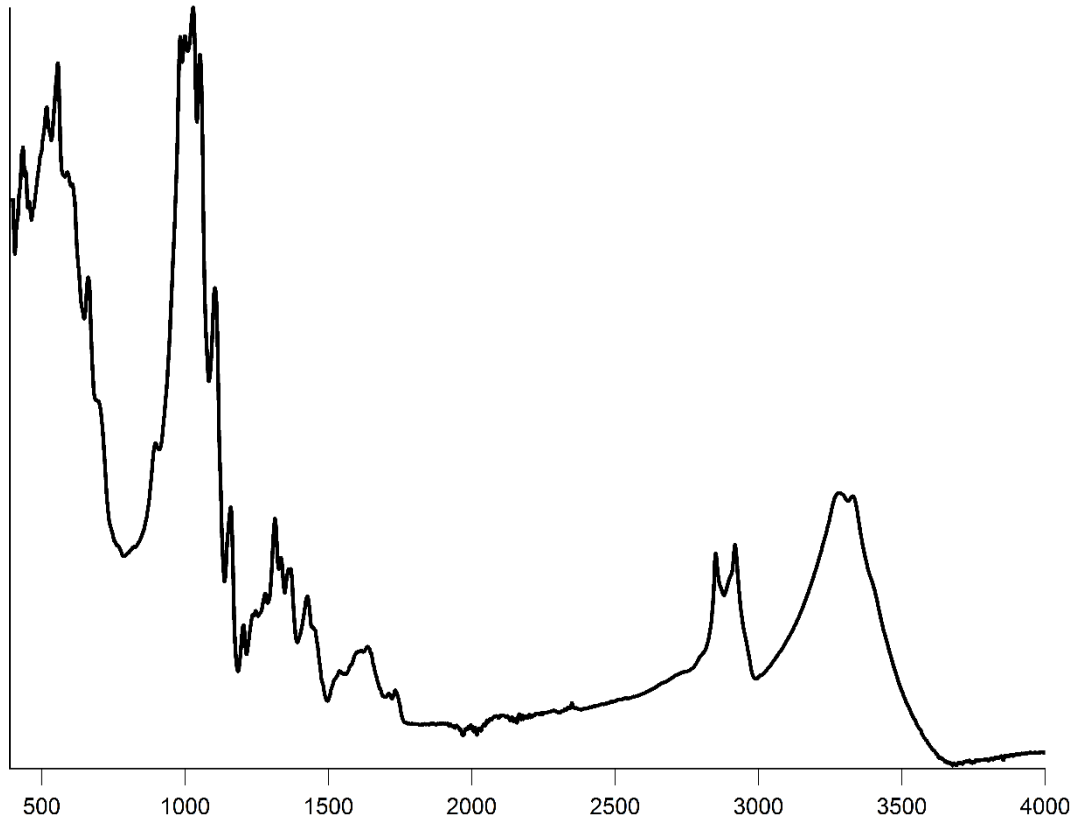


Figure 13: Cotton/Elastane 92/8

Appendix 2

CP-MAS ^{13}C NMR spectra of textile fibers

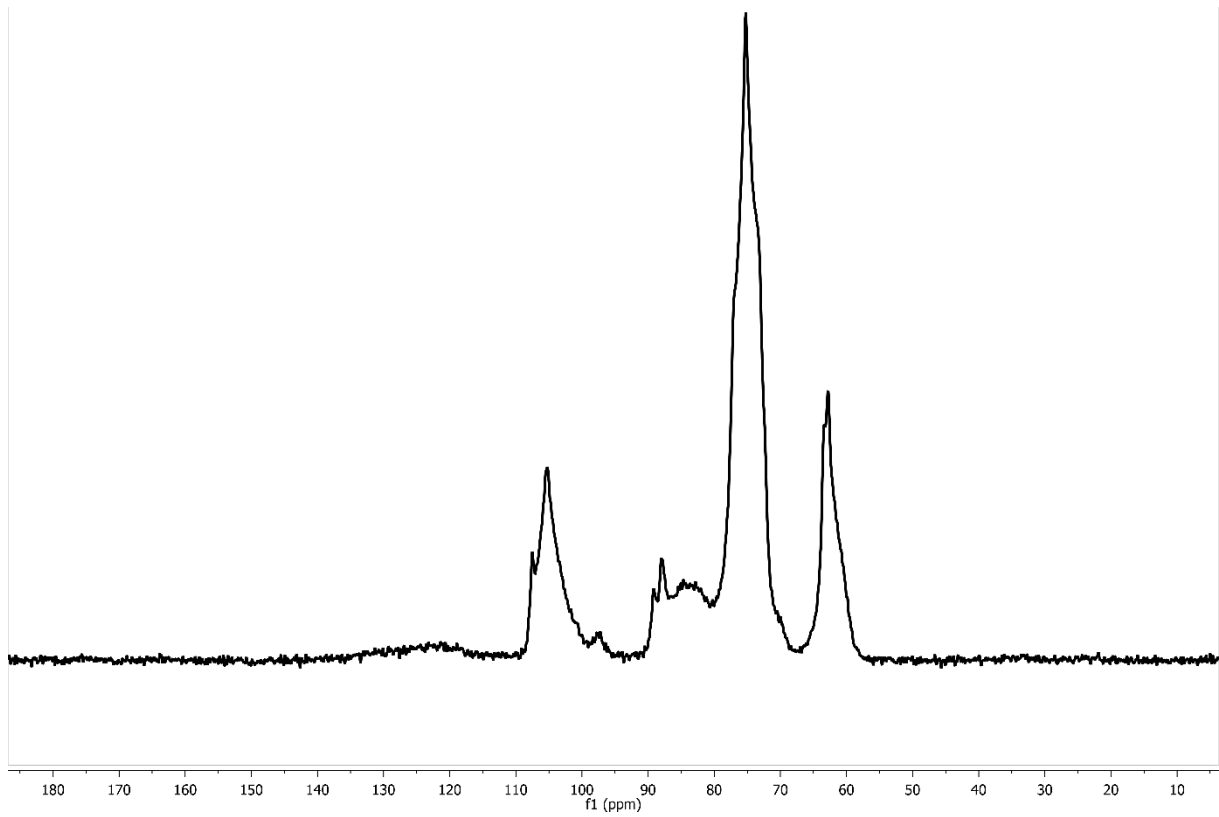


Figure 1: Viscose

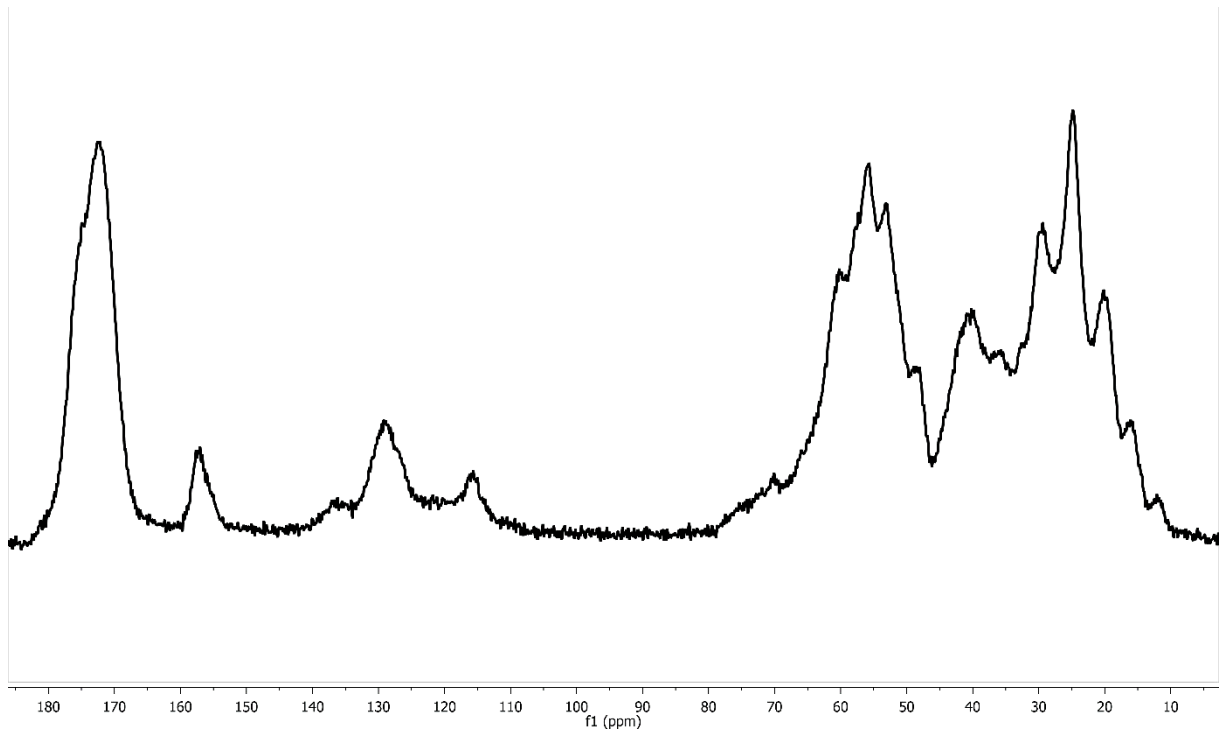


Figure 2: Wool

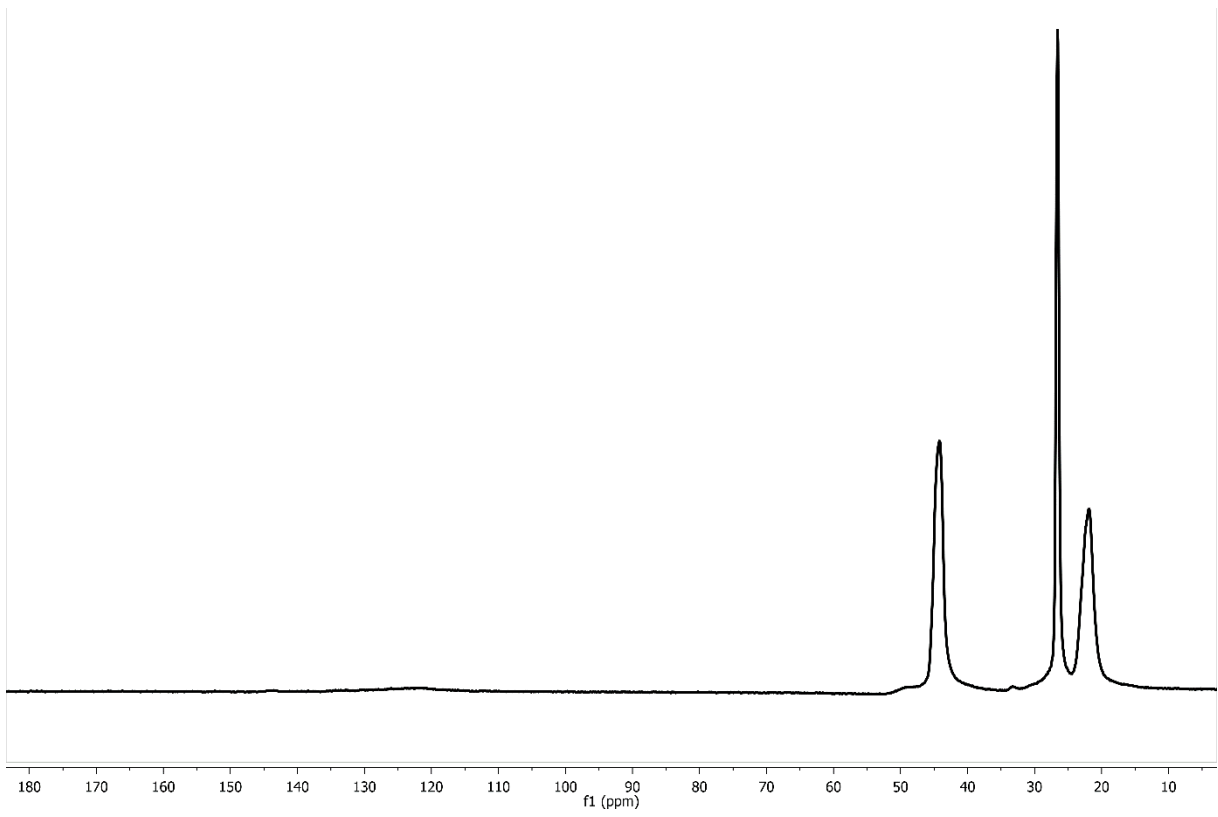


Figure 3: Polypropylene

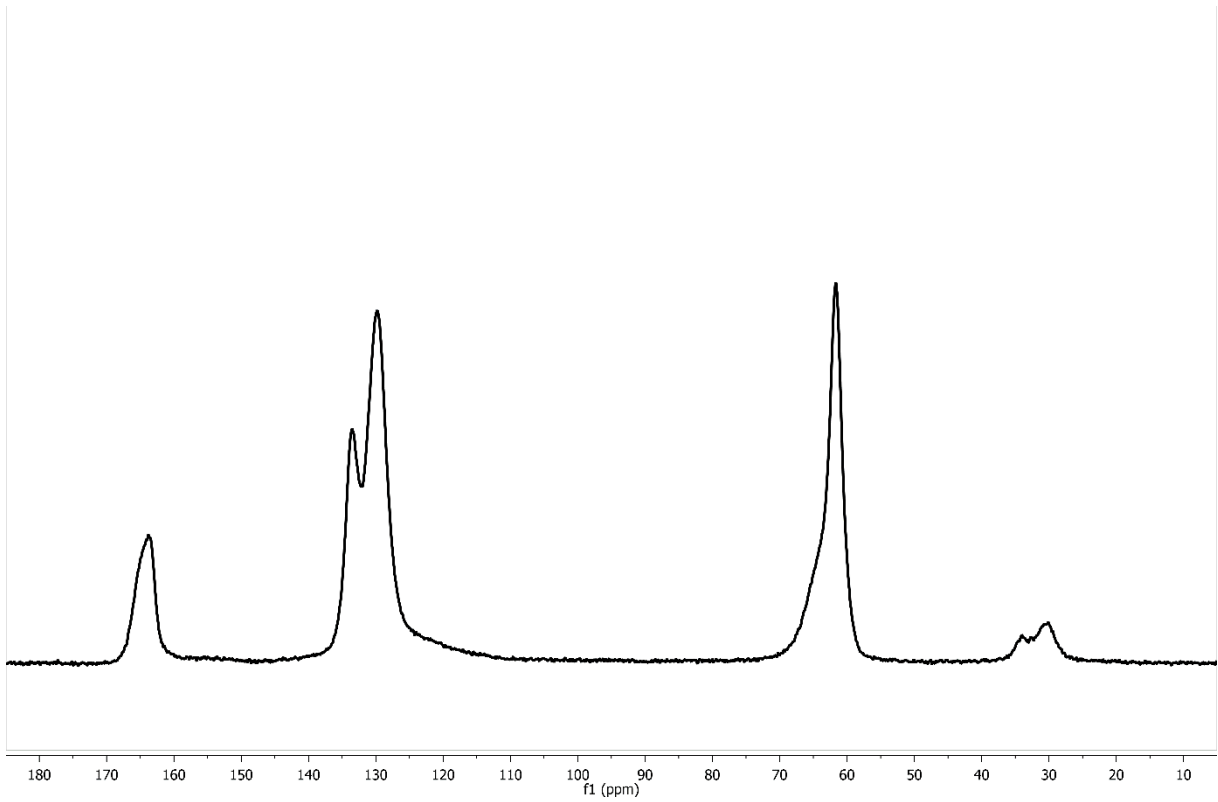


Figure 4: Polyester

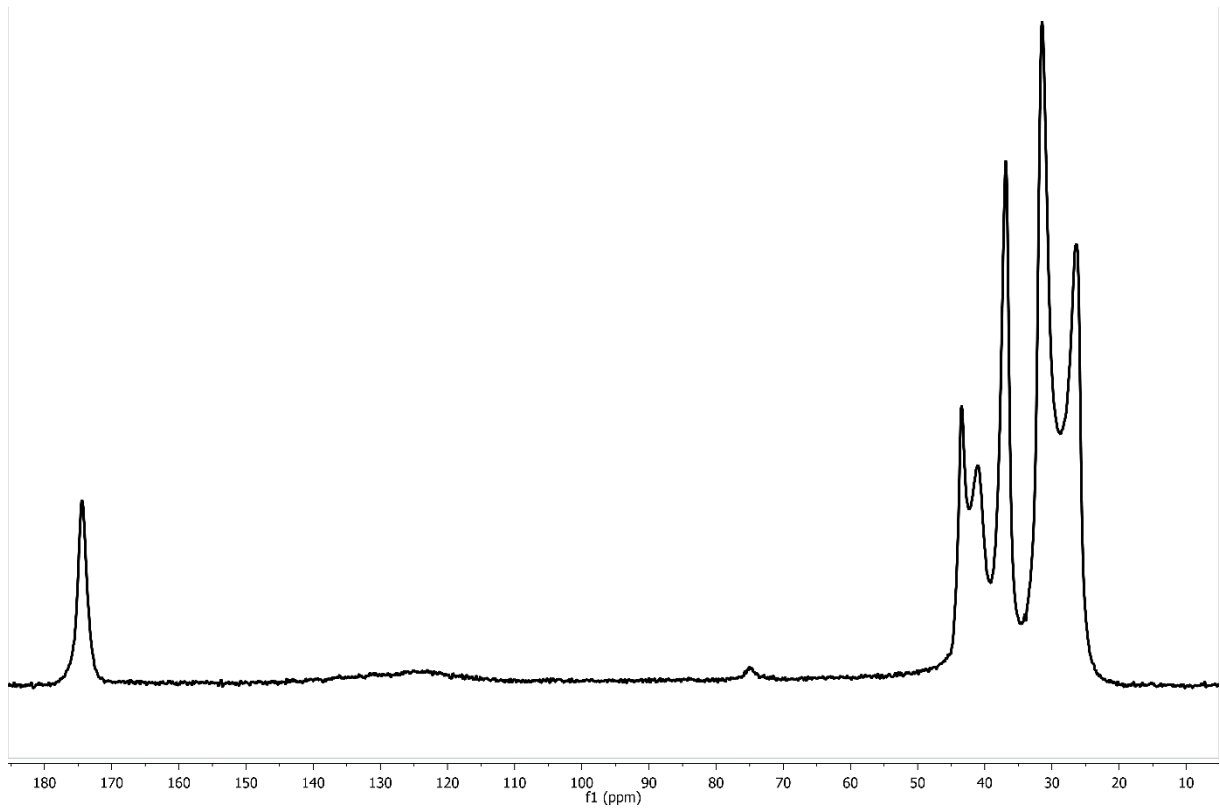


Figure 5: Polyamide

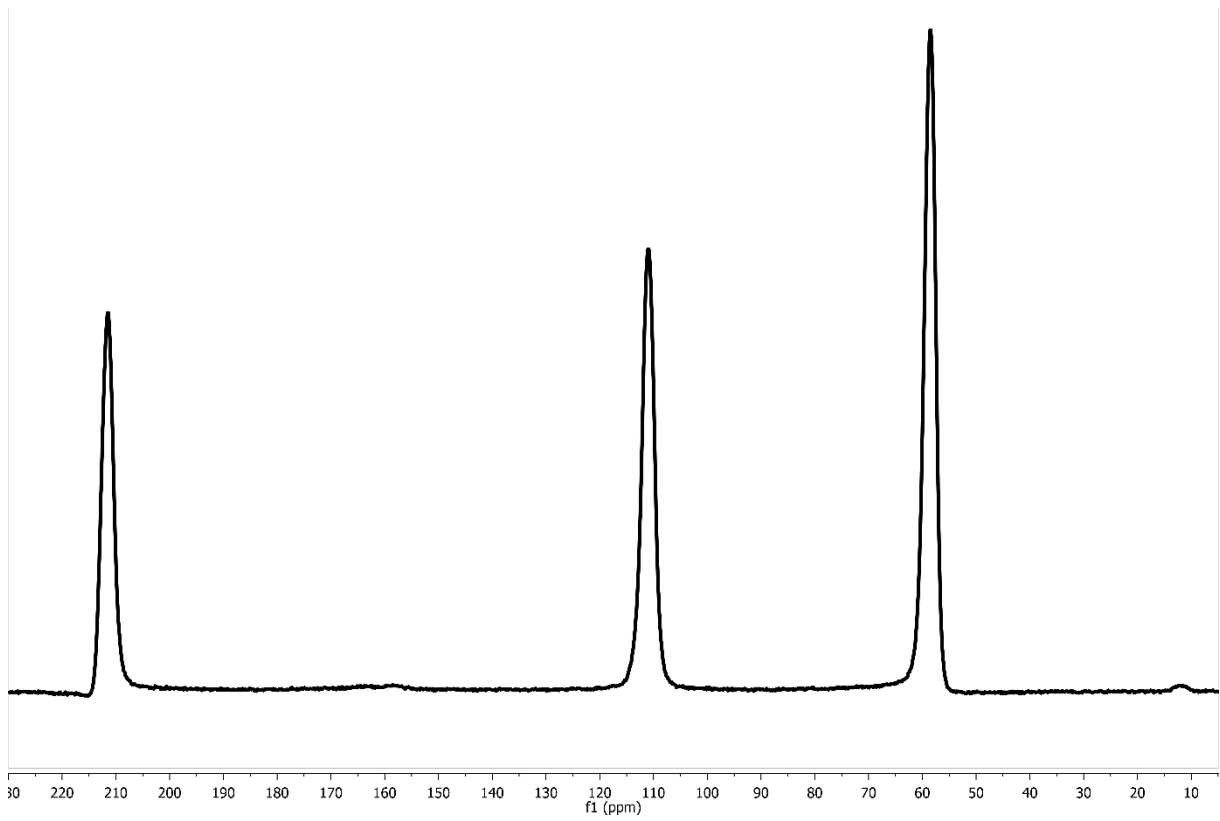


Figure 6: Polylactic acid

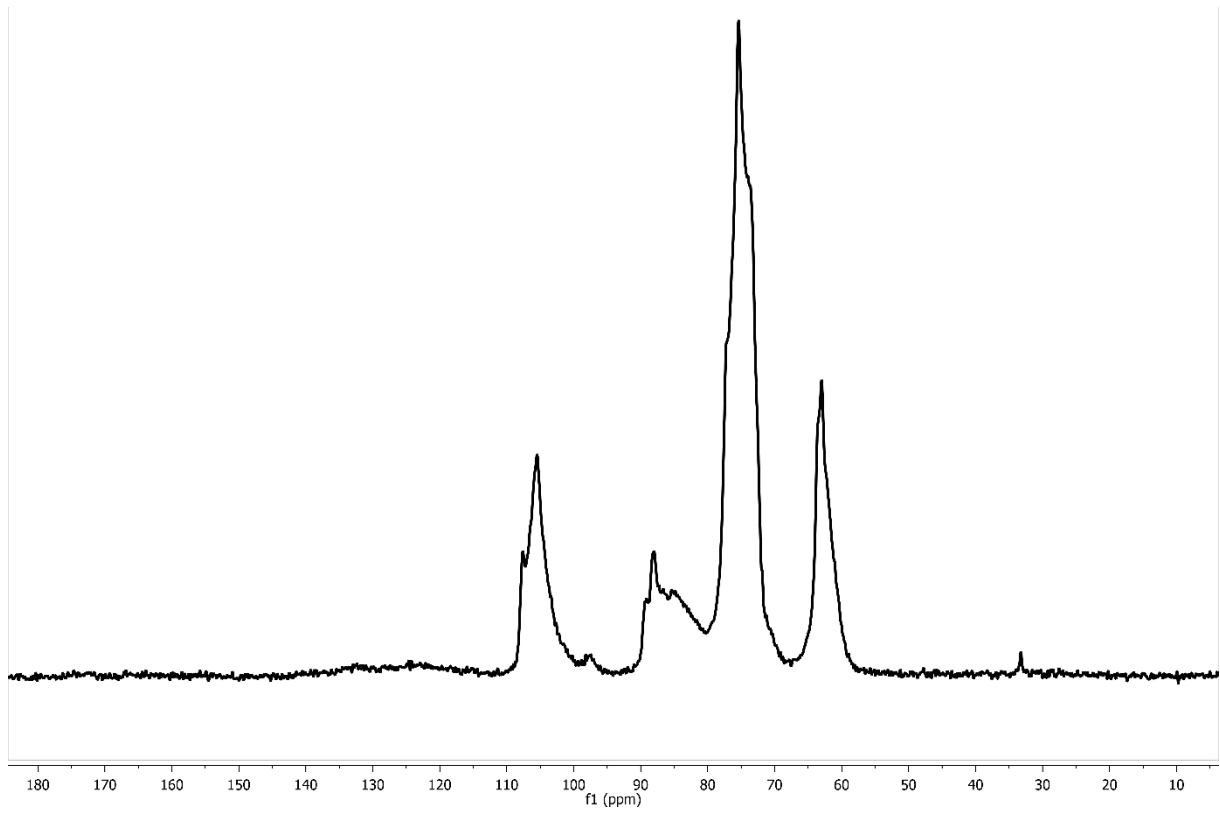


Figure 7: Lyocell

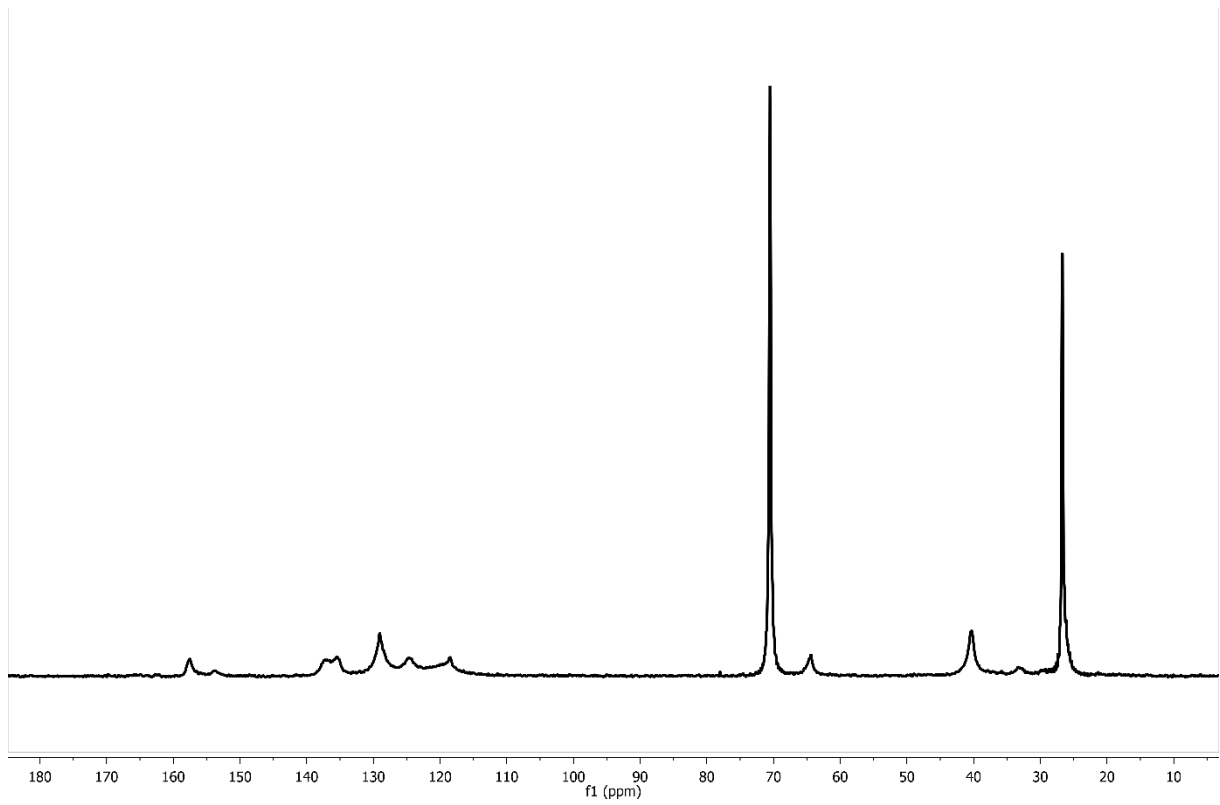


Figure 8: Elastane

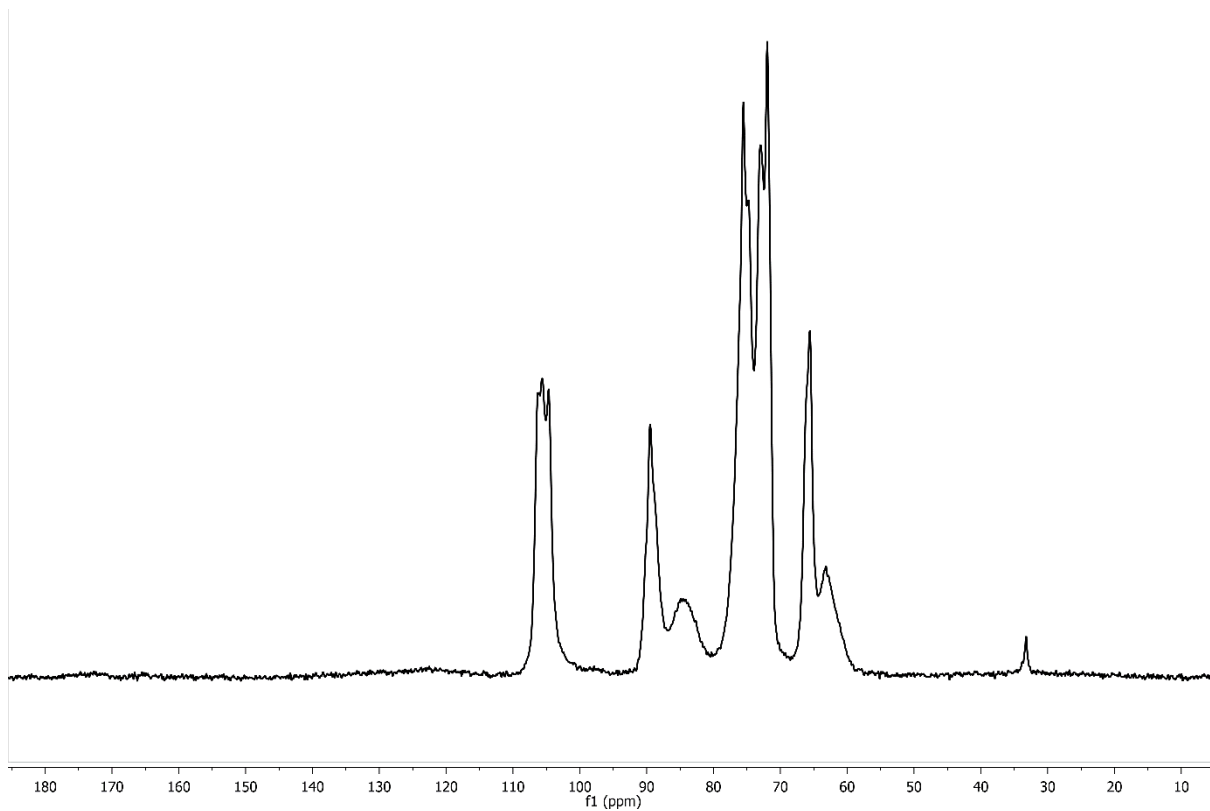


Figure 9: Cotton

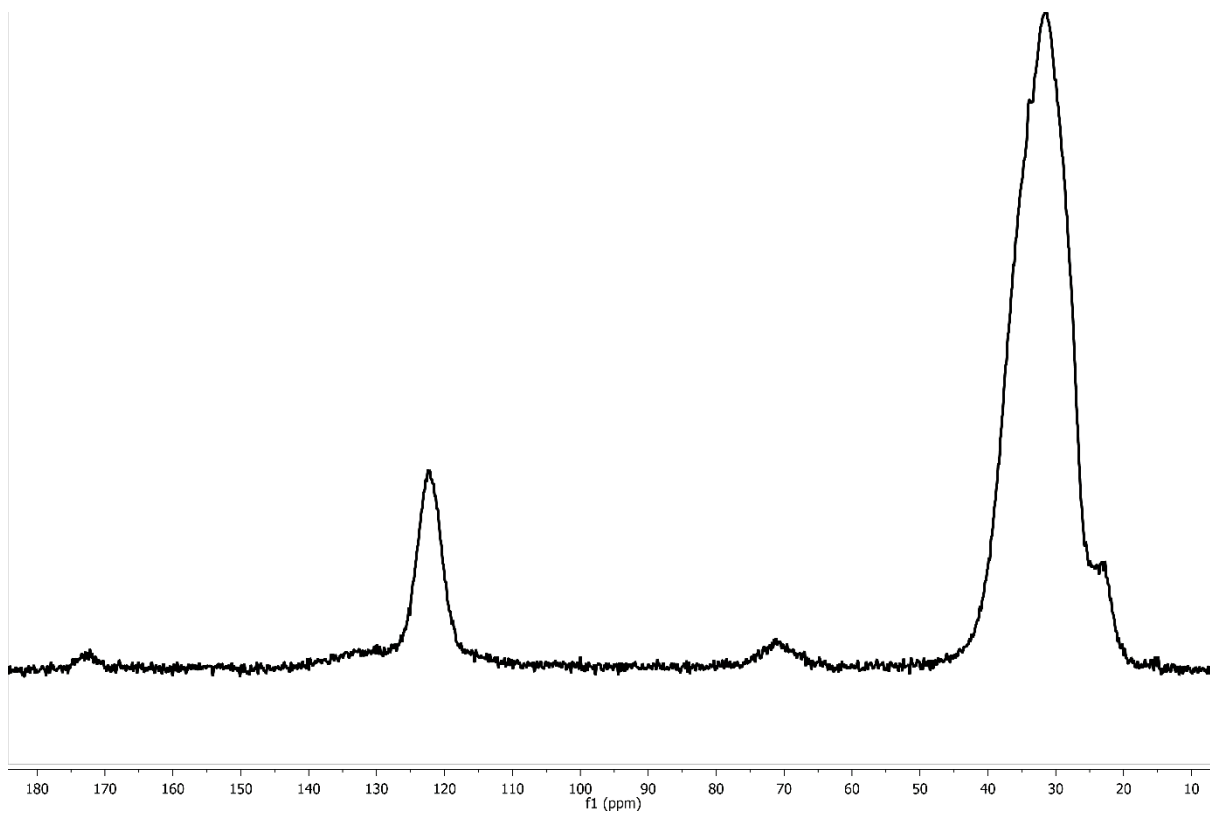


Figure 10: Acrylic

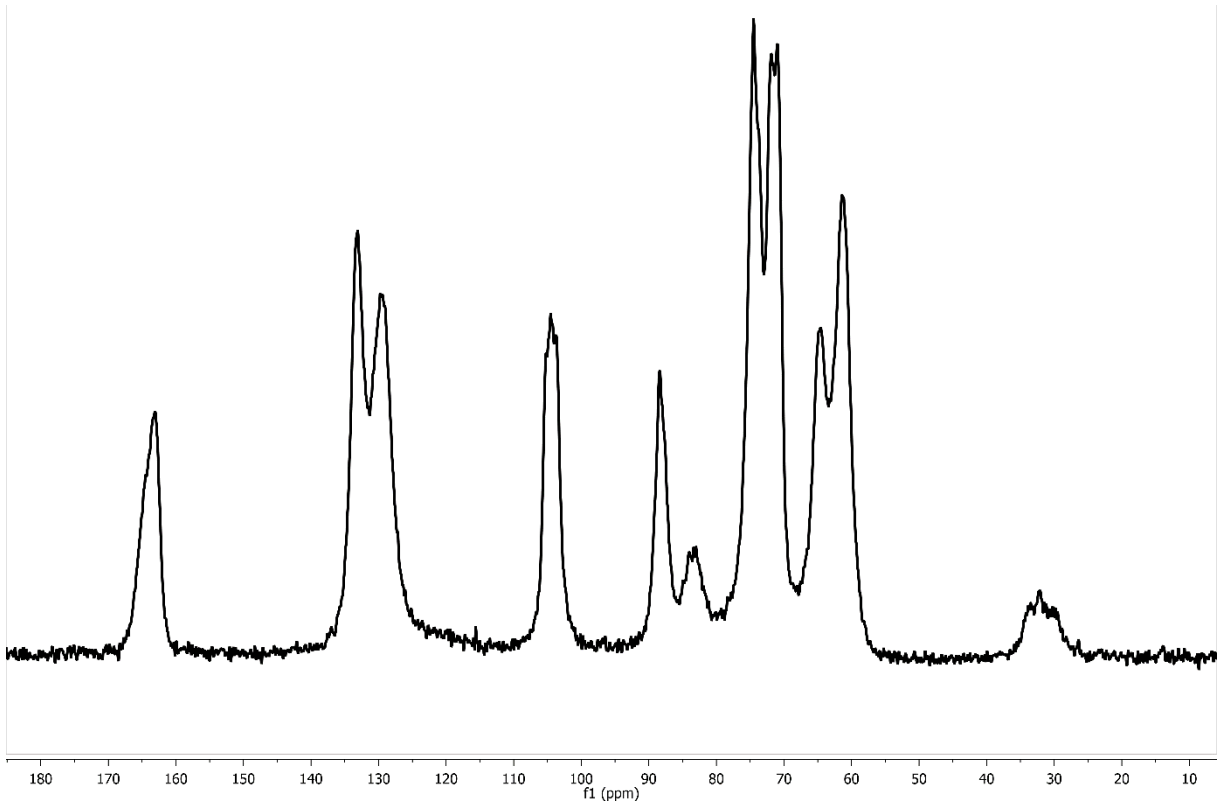


Figure 11: Cotton/polyester blend 50/50

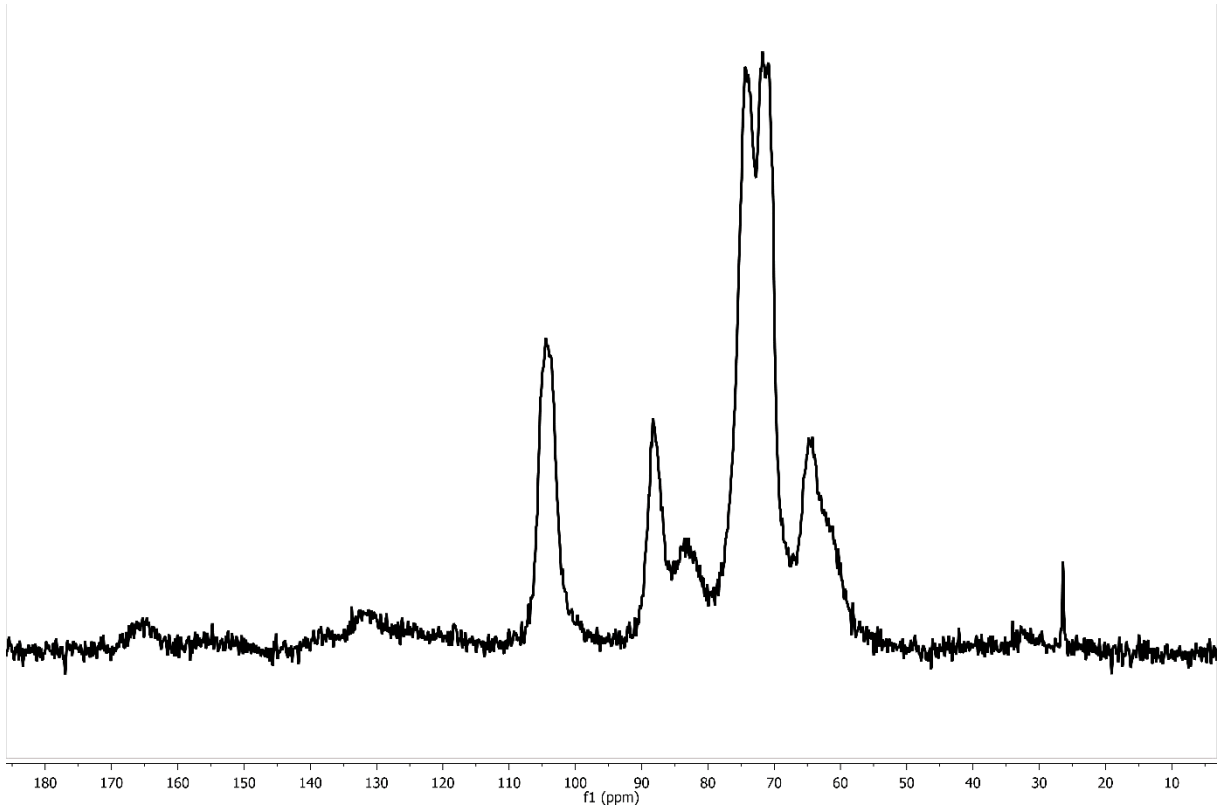


Figure 12: Cotton/Elastane blend 92/8